FINAL REPORT

U.F. Project No: 49104504972-12
Contract No: BC-354
RPWO#: 83

Evaluation of Early Strength Requirement of Concrete for Slab Replacement Using APT

Mang Tia
Wasantha Kumara

Department of Civil & Coastal Engineering
College of Engineering
UNIVERSITY OF FLORIDA
Gainesville, FL

March 2005

ACKNOWLEDGMENTS

The Florida Department of Transportation (FDOT) is gratefully acknowledged for providing the financial support for this study. The FDOT Materials Office provided the additional testing equipment, materials and personnel needed for this investigation. Sincere thanks go to the project manager, Mr. Michael Bergin, and the director of FDOT APT facility, Dr. Bouzid Choubane, for providing the technical coordination and advices throughout the project. Sincere gratitude is extended to the FDOT Materials Office personnel, particularly to Dr. Alexander Appea, Messrs. Tom Byron, Steve Ross, Aaron Philpott, Charles Ishee, Richard DeLorenzo, Salil Gokhale, Abdenour Nazef, Jerry Moxley and Vidal Francis.

TABLE OF CONTENTS

page

ACKNOWLEDGEMENTS i

LIST OF TABLES iv

LIST OF FIGURES v

TECHNICAL SUMMARY ix

CHAPTER

1 INTRODUCTION 1

1.1 Background 1

1.2 Scope of Report 2

2 CONSTRUCTION OF TEST TRACK 3

2.1 Layout of Test Slabs 3

2.2 Construction of Test Track 3

2.3 Sawing of Joints 6

3 STRESS ANALYSIS AND INSTRUMENTATION OF TEST SLABS 7

3.1 Stress Analysis 7

3.2 Instrumentation Layout 18

3.2.1 Wheatstone Bridge Circuits 18

3.2.2 Placement of Gauges 19

4 CONSTRUCTION OF REPLACEMENT TEST SLABS 22

4.1 Description of Five Test Slabs 22

4.2 Removal of Existing Slabs 22

4.3 Construction of Concrete Test Slabs 25

4.3.1 Dowel Bar Placement 25

4.3.2 Concrete Mix Used in the Test Slabs 26

4.3.3 Concrete Placement 28

4.3.4 Concrete Finishing and Sawing of Joints 34

5 TESTING OF THE TEST SLABS 36

5.1 HVS Loading 36

5.1.1 Slab 1C 36

5.1.2 Slab 1G 36
5.1.3 Slab 2C 41
5.1.4 Slab 2E 41
5.1.5 Slab 2G 45
5.2 Temperature Data 46
5.3 Impact Echo Test 49
5.4 FWD Test 53
6 OBSERVED PERFORMANCE OF THE TEST SLABS 54
6.1 Crack Initiation and Propagation 54
6.1.1 Cracks on Slab 1C 54
6.1.2 Cracks on Slab 1G 57
6.1.3 Cracks on Slab 2C 59
6.1.4 Cracks on Slab 2E 63
6.1.5 Cracks on Slab 2G 64
7 ANALYSIS OF DATA 67
7.1 Estimation of Model Parameters 67
7.2 Analysis of Dynamic Strain Data 71
7.2.1 Analysis of Measured Dynamic Strains for Detection of Cracks 72
7.2.2 Comparison of Measured Strains with Computed Strains 74
7.3 Analysis of Static Strain Data 78
7.4 Impact Echo Test Results 81
7.5 Analysis of Performance of Concrete Mixes 86
7.5.1 Computation of Stresses in the Test Slabs 86
7.5.2 Relating Stress/Strength Ratio to Observed Performance 93
7.5.3 Required Concrete Properties for Performance 94
8 CONCLUSIONS AND RECOMMENDATIONS 99
8.1 Summary of Findings 99
8.2 Conclusions 101
8.3 Recommendations 102

APPENDIX A FWD DATA 103

LIST OF TABLES

Table		page
1	Properties of the Concrete Used on the Initial Concrete Test Track	6
2	Strain Gauge Locations and Identification Numbers	21
3	Fresh Concrete Properties	26
4	Mix Designs of Concrete Used in Test Slabs	27
5	Compressive Strength, Elastic Modulus and Flexural Strength Data	29
6	Schedule of Testing and Data Collection for Test Slab 1C	37
7	Schedule of Testing and Data Collection for Test Slab 1G	39
8	Schedule of Testing and Data Collection for Test Slab 2C	42
9	Schedule of Testing and Data Collection for Test Slab 2E	43
10	Schedule of Testing and Data Collection for Test Slab 2G	45
11	Computation of Stress to Strength Ratios for Test Slab 1C (Mix 1)	88
12	Computation of Stress to Strength Ratios for Test Slab 1G (Mix 2)	89
13	Computation of Stress to Strength Ratios for Test Slab 2C (Mix 3)	90
14	Computation of Stress to Strength Ratios for Test Slab 2E (Mix 4)	91
15	Computation of Stress to Strength Ratios for Test Slab 2G (Mix 5)	92

LIST OF FIGURES

Figure		page
1	Layout of concrete slabs on test track	4
2	Placement of concrete on test track	5
3	Finished concrete test track	5
4	Making a 3-inch deep saw cut at the joint	6
5	Loading positions used in the stress analysis	8
6	Distribution of maximum principal stresses due to a 12-kip load at the slab corner for the condition of no load transfer at the joints	9
7	Distribution of stresses in the XX direction due to a 12-kip load at the slab corner for the condition of no load transfer at the joints	10
8	Distribution of stresses in the YY direction due to a 12-kip load at the slab corner for the condition of no load transfer at the joints	11
9	Distribution of maximum principal stresses due to a 12-kip load at the slab corner for the condition of good load transfer at the joints	12
10	Distribution of stresses in the XX direction due to a 12-kip load at the slab corner for the condition of good load transfer at the joints	13
11	Distribution of stresses in the YY direction due to a 12-kip load at the slab corner for the condition of good transfer at the joints	14
12	Distribution of maximum principal stresses on the adjacent slab due to a 12-kip load at the slab corner for the condition of good load transfer at the joints	15
13	Distribution of stresses in the XX direction on the adjacent slab due to a 12-kip load at the slab corner for the condition of good load transfer at the joints	16
14	Distribution of stresses in the YY direction on the adjacent slab due to a 12-kip load at the slab corner for the condition of good load transfer at the joints	17
15	Distribution of maximum principal stresses due to a 12-kip load at the mid-edge for the condition of no load transfer at the joints	18
16	Strain gauge arrangements in a half bridge circuit	19
17	Connection of the active and dummy strain gauges in the half bridge circuit	19
18	Instrumentation layout for Test Slab 1C	20

19 Instrumentation layout for Test Slabs 1G, 2C, 2E and 2G 21
20 Cutting of a concrete slab (12 ft ×16 ft) into small pieces (3 ft × 4 ft) 23
21 Separated concrete pieces after cutting with diamond bladed saw........................23
22 Removal of separated pieces using a lifter 24
23 Removal of concrete pieces adjacent to the surrounding slabs.............................24
24 Correcting the damaged portion of the asphalt base 25
25 Dowel bars epoxied to an adjacent slab before placement of the test slab 26
26 Comparison of compressive strength of the concrete mixes used 30
27 Formwork for the free edge of Test Slab 1C 31
28 Placing concrete around strain gauges 32
29 Placement of concrete for a test slab...33
30 Placement of concrete around dummy gauges in wooden blocks 33
31 Leveling of concrete surface 34
32 Making a 3-inch deep saw cut at the joint 35
33 Temperature differentials at Slab 1C 47
34 Temperature differentials at Slab 1G 47
35 Temperature differentials at Slab 2C 48
36 Temperature differentials at Slab 2E 48
37 Temperature differentials at Slab 2G 49
38 Schematic representation of test set-up for wave speed measurement 50
39 Waveforms from impact echo test for P-wave speed measurement 50
40 Steel template for marking impact and receiver locations.....................................51
41 Receiver and impact locations on test slab for impact echo test............................52
42 Shrinkage cracks on Test Slab 1C 54
43 Corner crack on Slab 1C 55
44 Cracked Slab 1C at the end of HVS testing..55
45 Crack map of Slab 1C 56
46 Corner crack at the southern end of Slab 1G 57
47 Transverse cracks at the mid-edge of Slab 1G..58
48 Crack propagation at the mid-edge of Slab 1G with additional loading................58
49 Crack map of Slab 1G...59

50 Transverse cracks at mid-edge of Slab 2C....60
51 Cracks on Slab 2C at the end of HVS testing....61
52 Crack map of Slab 2C....62
53 Transverse crack on Slab 2E at the middle of the slab....63
54 Crack map of Slab 2E....64
55 Transverse cracks on Slab 2G at the middle of the slab....65
56 Crack map of Slab 2G....66
57 Measured and computed deflection basins caused by a 9-kip FWD load at slab center for Slab 1G....68
58 Measured and computed deflection basins caused by a 9-kip FWD load at slab center for Slab 2C....69
59 Measured and computed deflection basin caused by a 9-kip FWD load at slab joint for Slab 1G....70
60 Measured and computed deflection basins caused by a 9-kip FWD load at a free edge for Slab 1G....71
61 Measured dynamic strains from gauge 3 on Slab 2C....72
62 Measured dynamic strains from gauge 4 on Slab 2E....73
63 Maximum measured compressive strain from gauge 4 on Slab 2E....74
64 Measured and computed strains for gauge 1 on Slab 1C....75
65 Measured and computed strains for gauge 2 on Slab 1C....75
66 Measured and computed strains for gauge 4 on Slab 1C....76
67 Measured and computed strains for gauge 5 on Slab 1C....76
68 Measured and computed strains for gauge 6 on Slab 1C....77
69 Measured and computed strains for gauge 7 on Slab 1C....77
70 Measured strains at Slab 1G in the first method of applying a static load....79
71 Measured strains at Slab 2G in the second method of applying a static load....80
72 Comparison of maximum measured dynamic and static strains....81
73 Grid lines for impact echo test and location of corner crack on Slab 1G....82
74 Measured P-wave speed along line 3 at corner of Slab 1G....83
75 Measured P-wave speed along line 4 at corner of Slab 1G....83

76 Measured P-wave speed along line 8 at corner of Slab 1G 84
77 Measured P-wave speed along line 10 at corner of Slab 1G 84
78 Measured P-wave speed along line 15 at corner of Slab 1G 85
79 Measured P-wave speed along line 16 at corner of Slab 1G 85
80 Stress/ flexural strength ratio versus HVS passes...93
81 Computed stress/strength ratio versus compressive strength of concrete using ACI equations for relating f_c, E and flexural strength...................................96
82 Relationship between compressive strength and elastic modulus 96
83 Relationship between flexural strength and compressive strength.........................97
84 Computed stress/strength ratio as a function of compressive strength using the developed relationship between f_c, E and flexural strength 98

TECHNICAL SUMMARY

Purpose of Study

Full slab replacement is a common method for repair of badly deteriorated concrete pavement slabs in Florida. This type of repair work is typically performed at night, and the repaired slabs are opened to traffic by the next morning. It is essential that this repair work be finished in a minimal amount of time. High early strength concrete is typically used in this application in order to have sufficient strength within a few hours after placement. Florida Department of Transportation (FDOT) currently specifies the slab replacement concrete to have a minimum 6-hour compressive strength of 2200 psi (15.2 MPa) and a minimum 24-hour compressive strength of 3000 psi (20.7 MPa). Due to a lack of research in this area, there are uncertainties on the optimum concrete mixtures to be used in this application. Questions arise as to what are the required curing time and the required early-age properties of the concrete for this application. This research study was conducted to answer these questions.

Scope of Study

In this study, five 9-inch thick concrete replacement slabs were constructed at the accelerated pavement testing facility at the FDOT Materials Research Park in Gainesville, Florida. The five test slabs were tested by a Heavy Vehicle Simulator (HVS), which applied a 12-kip super single wheel load in a uni-directional mode along the edge of the slab beginning at 6 hours after the placement of concrete. Two of the test slabs (1C and 2G) used a concrete with a cement content of 850 lbs per cubic yard of concrete, while the other three test slabs (1G, 2C and 2E) used a concrete with a cement content of 725 lbs per cubic yard of concrete. Both concrete mixes contained an accelerating admixture, and had a water-cement ratio of 0.30.

Summary of Findings

The results of this experiment showed that Slabs 1C and 1G performed well, while Slabs 2C, 2E and 2G cracked prematurely under the 12-kip wheel loads. The performance of the test slabs was independent of the cement content of the concrete used.

The FEACONS (Finite Element Analysis of CONcrete Slabs) computer program was used to model the response of the test slabs and to compute the stresses in the concrete slabs due to the applied loads and the temperature differentials in the concrete slabs. The good performance of Slabs 1C and 1G was attributed to the fact that the temperature-load induced stresses were much lower than the flexural strengths of the concretes. The premature cracking of Slabs 2C and 2G was attributed to the fact that the temperature-load induced stresses exceeded the estimated flexural strength of the concrete during the early age of the concretes.

The premature cracking of Slab 2E could not be explained by the computed temperature-load induced stresses. From the appearance of the deep transverse crack across the middle of the slab, it was postulated that the cracking might be caused by the locking-up of the dowel bars at both joints.

Impact echo tests were used successfully in this study to detect cracks in a concrete slab. This was manifested by a sudden drop in the apparent measured speed of P waves across the location of cracks. Cracks in the concrete slab were also successfully detected from observed changes in the measured strains from strain gages that had been installed in the concrete.

The predicted strains in the concrete slab as calculated by the FEACONS program matched fairly well with the measured strains from the installed strain gages. The measured maximum strains caused by a moving HVS wheel load were found to match fairly well with the measured maximum strains caused by a static wheel load of the same magnitude. This indicates that it is proper to model a moving load of this type by a static load as used in the FEACONS program.

Plots of stress to flexural strength ratio versus compressive strength of concrete were developed for a typical 9-inch concrete replacement slab subjected to a 12-kip wheel load and different temperature differentials in the concrete slab. When the ACI equations were used to relate the compressive strength to elastic modulus and flexural strength of concrete (as presented in Figure 76 in report), a compressive strength of 1600 psi or above at the time of the loading of the concrete slab, with a temperature differential of 10° F, would be required to ensure that the induced stress would not exceed the flexural strength. When the relationships between the compressive strength, elastic modulus and flexural strength as developed from the limited test data from this study were used (as shown in Figure 79 in report), a compressive strength of 1100 psi or above at the time of the loading of the concrete slab, with a temperature differential of 10° F, would be required to ensure that the induced stress would not exceed the flexural strength.

Conclusions

The results from this study show that the performance of a concrete replacement slab depends not just on the cement content of the concrete mix, as two concrete slabs with the same concrete mix design can have drastically different performance. The performance of a concrete replacement slab will depend on whether or not the concrete will have sufficient strength to resist the anticipated temperature-load induced stresses in the concrete slab. The strength development of a concrete depends not only on the mix design but also the condition under which the concrete is cured. The anticipated temperature-load induced stresses are a function of the slab thickness, effective modulus of subgrade reaction, modulus of the concrete, coefficient of thermal expansion of the concrete, anticipated loads and anticipated temperature differentials in the concrete slab. The anticipated stress must be lower than the anticipated flexural strength of the concrete at all times to ensure good performance.

Based on the limited test results from this study, it appears that for a 9-inch slab placed on a strong foundation (as in the case of the asphalt base used in this study) and a maximum temperature differential of +10° F in the concrete slab, a minimum required compressive strength of 1100 to1600 psi for the concrete at the time of application of traffic loads may be adequate. It may be feasible to lower the minimum required compressive strength of 2200 psi at 6 hours, as specified by the current FDOT specifications, to 1600 psi at 6 hours, subject to further testing and verification.

Recommendations

Due to the limited scope of this study and the limited amount of testing performed in this study, no recommendation for changes in FDOT specifications for concrete replacement slab is made at this point. It is recommended that further testing and research in this subject area be conducted, with particular focus on the following areas:

1. The use of maturity meter to accurately determine the strength of the in-place concrete, and to determine the time when the concrete will have sufficient strength to be open to traffic.
2. Determination of the relationships between compressive strength, flexural strength and elastic modulus of typical concretes used in replacement slabs in Florida. Accurate determination of these relationships is needed in order to determine the required strength of the concrete before the pavement slab can be open to traffic.
3. Determination of temperature distributions in typical concrete pavement slabs in Florida. This information is needed in order to accurately determine the maximum temperature-load induced stresses in the concrete slabs.

CHAPTER 1
INTRODUCTION

1.1 Background

Full slab replacement is a common method for repair of badly deteriorated concrete pavement slabs. In Florida, this type of repair work is typically performed at night, and the repaired slabs are opened to traffic by the next morning. It is essential that this repair work be finished in a minimal amount of time. High early strength concrete is typically used in this application in order to have sufficient strength within a few hours after placement.

Florida Department of Transportation (FDOT) currently specifies the slab replacement concrete to have a minimum 6-hour compressive strength of 2200 psi (15.2 MPa) and a minimum 24-hour compressive strength of 3000 psi (20.7 MPa)[1]. In the literature review, only a very few literature sources were found on comprehensive studies on slab replacement. The California Department of Transportation (Caltrans) has conducted research on the use of fast setting hydraulic cement concrete (FSHCC) in slab replacement using the HVS. The fatigue resistance of the FSHCC was found to be similar to the fatigue resistance of the normal Portland cement concrete [2]. Caltrans has developed several standard special provisions (SSP) for slab and lane/shoulder replacement. However, there is no SSP for slab replacement with dowel bars. The current specification for slab replacement with no dowel requires that the minimum modulus of rupture at opening to traffic should be 2.3 MPa (333 psi) and 4.3 MPa (623 psi) at 7 day [3].

Due to a lack of research in this area, there are uncertainties on the optimum concrete mixtures to be used in this application. Questions arise as to the required curing time and the required early-age properties of the concrete for this application. This research study was conducted to address these questions. In this study, the behavior and performance of the concrete replacement slabs under realistic Florida conditions were evaluated using full-scale testing by means of a Heavy Vehicle Simulator (HVS).

1.2 Scope of Report

This report presents all the work performed in this study, which includes construction of the test track; construction of the replacement test slabs; instrumentation of the test slabs; HVS testing; analysis of test results; and the findings and recommendations. This final report consists of the following eight chapters:

Chapter 1. Introduction and background

Chapter 2. Construction of test track

Chapter 3. Stress analysis and instrumentation of test slabs

Chapter 4. Construction of replacement test slabs

Chapter 5. Testing of the test slabs

Chapter 6. Observed performance of the test slabs

Chapter 7. Analysis of test data

Chapter 8. Summary and recommendations

CHAPTER 2
CONSTRUCTION OF TEST TRACK

2.1 Layout of Test Slabs

The concrete test track to be used for this study was constructed over the existing two-inch thick asphalt surface at the APT facility at the FDOT State Materials Research Park on September 25, 2002, by a concrete contractor with the coordination of FDOT personnel. This concrete test track consisted of two 12-ft (3.7-m) wide lanes. Each test lane consisted of three 12 ft × 16 ft (3.7 m × 4.9 m) test slabs, placed between six 12 ft × 12 ft (3.7 m × 3.7 m) confinement slabs. Figure 1 shows the layout of the concrete slabs on this test track. The thickness of the concrete slabs was 9 inches (23 cm).

2.2 Construction of Test Track

A debonding agent (a white-pigmented curing compound) was applied on the asphalt surface before placement of the concrete slab. Concrete meeting FDOT's specifications for Florida Class 1 concrete (with a minimum 28-day compressive strength of 3000 psi [21 MPa]) was used. Since the 12 ft × 16 ft (3.7 m × 4.9 m) slabs were to be removed before testing, tie bars (for tying the adjacent lanes together) were placed only in the 12 ft × 12 ft (3.7 m × 3.7 m) confinement slabs. Figure 2 shows the placement of concrete for the test track. Figure 3 shows the finished concrete test track. Samples of concrete were taken from two randomly selected trucks (trucks no. 2 and 7). The slump, air content, and temperature of the fresh concrete were measured. The water cement ratio of the concrete was estimated from the amount of water and cement used. Compressive strength tests were run on the hardened concrete at 24 hours, 7 days and 28 days. The results of these tests are displayed in Table 1.

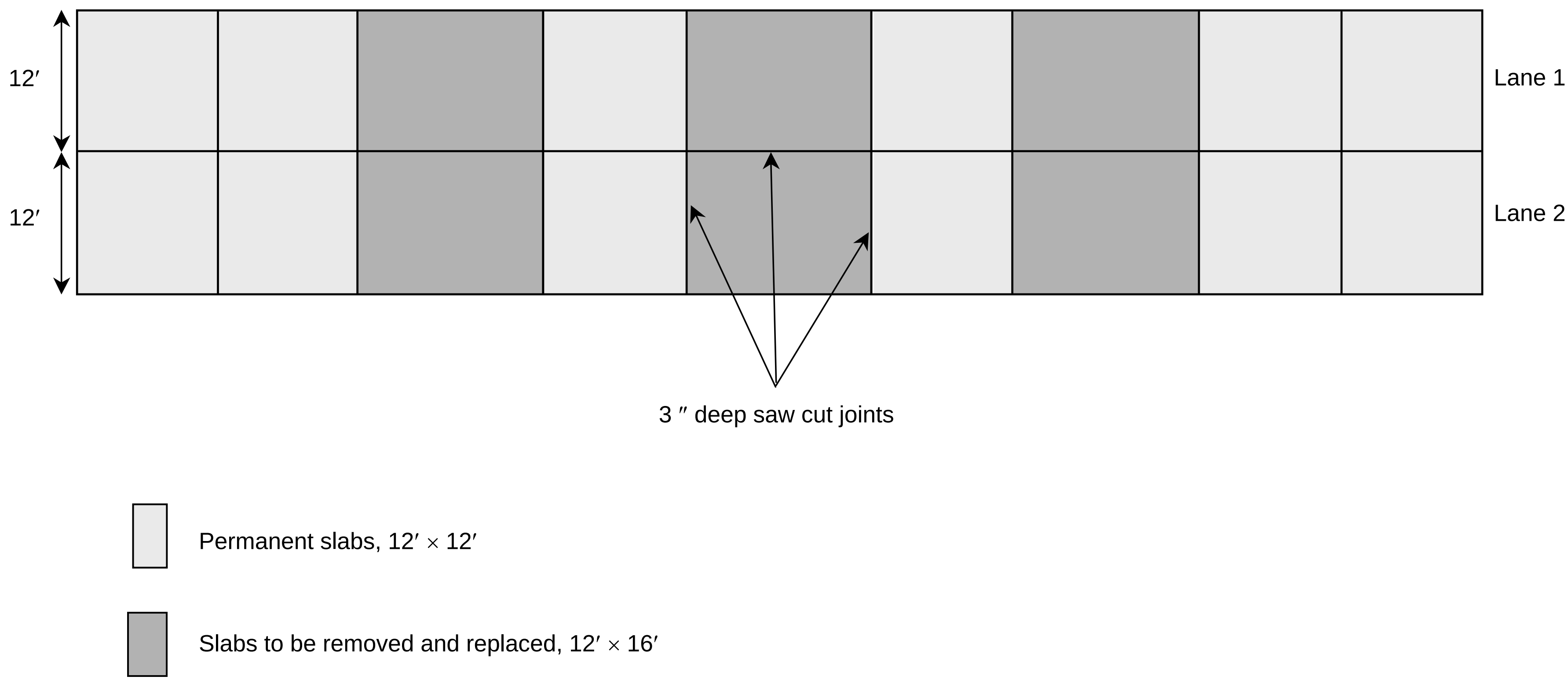

Figure 1. Layout of concrete slabs on test track

Figure 2. Placement of concrete on test track

Figure 3. Finished concrete test track

Table 1. Properties of the Concrete Used on the Initial Concrete Test Track

Truck No.	Slump (inch)	Temp. (° F)	Air (%)	W/C	Sample No.	Strength, psi		
						24 hrs	7 days	28 days
2	3.00	93° F	2.50%	0.5	1	1310	3940	5270
					2	1450	3730	5590
					Average	**1380**	**3840**	**5430**
7	3.25	90° F	3.25%	0.45	1	–	–	5040
					2	–	–	5270
					3	–	–	4980
					Average			**5100**

2.3 Sawing of Joints

After placement and finishing of the concrete on the test track, 3-in. (7.6 cm) deep saw cuts were made to form the joints for the slabs. A diamond-bladed saw was used for these cuts to ensure a smooth, straight vertical surface. Figure 4 shows a photo of this sawing operation.

Figure 4. Making a 3-inch deep saw cut at the joint

CHAPTER 3
STRESS ANALYSIS AND INSTRUMENTATION OF TEST SLABS

3.1 Stress Analysis

The FEACONS IV (Finite Element Analysis of CONcrete Slabs version IV) program was used to analyze the anticipated stresses on the test slabs when loaded by the HVS test wheel. The FEACONS program was developed at the University of Florida for the FDOT for analysis of concrete pavements subject to load and thermal effects. This program was chosen for use since both the University of Florida and FDOT have extensive experience with this program and the reliability of this program has been demonstrated in previous studies. In the FEACONS program, a concrete slab is modeled as an assemblage of rectangular plate bending elements with three degrees of freedom at each node. The three independent displacements at each node are (1) lateral deflection, w, (2) rotation about the x-axis, θ_x, and (3) rotation about the y-axis, θ_y. The corresponding forces at each node are (1) the downward force, f_w, (2) the moment in the x direction, $f_{\theta x}$, and (3) the moment in the y direction, $f_{\theta y}$.

The FEACONS program was used to analyze the stresses in the test slabs when subjected to a 12-kip (53-kN) single wheel load with a tire pressure of 120 psi (827 kPa) and a contact area of 100 in^2 (645 cm^2), and applied along the edge of the slab, which represents the most critical loading location. Analysis was done for two different load positions, namely (1) load at the corner of the slab, and (2) load at the middle of the edge, as shown in Figure 5.

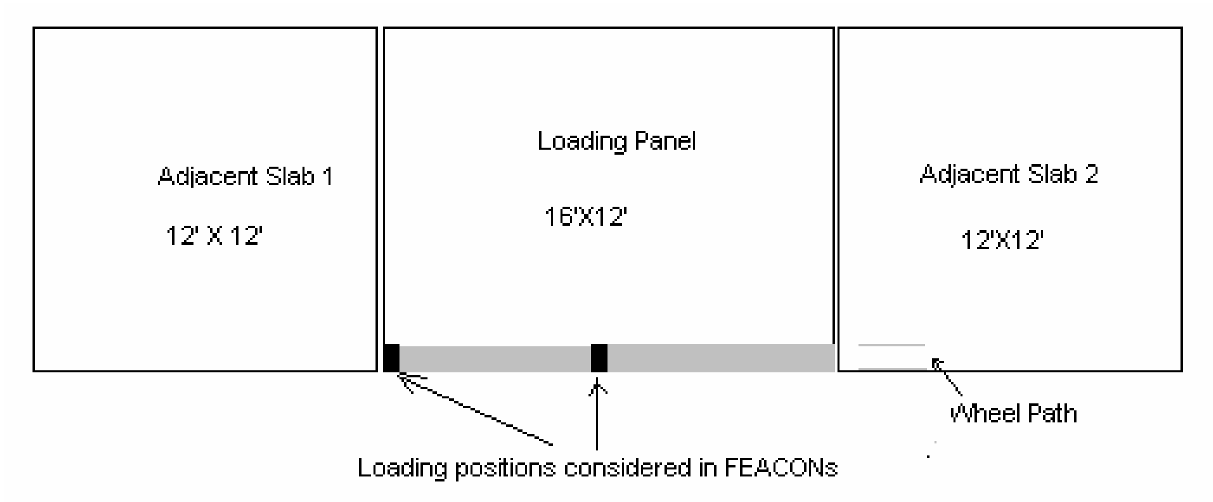

Figure 5. Loading positions used in the stress analysis

The elastic modulus of the concrete was assumed to be 5,000 ksi (34.45 GPa) and the modulus of subgrade reaction was assumed to be 0.4 kci (272 MN/m^3). The thickness of the concrete slabs was 9 inches (23 cm). Other pavement parameter inputs needed for the analysis are the joint shear stiffness (which models the shear load transfer across the joint), the joint torsional stiffness (which models the moment transfer across the joint) and the edge stiffness (which models the load transfer across the edge joint). The values for these parameters are usually determined by back-calculation from the deflection basins from NDT loads (such as FWD) applied at the joints and edges. In the absence of data for determination of these parameters, two conditions were used in the analysis. One condition was for the case of no load transfer. In this case, all the edge and joint stiffnesses were set to be zero. The other condition was for the case of good load transfer. In such a case, typical joint and edge stiffness values for good joint and edge conditions were used in the analysis. A shear stiffness of 500 ksi (3445 kPa), a torsional stiffness of 1000 ksi (6.89 MPa), and an edge stiffness of 30 ksi (207 kPa) were used for this condition.

Figure 6 shows the distribution of the maximum principal stresses at the top of the test slab caused by a 12 kip (53-kN) wheel load at the slab corner, for the condition of no load transfer at the joints and edges. Figures 7 and 8 show the distribution of the stresses in the X (longitudinal) and Y (lateral) direction, respectively, for the same loading and load transfer condition.

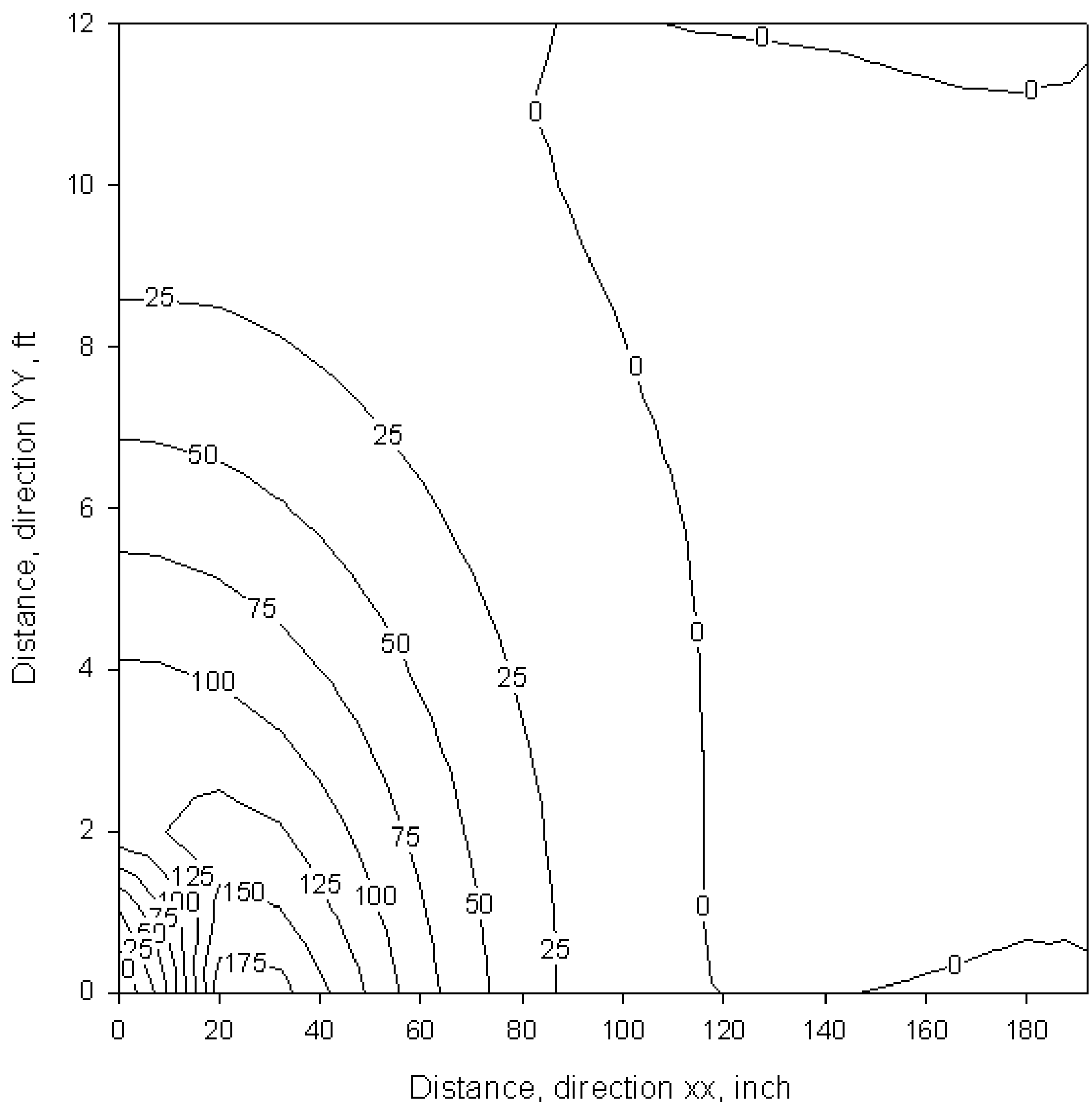

Figure 6. Distribution of maximum principal stresses due to a 12-kip load at the slab corner for the condition of no load transfer at the joints

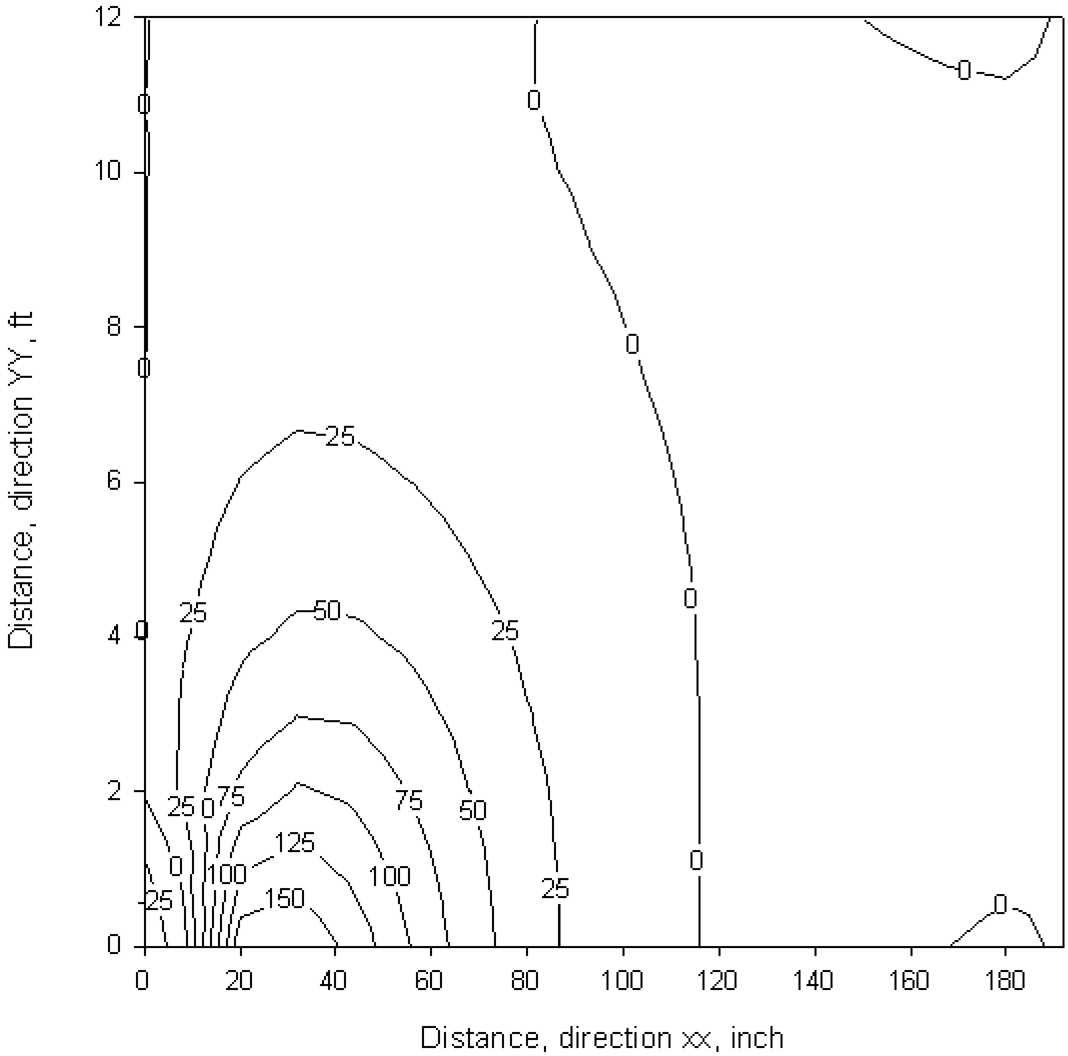

Figure 7. Distribution of stresses in the XX direction due to a 12-kip load at the slab corner for the condition of no load transfer at the joints

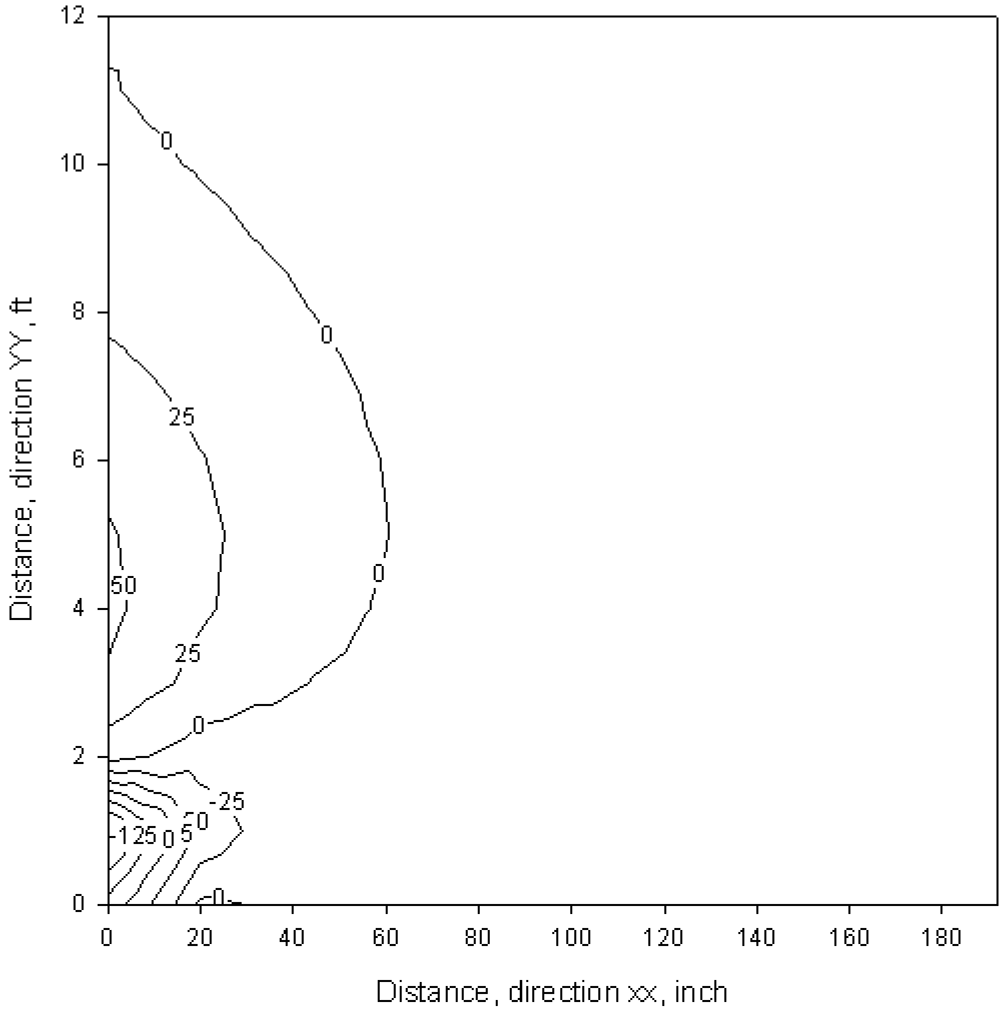

Figure 8. Distribution of stresses in the YY direction due to a 12-kip load at the slab corner for the condition of no load transfer at the joints

Figure 9 shows the distribution of the maximum principal stresses in the test slab caused by a 12-kip wheel load at the slab corner, for the condition of good load transfer at the joints and edges. Figures 10 and 11 show distribution of the stresses in the X (longitudinal) and Y (lateral) direction, respectively, for the same loading and load transfer condition.

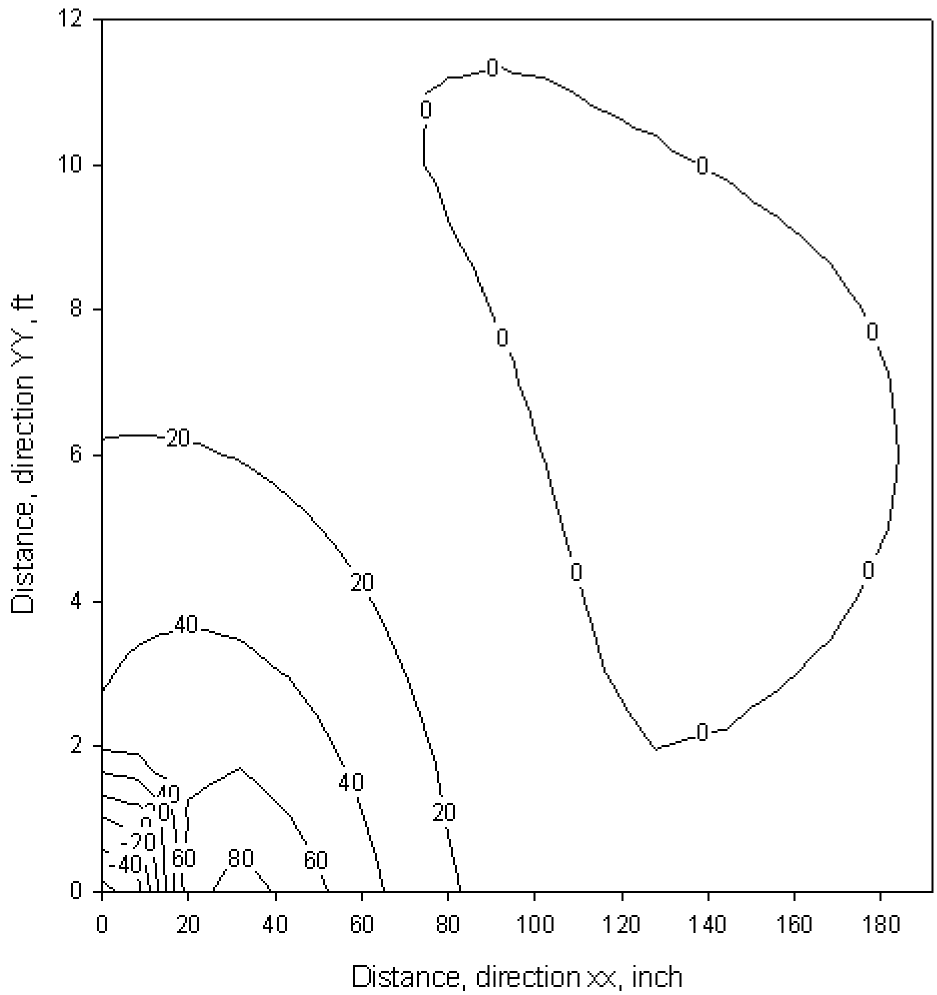

Figure 9. Distribution of maximum principal stresses due to a 12-kip load at the slab corner for the condition of good load transfer at the joints

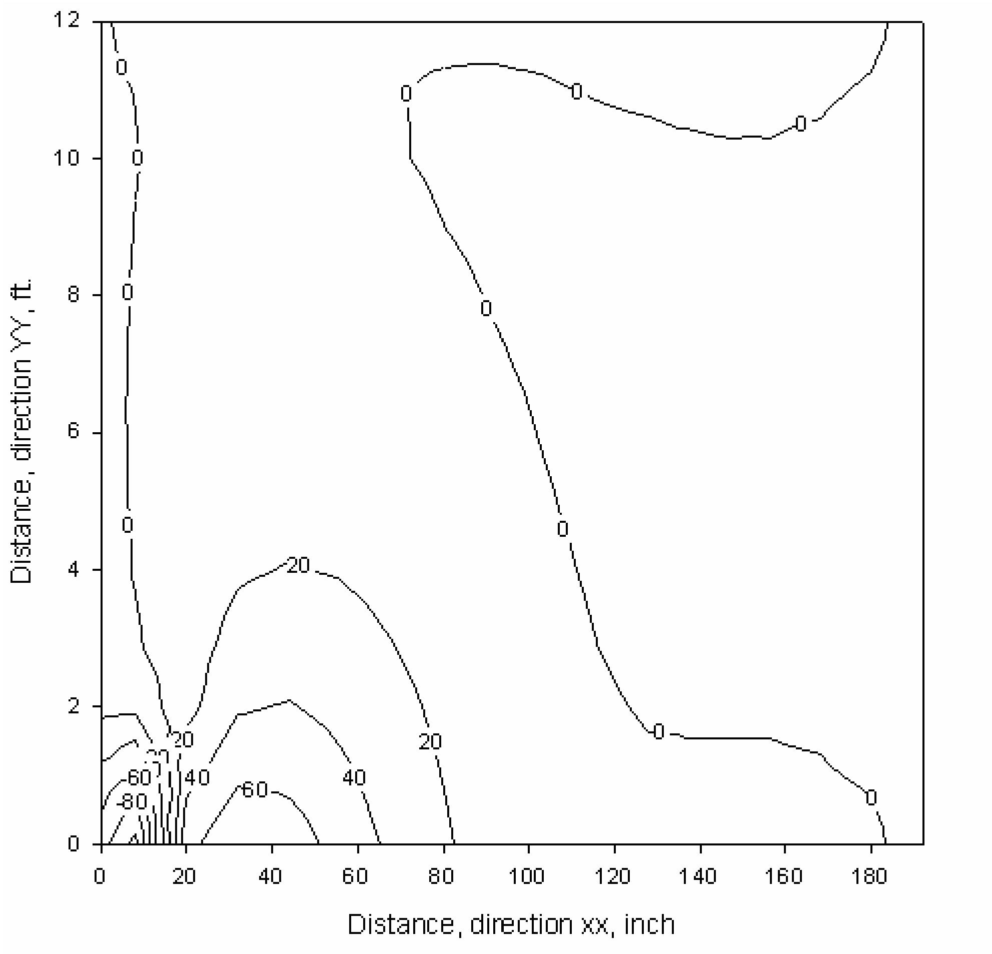

Figure 10. Distribution of stresses in the XX direction due to a 12-kip load at the slab corner for the condition of good load transfer at the joints

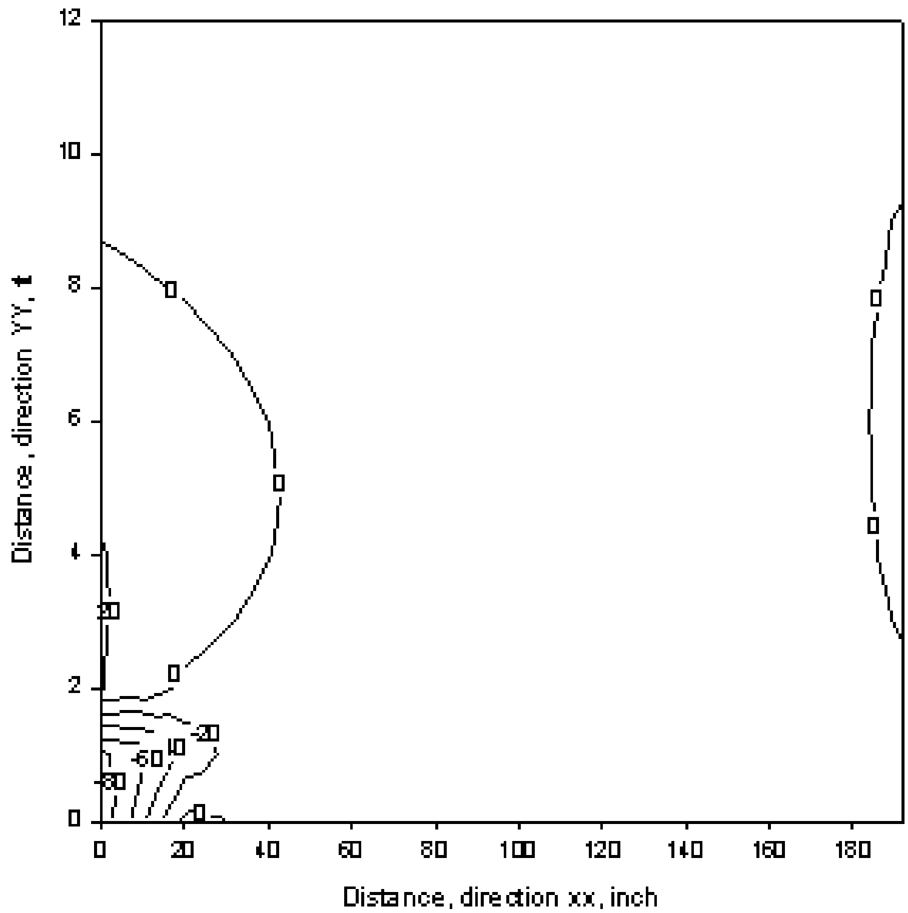

Figure 11. Distribution of stresses in the YY direction due to a 12-kip load at the slab corner for the condition of good transfer at the joints

Figure 12 shows the distribution of the maximum principal stresses on the adjacent slab caused by a 12-kip (53-kN) load at the slab corner, for the condition of good load transfer at the joints and edges. Figures 13 and 14 show the distribution of the stresses in the XX and YY directions, respectively, on the adjacent slab, for the same loading and load transfer condition.

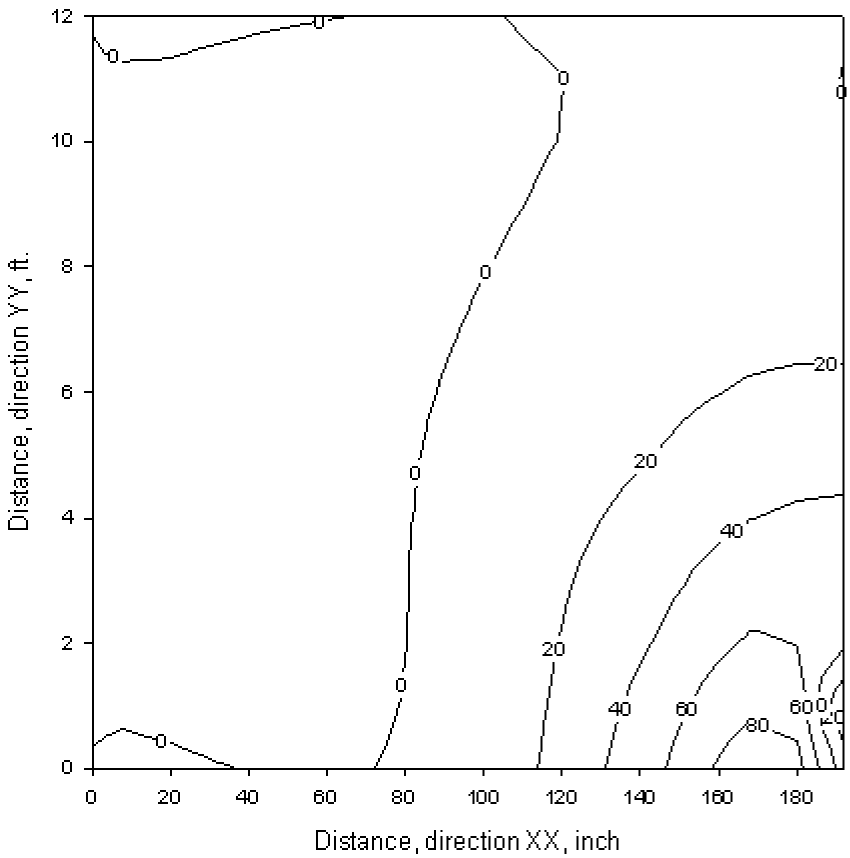

Figure 12. Distribution of maximum principal stresses on the adjacent slab due to a 12-kip load at the slab corner for the condition of good load transfer at the joints

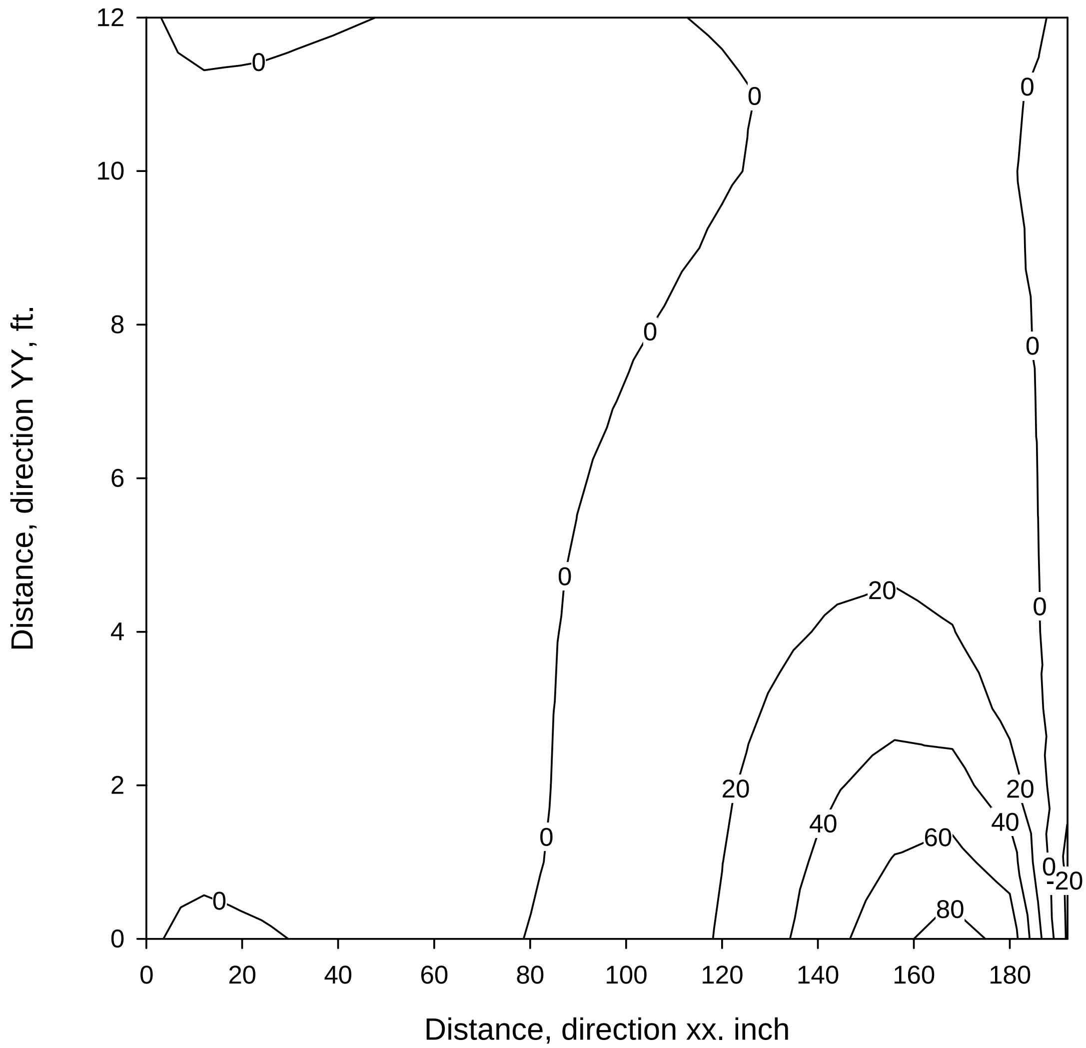

Figure 13. Distribution of stresses in the XX direction on the adjacent slab due to a 12-kip load at the slab corner for the condition of good load transfer at the joints

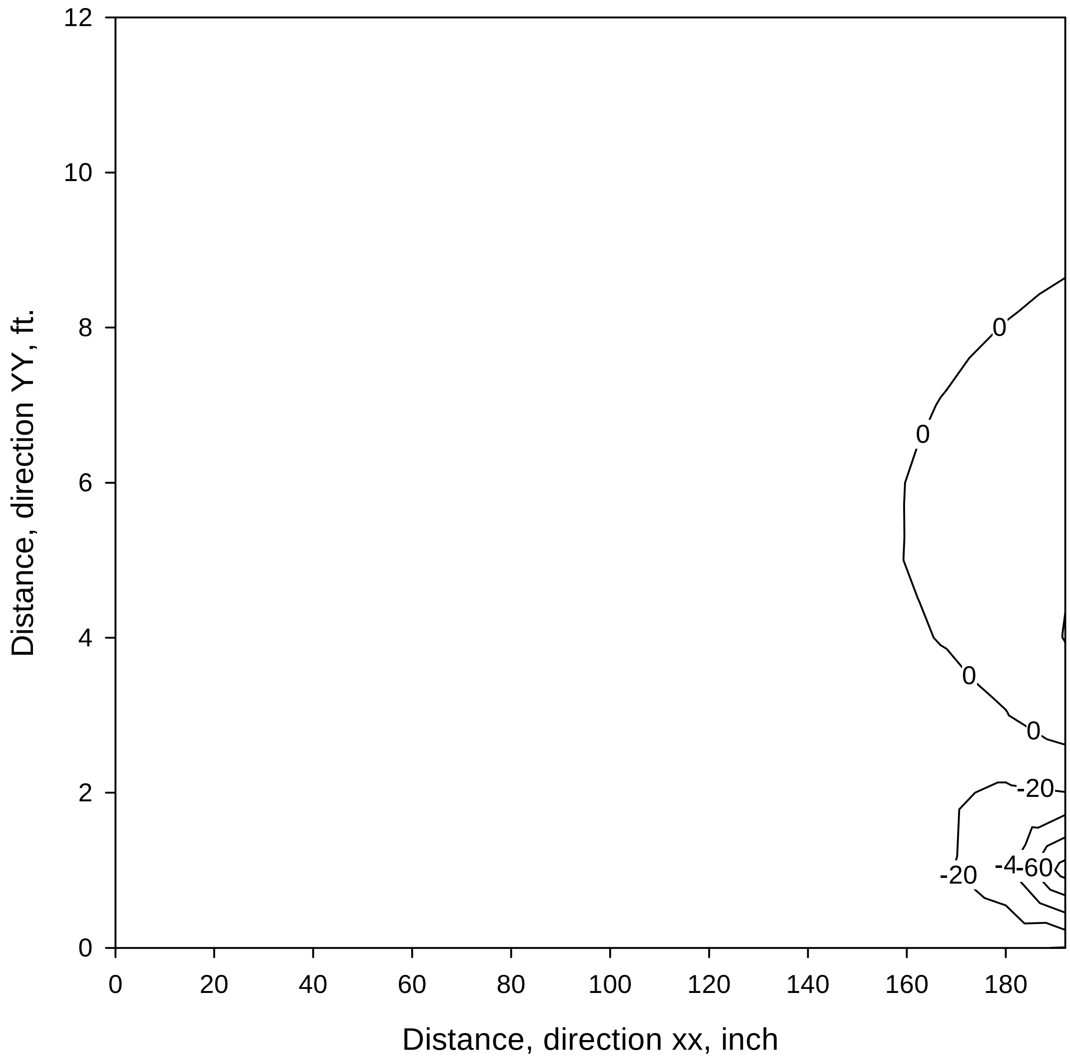

Figure 14. Distribution of stresses in the YY direction on the adjacent slab due to a 12-kip load at the slab corner for the condition of good load transfer at the joints

Figure 15 shows the distribution of the maximum principal stresses on the test slab caused by a 12-kip (53-kN) load at mid edge, for the condition of no load transfer across the joints and edges.

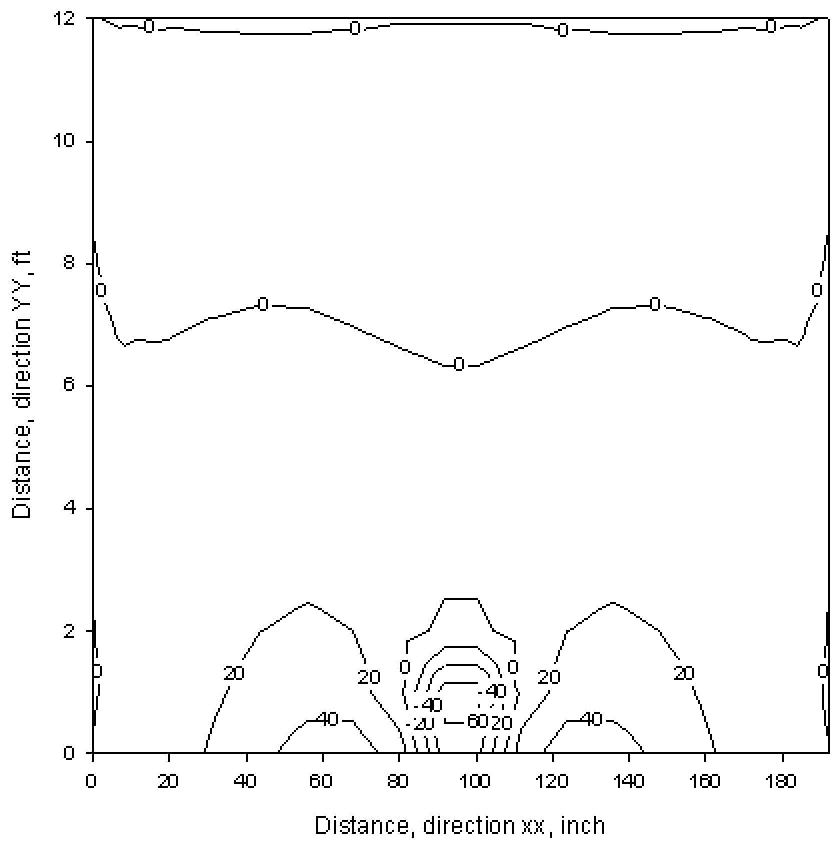

Figure 15. Distribution of maximum principal stresses due to a 12-kip load at the mid-edge for the condition of no load transfer at the joints

3.2 Instrumentation Layout

3.2.1 Wheatstone Bridge Circuits

Strain gauges were placed in the concrete test slabs to monitor the strains in them. Wheatstone half-bridge circuits were used. One strain gauge was used as an active gage to monitor the load-induced strain, while another one was used as a dummy gauge for temperature compensation. The Wheatstone half-bridge circuit used is shown in Figures 16 and 17. The active gauge with a resistance of R_A is subjected to a temperature-induced strain (y) and a load-induced strain (x) simultaneously. The dummy gauge with a resistance of R_D, is subjected only to a temperature-induced strain (y). The effect of the temperature-induced strain “(1+y)” is canceled out in this half bridge circuit, and only the load-induced strain is measured.

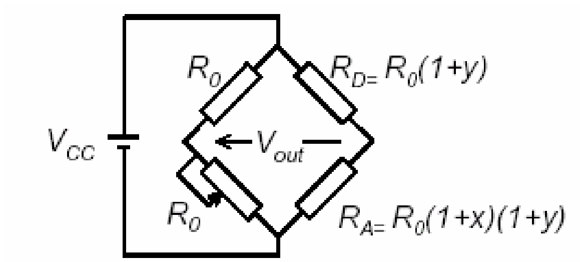

Figure 16. Strain gauge arrangements in a half bridge circuit

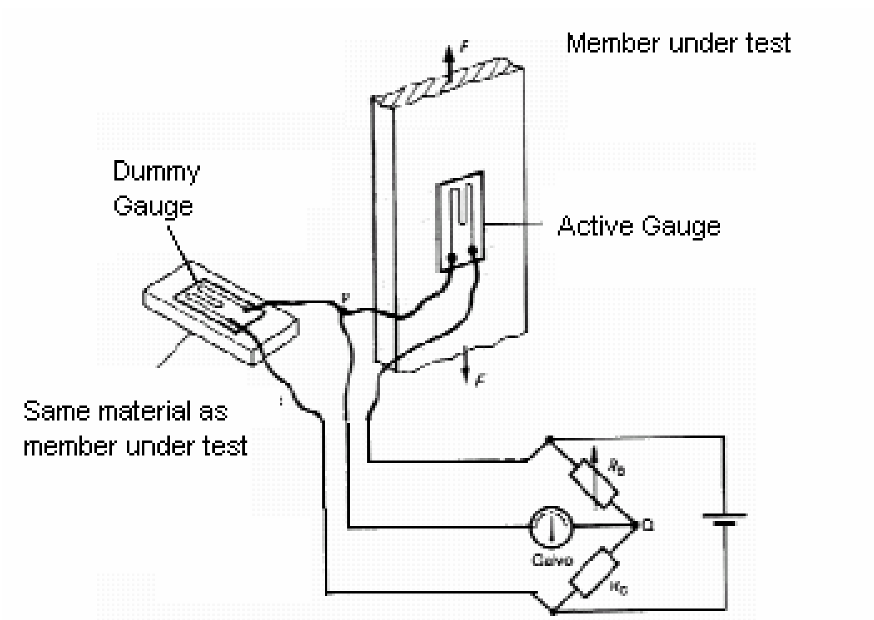

Figure 17. Connection of the active and dummy strain gauges in the half bridge circuit

3.2.2 Placement of Gauges

The locations for the strain gauges were selected based on the computed anticipated stress distribution on the test slab. Slab 1C was instrumented with seven strain gauges and two sets of thermocouples as shown in Figure 18. The dummy gauges and a set of thermocouples were placed in concrete blocks made of the same concrete mixture for temperature compensation of the strain gauges. A set of thermocouples consisted of 6 gauges (k type junctions). Five gauges were placed in the concrete at 0.5, 2.5, 4.5, 6.5, 8.5 inches from the surface and one gauge was placed in the asphalt at 1 inch below the asphalt surface. This was achieved by fixing the thermocouples to a fiberglass rod. Figure 19 shows the instrumentation setup for Test Slabs 1G, 2C, 2E and 2G. The strain gauge locations and the assigned numbers are shown in Table 2. The main difference between the second instrumentation plan and the first plan is that strain gauge number 4 in the first plan was moved to the northern end of the slab at 30 inches from the northern joint in the second plan. This strain gauge would replicate strain gauge No. 3, since both gauges were on the wheel path and 30 inches from the joint.

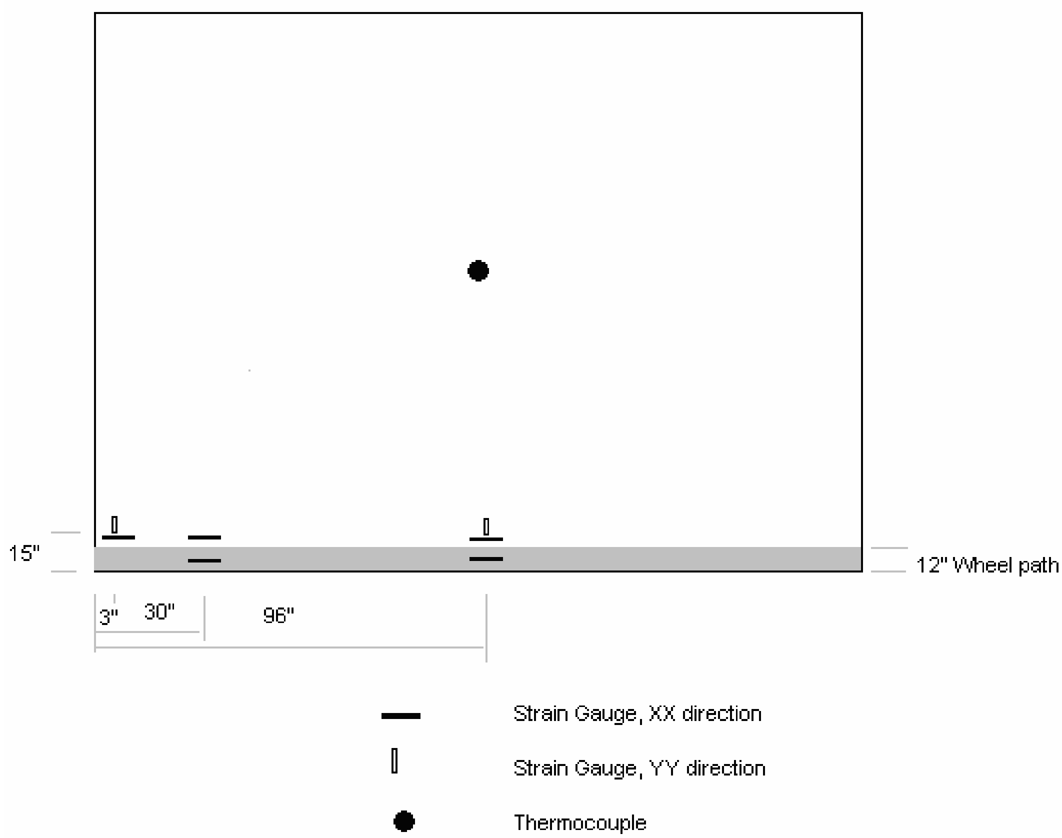

Figure 18. Instrumentation layout for Test Slab 1C

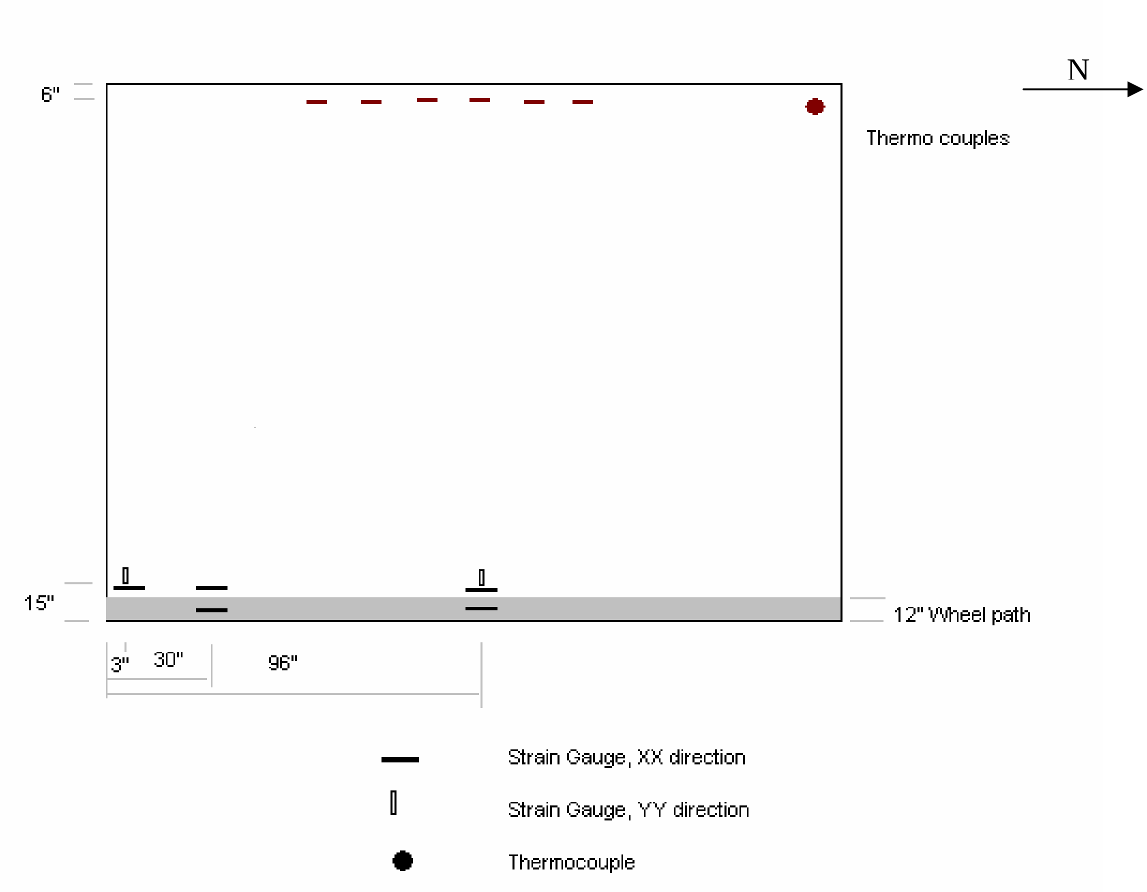

Figure 19. Instrumentation layout for Test Slabs 1G, 2C, 2E and 2G

Table 2. Strain Gauge Locations and Identification Numbers

Slab No.	Gauge No.	Direction	Location
1C	1	XX	3″ from south end, outside wheel path
	2	YY	3″ from south end, outside wheel path
	3	XX	30″ from south end, on wheel path
	4	XX	30″ from south end, outside wheel path
	5	XX	96″ from south end, on wheel path
	6	XX	96″ from south end, outside wheel path
	7	YY	96″ from south end, outside wheel path
1G, 2C, 2E, 2G	1	XX	3″ from south end, outside wheel path
	2	YY	3″ from south end, outside wheel path
	3	XX	30″ from south end, on wheel path
	4	XX	96″ from south end, on wheel path
	5	XX	96″ from south end, outside wheel path
	6	YY	96″ from south end, outside wheel path
	7	XX	30″ from north end, on wheel path

CHAPTER 4
CONSTRUCTION OF REPLACEMENT TEST SLABS

4.1 Description of Five Test Slabs

Five concrete test slabs designated as 1C, 1G, 2C, 2E and 2G were placed on the concrete test track at the APT facility at the FDOT State Materials Research Park on August 12, 2003, September 16, 2003, October 13, 2003, March 2, 2004, and March 30, 2004, respectively, by a concrete contractor with the coordination of FDOT personnel and U.F. investigators. Two different concrete mixes were used for these five test slabs with two slabs, 1C and 2G, using a concrete mix with a high cement content (850 lb/yd^3) and the other three slabs, 2C, 1G, 2E, using a concrete mix with a low cement (725 lb/yd^3). Concrete samples were obtained and test specimens were prepared for compressive strength, elastic modulus, flexural strength and shrinkage evaluation.

4.2 Removal of Existing Slabs

Slab removal for the first slab replacement test was conducted on July 17, 2003 under the supervision of FDOT personal. A 12 ft × 16 ft slab was separated into 3 ft × 4 ft pieces using a diamond bladed saw as shown in Figures 20 and 21. Each separated piece was removed using the weight lifter as shown in Figure 22. Special attention was given to protect the surrounding slabs. Steel plates were placed along the joint to protect the adjacent slab from damage as the broken pieces were removed, as shown in Figure 23. The damaged places of the asphalt base were patched using a cold asphalt mix and compacted using a vibrator as shown in Figure 24.

Figure 20. Cutting of a concrete slab (12 ft ×16 ft) into small pieces (3 ft × 4 ft)

Figure 21. Separated concrete pieces after cutting with diamond bladed saw

Figure 22. Removal of separated pieces using a lifter

Figure 23. Removal of concrete pieces adjacent to the surrounding slabs

Figure 24. Correcting the damaged portion of the asphalt base

4.3 Construction of Concrete Test Slabs

4.3.1 Dowel Bar Placement

Dowel bars were placed in drilled holes made on the adjacent slabs in one-foot intervals starting six inch from the edge. The dowel bars were fixed to the adjacent slabs using an epoxy and the open ends of the bars to be embedded in the concrete of the test slab were sprayed with a lubricant to allow movement in the longitudinal direction. Figure 25 shows the dowel bars epoxied to an adjacent slab before placement of the concrete test slab.

Figure 25. Dowel bars epoxied to an adjacent slab before placement of the test slab

4.3.2 Concrete Mix Used in the Test Slabs

Two different concrete mix designs were used in the test slab. Fresh concrete properties are shown in Table 3. The mix design details are shown in Table 4.

Table 3. Fresh Concrete Properties

Test Property	Mix 1 (Slab 1C)	Mix 2 (Slab 1G)	Mix 3 (Slab 2C)	Mix 4 (Slab 2E)	Mix 5 (Slab 2G)
Slump-Pre Accelerator	3.5″	6.75″	9.25″	8.5″	10.5″
Slump-W / Accelerator	2.5″	3.75″	10″	2.5″	7.75″
Temperature (° F)	95	89	85	87	85
Unit weight (pcf)	141.2	144.4	142.7	137.3	143.6
Air (%)	1.25	1.75	1.75	5.25	0.75
RH (%)	90	81	98	66	76

Table 4. Mix Designs of Concrete Used in Test Slabs

Slab No.	Material	Target (wt./yd^3)	Actual (wt./yd^3)	Moisture (%)	Aggregate Source
1C Mix 1	Cement	850 lb	844 lb		
	D57 Stone	1785 lb	1775 lb	2.0	Pit # 08-012
	DOT Sand	1114 lb	1111 lb	6.1	Pit # 76-349
	Air entrain. admixture (Darex)		927 oz		
	Superplasticizer (Adva-540)		51 oz		
	Accelerator (Daraccel)		385 oz		
	Water		20.6 gal		
	W/C	0.30			
1G Mix 2	Cement	725 lb	720 lb		
	D57 Stone	1771 lb	1754 lb	1.2	Pit # 08-012
	DOT Sand	1173 lb	1169 lb	4.2	Pit # 76-349
	Superplasticizer (Adva-540)		48.5 oz		
	Accelerator (Daraccel)		385 oz		
	Water		19 gal		
	W/C	0.30			
2C Mix 3	Cement	725 lb	718 lb		
	D57 Stone	1775 lb	1760 lb	1.4	Pit # 08-012
	DOT Sand	1173 lb	1166 lb	6.1	Pit # 76-349
	Superplasticizer (Adva-540)		51 oz		
	Accelerator (Daraccel)		385 oz		
	Water		18.6 gal		
	W/C	0.30			
2E Mix 4	Cement	725 lb	725 lb		
	D57 Stone	1775 lb	17780 lb	1.6	Pit # 08-012
	DOT Sand	1173 lb	1175 lb	4.4	Pit # 76-349
	Superplasticizer (Adva-540)		48 oz		
	Accelerator (Daraccel)		384 oz		
	Water		21.1 gal		
	W/C	0.30			
2G Mix 5	Cement	850	852 lb		
	D57 Stone	1785 lb	1780 lb	1.9	Pit # 08-012
	DOT Sand	1114 lb	1048 lb		Pit # 76-349
	Superplasticizer (Adva-540)		55 oz		
	Accelerator (Daraccel)		384 oz		
	Water		24.3 gal		
	W/C	0.30			

4.3.3 Concrete Placement

Samples of concrete were taken from the concrete truck before the accelerating admixture was added for conductance of the slump, unit weight and air content tests. Samples of concrete were again taken after the addition of the accelerating admixture for slump test and for fabrication of test specimens for compressive strength, elastic modulus and shrinkage evaluation. The compressive strength, elastic modulus, flexural strength data for the five mixes placed are shown in Table 5 and the compressive strength data are plotted in Figure 26.

The first test slab (1C) to be replaced was confined by three adjacent slabs and had one free edge. Figure 27 shows the formwork for the free edge of Slab 1C. The other four test slabs (1G, 2C, 2E & 2G) to be placed were free at both longitudinal edges. So formwork was used for on both edges of these test slabs.

A debonding agent (a white-pigmented curing compound) was applied on the asphalt surface before placement of the concrete on the asphalt.

PVC pipes were placed around the strain gauges to protect them from concrete handling instruments during the placement of concrete. The concrete was placed manually around the strain gauges inside the PVC pipes. Figure 28 shows a picture of how the concrete was placed in two PVC cylinders where the strain gauges were held in position. After the concrete was placed to the same thickness on both the inside and outside of the PVC pipe, the PVC pipe was then pulled out manually. Figure 29 shows the placement of concrete for a test slab. The concrete was placed manually in the wooden blocks where the dummy strain gauges were located. Figure 30 shows the placement of concrete around the dummy gauges. Vibrators were used to consolidate the concrete in the test slab and the dummy gauge blocks.

Table 5. Compressive Strength, Elastic Modulus and Flexural Strength Data

Time	Mix 1 (Slab 1C)			Mix 2 (Slab 1G)			Mix 3 (Slab 2C)			Mix 4 (Slab 2E)			Mix 5 (Slab 2G)		
	Comp.[1] $\times 10^3$ psi	E[2]* $\times 10^3$ psi	R[3]* $\times 10^3$ psi	Comp.[1] $\times 10^3$ psi	E[2] $\times 10^3$ psi	R[3] $\times 10^3$ psi	Comp.[1] $\times 10^3$ psi	E[2] $\times 10^3$ psi	R[3] $\times 10^3$ psi	Comp.[1] $\times 10^3$ psi	E[2] $\times 10^3$ psi	R[3] $\times 10^3$ psi	Comp.[1] $\times 10^3$ psi	E[2] $\times 10^3$ psi	R[3] $\times 10^3$ psi
4 hr	980	1267	235	710	–		480	1388.5	164	630	1730		670	1569	
6 hr	1700	1577	309	1100	–	274	860	–	220	1250	–	260	1210	1775	250
8 hr	2260	1854	357	1520	–	292	1170	2629.5	257	1560	2620		1830	2514	
1 day	4750	2749	517	3340	3302.5	433	2770	3223.0	395	3440	2920	525	3850	2789	530
3 days	5280	3300	545	4803	–	520	3883	–	467	4340	–		4650	2953	
7 days	5960	3540	579	5540		558	5020		531	4980	3300	650	5530		600
9 days		3579	582		–	563		3826.0			–				
28 days	6653	3950	612	6520	3952.0	606	6510	–	605	5810	–	760	6400	–	760

[1] Compressive strength
[2] Elastic modulus
[3] Flexural strength
* Estimated data

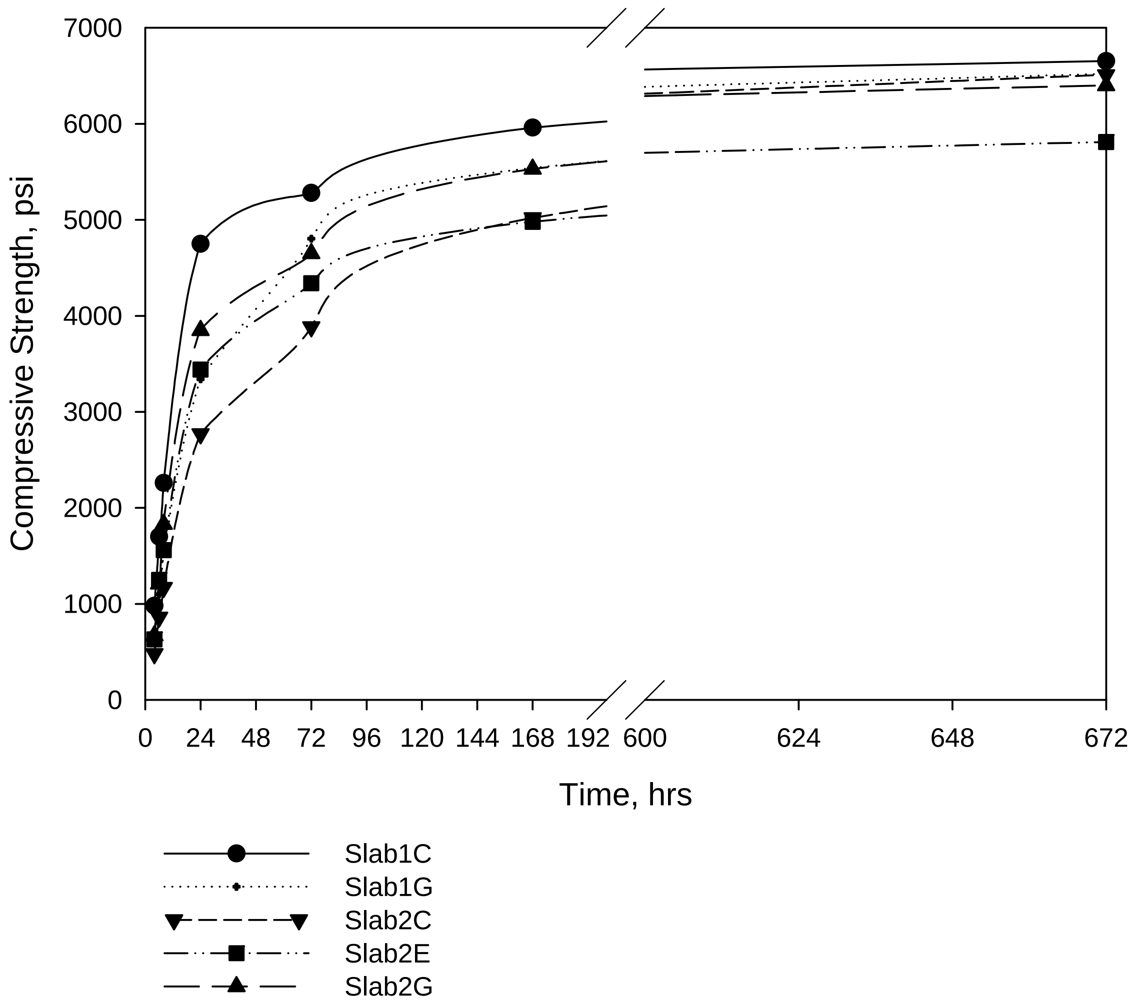

Figure 26. Comparison of compressive strength of the concrete mixes used

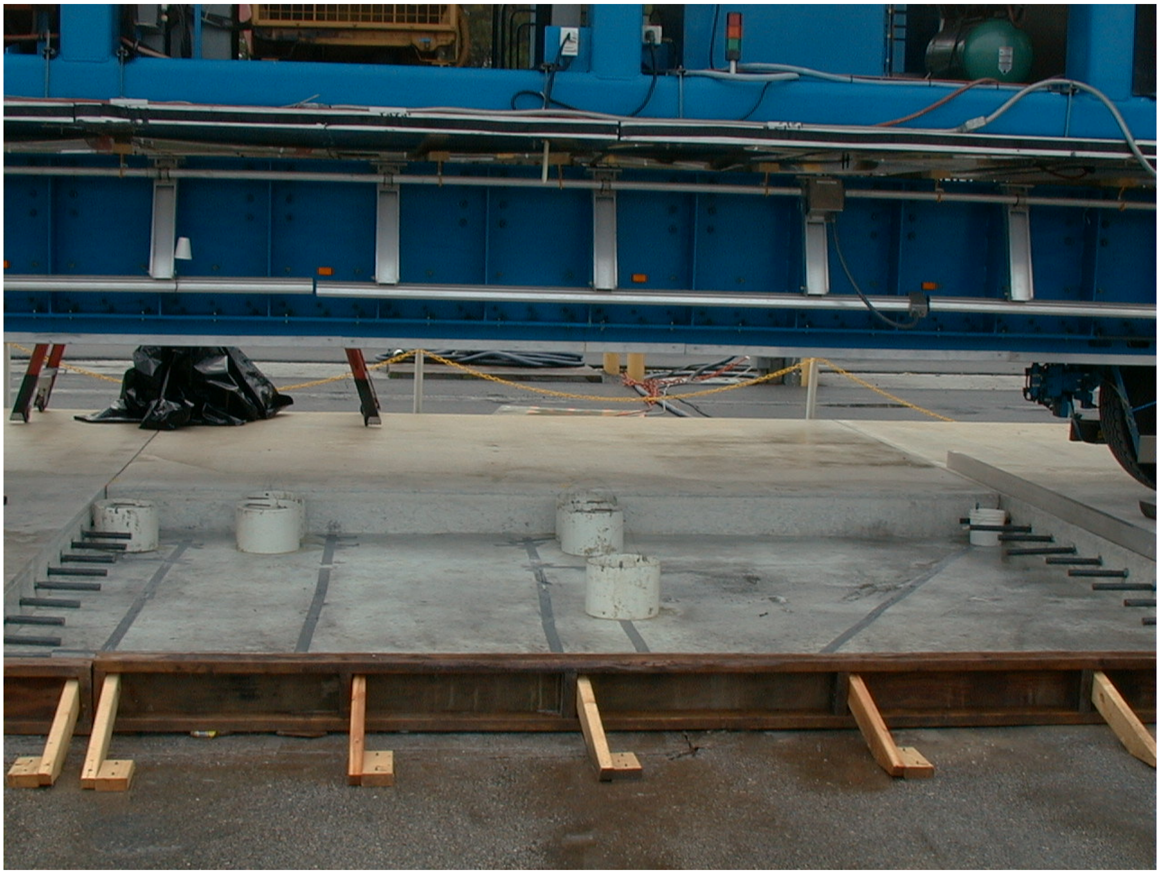

Figure 27. Formwork for the free edge of Test Slab 1C

Figure 28. Placing concrete around strain gauges

Figure 29. Placement of concrete for a test slab

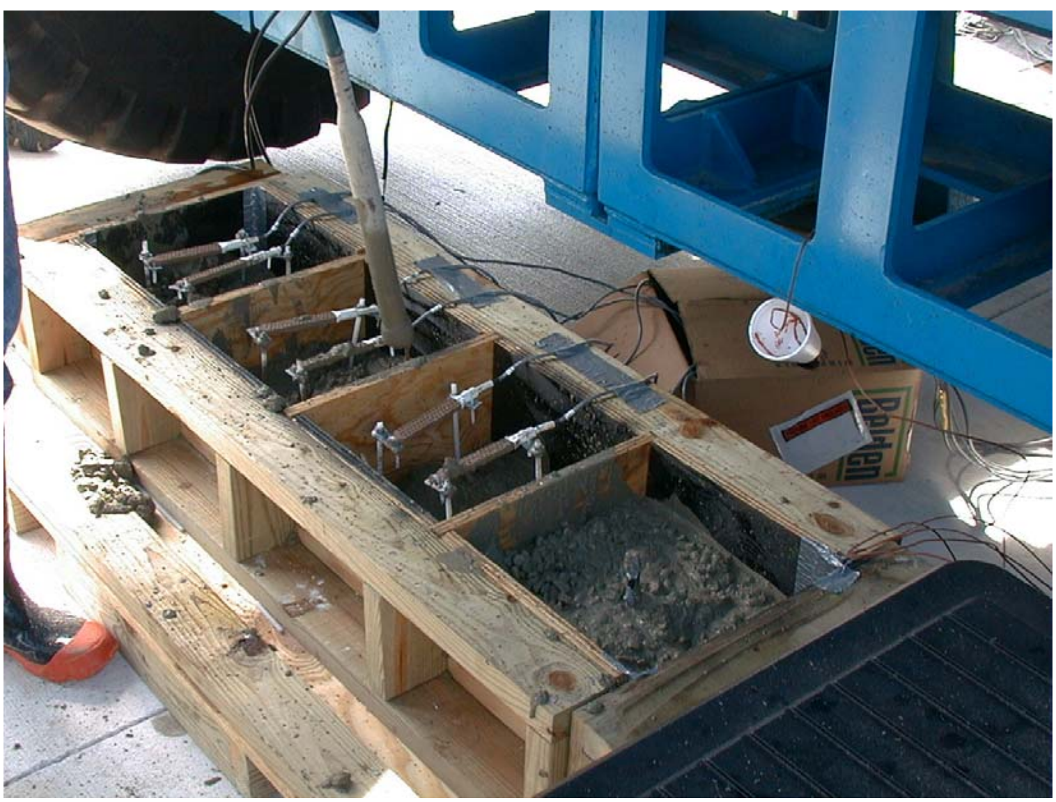

Figure 30. Placement of concrete around dummy gauges in wooden blocks

4.3.4 Concrete Finishing and Sawing of Joints

A vibrating leveling bar was used to level off the concrete. Figure 31 shows the leveling of the concrete surface of the test slab. The concrete surface was finished with additional hand troweling. A broom was passed over the concrete surface to produce a rough surface texture before it hardened. After placement and finishing of the concrete, 3-in. (7.6 cm) deep saw cuts were made to form the joints for the slabs. Figure 32 shows a picture of this sawing operation.

Figure 31. Leveling of concrete surface

Figure 32. Making a 3-inch deep saw cut at the joint

CHAPTER 5
TESTING OF THE TEST SLABS

5.1 HVS Loading

5.1.1 Slab 1C

HVS loading was originally planned to start at 6 hours after the start of the placement of the concrete. However, due to mechanical problem with the HVS, loading was not started until 8 hours after the start of concrete placement for Test Slab 1C. The schedule for testing and data collection for Test Slab 1C is shown in Table 6. HVS loading using a12-kip (53 kN) super single wheel was applied along the edge of the slab for 7 days with a total load repetitions of 86,000. After stopping for one day for HVS maintenance, the HVS load was then raised to 15 kips (67 kN) and applied for 5 more days with an additional 59,000 load repetitions. The HVS load was then raised to 18 kips (80 kN) and applied for 2 more days with an additional 11,300 load repetitions. Strain gauge readings due to static loads were taken for two loading positions, namely corner and mid edge.

5.1.2 Slab 1G

The schedule for testing and data collection for Test Slab 1G is shown in Table 7. HVS loading was started at 6 hours after the start of the placement of the concrete. HVS loading using a12-kip (53 kN) super single wheel was applied along the free edge of the slab for 9 days with a total load repetitions of 107,152. The HVS load was then raised to 15 kips (67 kN) and applied for 5 more days with an additional 55,067 load repetitions.

Table 6. Schedule of Testing and Data Collection for Test Slab 1C

Order of Testing	Date	Time Collected	Load	Remarks / # HVS Passes
Initial Strain Readings	8/12/2003	10:10 AM	–	
Curing Strains (1st 6 hr)	8/12/2003	11:20 AM	–	
Static Strain #1 (Corner)	8/12/2003	6:43 PM	12 kips	Strain reading at 6 hours after mixing of concrete was missed. Testing time was moved from originally scheduled 4:50 to 6:43 PM due to mechanical problems
Static Strain #2 (Corner)	8/12/2003	6:47 PM	"	
Static Strain # 3 (Center)	8/12/2003	6:50 PM	"	
Initial Dynamic Load	8/12/2003	6:53 PM	"	
Dynamic Strain 9 hr	8/12/2003	7:48 PM	"	
Static Strain #4 (Corner) 9 hr	8/12/2003	7:54 PM	"	
Static Strain # 5 (Center) 9 hr	8/12/2003	7:56 PM	"	
Dynamic Strain 10.5 hr	8/12/2003	9:14 PM	"	
Dynamic Strain 11 hr	8/12/2003	9:50 PM	"	
Dynamic Strain 12 hr	8/12/2003	10:48 PM	"	
Dynamic Strain 13 hr	8/12/2003	11:46 PM	"	
Static Strain # 5 (Corner) 13 hr	8/12/2003	11:52 PM	"	
Static Strain # 6 (Center) 13 hr	8/13/2003	11:55 PM	"	
Dynamic Strain 15 hr	8/13/2003	1:45 AM	"	
Static Strain Day 1 (Corner)	8/13/2003	9:28 AM	"	5311, 7:35 AM 8/13/03
Static Strain Day 1 (Center)	8/13/2003	9:35 AM	"	
Dynamic Strain Day 1	8/13/2003	10:51AM	"	
Static Strain Day 2 (Corner)	8/14/2003	8:52 AM	"	16950, 7:24 AM 8/14/03
Static Strain Day 2 (Center)	8/14/2003	8:56 AM	"	
Dynamic Strain Day 2	8/14/2003	10:50 AM	"	
Static Strain Day 3 (Corner)	8/15/2003	10:17 AM	"	29090, 7:20 AM 8/15/03
Static Strain Day 3 (Center)	8/15/2003	10:19 AM	"	
Dynamic Strain Day 3	8/15/2003	11:17 AM	"	
Static Strain Day 4 (Corner)	8/16/2003	8:23 AM	"	40044, 9:03 AM 8/16/03
Static Strain Day 4 (Center)	8/16/2003	8:27 AM	"	
Dynamic Strain Day 4	8/16/2003	8:46 AM	"	
Static Strain Day 5 (Corner)	8/17/2003	8:21 AM	"	50900, 7:33 AM 8/17/03

Table 6, continued

Order of Testing	Date	Time Collected	Load	Remarks / # HVS Passes
Static Strain Day 5 (Center)	8/17/2003	8:26 AM	"	
Dynamic Strain Day 5	8/17/2003	8:36 AM	"	
Static Strain Day 6 (Corner)	8/18/2003	8:52 AM	"	62540, 7:23 AM 8/18/03
Static Strain Day 6 (Center)	8/18/2003	8:55 AM	"	
Dynamic Strain Day 6	8/18/2003	10:13 AM	"	
Static Strain Day 7 (Corner)	8/19/2003	8:31 AM	"	74680, 7:01 8/19/03
Static Strain Day 7(Center)	8/19/2003	8:35 AM	"	
Dynamic Strain Day 7	8/19/2003	10:54 AM	"	
HVS Maintenance (Day 8)	8/20/2003		New Load	Electrical problems resulted in shutdown
Static Strain Day 9 (Corner)	8/21/2003	8:40 AM	15 kips	86001, 7:31 AM 8/19/03
Static Strain Day 9 (Center)	8/21/2003	8:46 AM	"	
Dynamic Strain Day 9	8/21/2003	10:52 AM	"	
Dynamic Strain Day 10	8/22/2003	10:03 AM	"	98440, 7:22 AM 8/22/03
Static Strain Day 10 (Corner)	8/22/2003	10:10 AM	"	
Static Strain Day 10(Center)	8/22/2003	10:13 AM	"	
Static Strain Day 11 (Corner)	8/23/2003	9:17 AM	"	110609, 9:08 AM 8/23/03
Static Strain Day 11 (Center)	8/23/2003	9:21 AM	"	
Dynamic Strain Day 11	8/23/2003	9:26 AM	"	
Dynamic Strain Day 12	8/24/2003	8:43 AM	"	122371, 9:00 AM 8/24/03
Static Strain Day 12 (Corner)	8/24/2003	8:49 AM	"	
Static Strain Day 12(Center)	8/24/2003	8:54 AM	"	
Static Strain Day 13 (Corner)	8/25/2003	8:55 AM	"	134088, 7:15 AM 8/25/03
Static Strain Day 13(Center)	8/25/2003	8:58 AM	"	
Dynamic Strain Day 13	8/25/2003	10:51 AM	"	
Load changes	8/25/2003	11:00 AM	18 kips	Pressure of super single tire adjusted to New Load
Static Strain Day 14 (Corner)	8/26/2003	8:50 AM	"	145000, 7:23 AM 8/26/03
Static Strain Day 14 (Center)	8/26/2003	8:56 AM	"	
Dynamic Strain Day 14	8/26/2003	10:51 AM	"	
Dynamic Strain Day 15	8/27/2003	6:07 AM	"	156300, 6:54 AM 8/27/03
Static Strains Day 15 (Corner)	8/27/2003	6:10 AM	"	
Static Strains Day 15 (Center)	8/27/2003	6:19 AM	"	Cracks detected on concrete slab on wheel path

Table 7. Schedule of Testing and Data Collection for Test Slab 1G

Order of Testing	Date	Time Collected	Load	# HVS Passes / Remarks
Curing Strain_1	9/16/2003	9:48:16 AM	No Load	
Curing Strain_2	9/16/2003	9:55:45 AM	"	
Static Strain_6hrs_Pt 1	9/16/2003	3:02:07 PM	12 kips	
Static Strain_6hrs_Pt 2	9/16/2003	3:04:23 PM	"	
Static Strain_6 hrs_Pt 3	9/16/2003	3:06:52 PM	"	
Dynamic Strain_6 hrs	9/16/2003	3:11:35 PM	"	
Dynamic Strain_6hrs	9/16/2003	3:13:39 PM	"	
Dynamic Strain_12hrs	9/16/2003	9:10:49 PM	"	
Static Strain_12hrs_Pt 1	9/16/2003	9:15:56 PM	"	
Static Strain_12hrs_Pt 2	9/16/2003	9:21:44 PM	"	
Static Strain_12hrs_Pt 3	9/16/2003	9:25:45 PM	"	
Dynamic Strain_24hrs	9/17/2003	9:00:37 AM	"	
Static Strain_24hrs_Pt 1	9/17/2003	9:12:03 AM	"	9134 @ 9:13 AM 9/17/03
Static Strain_24hrs_Pt 2	9/17/2003	9:15:18 AM	"	
Static Strain_24hrs_Pt 3	9/17/2003	9:17:58 AM	"	
Static Strain_Day 3_Pt 1	9/19/2003	9:09:13 AM	"	
Static Strain_Day 3_Pt 2	9/19/2003	9:12:58 AM	"	
Static Strain_Day 3 _Pt 3	9/19/2003	9:16:33 AM	"	
Static Strain Day 3_ Pt 4	9/19/2003	9:19:29 AM	"	4th point added for static strain data collection
Dynamic Strain_Day 3	9/19/2003	9:23:26 AM	"	33221 @ 9:46 AM 9/19/03
Dynamic Strain_Day 4	9/20/2003	9:01:56 AM	"	
Static Strain_Day 4_Pt 1	9/20/2003	9:05:31 AM	"	
Static Strain_Day 4_Pt 4	9/20/2003	9:09:44 AM	"	
Static Strain_Day 4_Pt 2	9/20/2003	9:15:53 AM	"	
Static Strain_Day 4_Pt 3	9/20/2003	9:19:16 AM	"	44987 @ 9:28 AM 9/20/03
Dynamic Strain_Day 5	9/21/2003	8:48:06 AM	"	
Static Strain_Day 5_Pt 1	9/21/2003	8:56:01 AM	"	
Static Strain_Day 5_Pt 4	9/21/2003	9:01:16 AM	"	
Static Strain_Day 5_Pt 2	9/21/2003	9:04:17 AM	"	
Static Strain_Day 5_Pt 3	9/21/2003	9:07:06 AM	"	57314 @9:15 AM 9/21/03
Dynamic Strain_Day 6	9/22/2003	8:54:05 AM	"	69942 @ 9:01 AM 9/22/03
Static Strain_Day 6_Pt 1	9/22/2003	9:05:54 AM	"	
Static Strain_Day 6_Pt 2	9/22/2003	9:09:24 AM	"	
Static Strain_Day 6_Pt 3	9/22/2003	9:18:15 AM	"	
Static Strain_Day 6_Pt 4	9/22/2003	9:21:06 AM	"	
Dynamic Strain_Day 7	9/23/2003	8:52:38 AM	"	82331 @ 9:01 AM 9/23/03
Static Strain_Day 7_Pt 1	9/23/2003	9:07:57 AM	"	
Static Strain_Day 7_Pt 2	9/23/2003	9:10:26 AM	"	
Static Strain_Day 7_Pt 3	9/23/2003	9:14:16 AM	"	
Static Strain_Day 7_Pt 4	9/23/2003	9:19:31 AM	"	

Table 7, continued

Order of Testing	Date	Time Collected	Load	# HVS Passes / Remarks
Dynamic Strain_Day 8	9/24/2003	9:33:20 AM	"	95187 @ 9:37 AM 9/24/03
Static Strain_Day 8 _Pt 1	9/24/2003	9:39:18 AM	"	
Static Strain_Day 8_Pt 2	9/24/2003	9:46:12 AM	"	
Static Strain_Day 8_Pt 3	9/24/2003	9:50:08 AM	"	
Static Strain_Day 8_Pt 4	9/24/2003	9:53:31 AM	"	
Dynamic Strain_Day 9	9/25/2003	8:41:22 AM	"	107152 @ 9:00 AM 9/25/03
Static Strain_Day 9_Pt 1	9/25/2003	9:07:04 AM	"	
Static Strain_Day 9_Pt 2	9/25/2003	9:09:59 AM	"	
Static Strain_Day 9_Pt 3	9/25/2003	9:13:31 AM	"	
Static Strain_Day 9_Pt 4	9/25/2003	9:17:27 AM	"	
Dynamic Strain_Day 9_15 kips	9/25/2003	10:50:47 AM	"	
Dynamic Strain_Day 10_15 kips	9/26/2003	9:02:21 AM	"	115996 @ 9:04 AM 9/26/03
Static Strain_Day 10_12 kips_Pt 1	9/26/2003	9:09:27 AM	"	
Static Strain_Day 10_12 kips_Pt 2	9/26/2003	9:11:26 AM	"	
Static Strain_Day 10_12 kips_Pt 3	9/26/2003	9:14:14 AM	"	
Static Strain_Day 10_12 kips_Pt 4	9/26/2003	9:15:55 AM	"	
Static Strain_Day 10_15 kips_Pt 1	9/26/2003	10:30:46 AM	15 kips	
Static Strain_Day 10_15 kips_Pt 1	9/26/2003	10:33:10 AM	"	
Static Strain_Day 10_15 kips_Pt 2	9/26/2003	10:36:49 AM	"	
Static Strain_Day 10_15 kips_Pt 3	9/26/2003	10:40:27 AM	"	
Static Strain_Day 10_15 kips_Pt 4	9/26/2003	10:45:14 AM	"	
Dynamic Strain_Day 11	9/27/2003	9:20:15 AM	"	127616 @ 10:00 AM 9/27/03
Static Strain_Day 11_Pt 1	9/27/2003	9:30:30 AM	"	
Static Strain_Day 11_Pt 2	9/27/2003	9:46:08 AM	"	
Static Strain_Day 11_Pt 3	9/27/2003	9:50:07 AM	"	
Static Strain_Day 11_Pt 4	9/27/2003	9:52:44 AM	"	Cracks detected on Strain Gage position # 3
Dynamic Strain_Day 12	9/28/2003	8:59:08 AM	"	139128 @ 9:20 AM 9/28/03
Static Strain_Day 12_Pt 1	9/28/2003	9:03:17 AM	"	
Static Strain_Day 12_Pt 4	9/28/2003	9:06:30 AM	"	
Static Strain_Day 12_Pt 2	9/28/2003	9:12:58 AM	"	
Static Strain_Day 12_Pt 3	9/28/2003	9:16:06 AM	"	
Dynamic Strain _Day 13	9/29/2003	8:38:39 AM	"	150160 @ 9:01 AM 9/29/03
Static Strain_Day 13_Pt 1	9/29/2003	9:05:30 AM	"	
Static Strain_Day 13_Pt 2	9/29/2003	9:09:31 AM	"	
Static Strain_Day 13_Pt 3	9/29/2003	9:13:23 AM	"	
Static Strain_Day 13_Pt 4	9/29/2003	9:16:25 AM	"	
Dynamic Strain_Day 14_15 kips	9/30/2003	8:49:43 AM	"	162219 @ 8:54 AM 9/30/03
Static Strain_Day 14_15 kips_Pt 1	9/30/2003	9:00:19 AM	"	
Static Strain_Day 14_15 kips_Pt 2	9/30/2003	9:03:33 AM	"	
Static Strain_Day 14_15 kips_Pt 3	9/30/2003	9:09:22 AM	"	
Static Strain_Day 14_15 kips_Pt 4	9/30/2003	9:11:53 AM	"	

For Test Slab 1C, strain gauge readings due to static loads were taken for two loading positions, namely corner (pt 1) and mid-edge (pt 2). For Test Slabs 1G, 2C, 2E and 2G, two more static loading positions were used. These were at the locations of strain gauges No. 3 and No. 4, which were on the wheel path and at 30 inches from the southern and northern joints of the slab, respectively. They were named as pt 3 and pt 4, respectively.

5.1.3 Slab 2C

The schedule for testing and data collection for Test Slab 2C is shown in Table 8. HVS loading was started at 6 hours after the start of the placement of the concrete. HVS loading using a12-kip (53 kN) super single wheel was applied along the free edge of the slab for 8 days with a total load repetitions of 93,323. Strain gauge readings due to static load were taken for 4 positions, pt 1, pt 2, pt 3 and pt 4, as described in the previous section, each day before continuing with dynamic loading.

5.1.4 Slab 2E

The schedule for testing and data collection for Test Slab 2E is shown in Table 9. HVS loading was started at 6 hours after the start of the placement of the concrete. HVS loading using a12-kip (53 kN) super single wheel was applied along the free edge of the slab for 9 days with a total load repetitions of 59,923. HVS loading was shutdown for 3 days due to a mechanical problem of the HVS. It resumed loading on 7^{th} day and continued until 10^{th} day. Strain readings due to static loads were taken at 4 positions each day.

Table 8. Schedule of Testing and Data Collection for Test Slab 2C

Order of Testing	Date	Time Collected	Load	# HVS Passes / Remarks
Curing Strain	10/13/2003	9:28:34 AM	12 kips	
Static Strain pt 1_6 hrs	10/13/2003	3:14:01 PM	"	
Static Strain pt 2_6 hrs	10/13/2003	3:17:23 PM	"	
Static Strain pt 3_6 hrs	10/13/2003	3:21:17 PM	"	
Static Strain pt 4_6 hrs	10/13/2003	3:28:35 PM	"	
Dynamic Strain_6 hrs	10/13/2003	3:35:22 PM	"	
Static Strain pt 1_12 hrs	10/13/2003	9:38:31 PM	"	
Static Strain pt 2_12 hrs	10/13/2003	9:25:46 PM	"	
Static Strain pt 3_12 hrs	10/13/2003	9:30:17 PM	"	
Static Strain pt 4_12 hrs	10/13/2003	9:34:51 PM	"	
Dynamic Strain_12 hrs	10/13/2003	9:42:14 PM	"	
Dynamic Strain_24 hrs	10/14/2003	8:51:38 AM	"	8914 @ 9:01 AM 10/14/03
Static Strain pt 1_24 hrs	10/14/2003	9:22:11 AM	"	
Static Strain pt 2_24 hrs	10/14/2003	9:26:48 AM	"	
Static Strain pt 3_24 hrs	10/14/2003	9:29:21 AM	"	
Static Strain pt 4_24 hrs	10/14/2003	9:31:59 AM	"	
Dynamic Strain_Continuous_Day 1	10/14/2003	11:49:04 AM	"	
Dynamic Strain_Day 2	10/15/2003	8:47:38 AM	"	21159 @9:02 AM 10/15/04
Static Strain pt 1_Day 2	10/15/2003	10:44:42 AM	"	
Static Strain pt 2_ Day 2	10/15/2003	10:40:12 AM	"	
Static Strain pt 3_ Day 2	10/15/2003	10:47:39 AM	"	
Static Strain pt 4_Day 2	10/15/2003	10:50:08 AM	"	
Dynamic Strain_Continuous_Day 2	10/15/2003	11:19:20 AM	"	
Dynamic Strain_Day 3	10/16/2003	8:53:53 AM	"	33176 @ 9:01 AM 10/16/04
Static Strain pt 1_Day 3	10/16/2003	9:03:36 AM	"	Cracks detected in mid slab area
Static Strain pt 2_Day 3	10/16/2003	9:06:21 AM	"	
Static Strain pt 3_Day 3	10/16/2003	9:09:16 AM	"	
Static Strain pt 4_Day 3	10/16/2003	9:11:35 AM	"	
Dynamic Strain_Continuous_Day 3	10/16/2003	11:21:48 AM	"	
Dynamic Strain _Day 4	10/17/2003	8:50:06 AM	"	45433 @ 9:03 AM 10/17/04
Static Strain pt1_Day 4	10/17/2003	9:09:41 AM	"	
Static Strain pt 2_Day 4	10/17/2003	9:12:01 AM	"	
Static Strain pt 3_Day 4	10/17/2003	9:14:38 AM	"	
Static Strain pt 4_Day 4	10/17/2003	9:17:08 AM	"	
Dynamic Strain_Day 4	10/17/2003	2:41:10 PM	"	
Dynamic Strain_Continuous_Day 4	10/17/2003	4:09:11 PM	"	
Dynamic Strain_Day 5	10/18/2003	9:14:57 AM	"	57476 @ 9:40 10/18/04
Static Strain pt 1_Day 5	10/18/2003	9:24:34 AM	"	
Static Strain pt 2_Day 5	10/18/2003	9:28:38 AM	"	
Static Strain pt 3_Day 5	10/18/2003	9:33:14 AM	"	

Table 8, continued

Order of Testing	Date	Time Collected	Load	# HVS Passes / Remarks
Static Strain pt 4_Day 5	10/18/2003	9:36:17 AM	"	
Dynamic Strain_Continuous_Day 5	10/18/2003	10:45:12 AM	"	
Static Strain pt 1_Day 6	10/19/2003	8:56:26 AM	"	69647 @ 9:16 10/19/04
Static Strain pt 2_Day 6	10/19/2003	8:59:43 AM	"	
Static Strain pt 3_Day 6	10/19/2003	9:07:30 AM	"	
Static Strain pt 4_Day 6	10/19/2003	9:12:17 AM	"	
Dynamic Strain_Continuous_Day 6	10/19/2003	9:57:17 AM	"	
Dynamic Strain_Day 7	10/20/2003	8:38:37 AM	"	Additional hairline cracks detected in wheel path
Static Strain pt 1_Day 7	10/20/2003	9:00:32 AM	"	82243 @ 8:57 10/20/04
Static Strain pt 2_Day 7	10/20/2003	9:03:27 AM	"	
Static Strain pt 3_Day 7	10/20/2003	9:05:41 AM	"	
Static Strain pt 4_Day 7	10/20/2003	9:08:05 AM	"	
Dynamic Strain_Continuous_Day 7	10/20/2003	3:22:43 PM	"	
Dynamic Strain_Day 8	10/21/2003	8:48:52 AM	"	93323 @ 9:02 10/21/04
Static Strain pt 1_Day 8	10/21/2003	9:01:00 AM	"	
Static Strain pt 2_Day 8	10/21/2003	9:03:11 AM	"	
Static Strain pt 3_Day 8	10/21/2003	9:06:31 AM	"	
Static Strain pt 4_Day 8	10/21/2003	9:08:53 AM	"	

Table 9. Schedule of Testing and Data Collection for Test Slab 2E

Order of Testing	Date	Time Collected	Load	# HVS Passes / Remarks
Curing Strain	3/2/2004	11:24:00 AM	12 kips	
Initial Static Strains	3/2/2004	4:27:00 PM	"	
Initial Static Strains #2	3/2/2004	4:33:00 PM	"	
Initial Dynamic Strains	3/2/2004	4:38:00 PM	"	
Initial Dynamic Strains (2 passes)	3/2/2004	4:47:00 PM	"	
Initial Dynamic Strains	3/2/2004	4:48:00 PM	"	
Initial Static Strain	3/2/2004	5:06:00 PM	"	
Initial Dynamic Strain	3/2/2004	5:19:00 PM	"	
Dynamic Strain	3/2/2004	6:25:00 PM	"	
Static	3/2/2004	6:30:00 PM	"	
Dynamic	3/2/2004	7:25:00 PM	"	
Static	3/2/2004	7:30:00 PM	"	
Dynamic	3/2/2004	8:28:00 PM	"	

Table 9, continued

Order of Testing	Date	Time Collected	Load	# HVS Passes / Remarks
Static	3/2/2004	8:33:00 PM	"	
Dynamic	3/2/2004	9:25:00 PM	"	
Static	3/2/2004	9:30:00 PM	"	
Dynamic	3/2/2004	10:27:00 PM	"	
Static	3/2/2004	10:32:00 PM	"	
Dynamic Day 2	3/3/2004	8:28:00 AM	"	7695
Static Day 2	3/3/2004	10:35:00 AM	"	
All Day Dynamic Day 2	3/3/2004	10:42:00 AM	"	
Static 1033 Day 3	3/4/2004	10:48:00 AM	"	
Dynamic Strain 1033 Day 3	3/4/2004	11:00:00 AM	"	19010
All day Dynamic Day 3	3/4/2004	12:15:00 PM	"	
Dynamic Strain Day 4	3/5/2004	8:51:00 AM	"	30780
Note:	3/5/2004	8:54:00 AM	"	HVS Shuts down due to Computer problems
Note:	3/8/2004	12:09:00 PM	"	HVS Resumes testing
Static Strain Day 7 (After Restart from problem)	3/8/2004	12:44:00 PM	"	30780
Dynamic Strain Day 7 (After restart)	3/8/2004	12:52:00 PM	"	
All Day Dynamic Day 7	3/8/2004	1:00:00 PM	"	
Note:	3/9/2004		"	Crack appears in center of slab going through the center gages: full length, total penetration
Dynamic Strain Day 8	3/9/2004	8:46:00 AM	"	40809
Static Strain Day 8	3/9/2004	10:40:00 AM	"	
All Day Dynamic Day 8 Part 1	3/9/2004	11:04:00 AM	"	52624
All Day Dynamic Day 8 Part 2	3/9/2004	1:36:00 PM	"	
Dynamic Day 9 (Before Restart)	3/10/2004	8:52:00 AM	"	59923
Static Strain Day 9	3/10/2004	10:47:00 AM	"	
Dynamic Day 9 (After Restart)	3/10/2004	10:59:00 AM	"	
All Day Dynamic Day 9 Part 1	3/10/2004	11:07:00 AM	"	
All Day Dynamic Day 9 Part 2	3/10/2004	3:52:00 PM	"	
Note	3/11/2004	9:07:00 AM	"	End of test

5.1.5 Slab 2G

The schedule for testing and data collection for Test Slab 2G is shown in Table 10. HVS loading was started at 6 hours after the start of the placement of the concrete. HVS loading using a12-kip (53 kN) super single wheel was applied along the free edge of the slab for 9 days with a total load repetitions of 80,000. Strain readings due to static load were taken at 4 positions each day.

Table 10. Schedule of Testing and Data Collection for Test Slab 2G

Order of Testing	Date	Time Collected	Load	# HVS Passes / Remarks
Curing Strain	3/30/2004	11:12:06 AM	12 kips	0
Initial Static	3/30/2004	4:35:19 PM	"	
Initial Dynamic	3/30/2004	4:41:40 PM	"	
Statics Day 1	3/31/2004	10:10:12 AM	"	
Dynamic Day 1	3/31/2004	10:15:41 AM	"	
Dynamic Day 2	4/1/2004	10:14:35 AM	"	
Statics Day 2	4/1/2004	10:33:11 AM	"	10091
Continuous Day 2	4/1/2004	10:58:40 AM	"	
Statics Day 3	4/2/2004	10:55:39 AM	"	20000
Continuous Day 3	4/2/2004	11:01:50 AM	"	
Dynamic Day 3	4/2/2004	8:17:09 AM	"	
Dynamic Day 4	4/3/2004	8:46:53 AM	"	30316
Continuous Day 4	4/3/2004	10:53:30 AM	"	
Continuous Day 5	4/4/2004	5:39:56 PM	"	
Statics Day 5	4/4/2004	5:23:20 PM	"	40950
Dynamic Day 6	4/5/2004	8:33:06 AM	"	Cracks noticed on slab early in the morning
Statics Day 6	4/5/2004	10:57:51 AM	"	50933
Continuous Day 6	4/5/2004	12:34:54 PM	"	
Dynamic Day 7	4/6/2004	8:58:54 AM	"	Cracks extend towards the middle of the slab
Statics Day 7	4/6/2004	10:49:41 AM	"	60000
Continuous Day 7	4/6/2004	11:03:51 AM	"	
Dynamic Day 8	4/7/2004	8:21:53 AM	"	Very extensive cracks towards the middle
Statics Day 8	4/7/2004	10:12:07 AM	"	70000
Continuous Day 8	4/7/2004	10:16:36 AM	"	
Dynamic Day 9	4/8/2004	8:47:19 AM	"	
Statics Day 9	4/8/2004	10:47:29 AM	"	80000
Continuous Day 9	4/8/2004	11:13:19 AM	"	End of test

5.2 Temperature Data

Three sets of thermocouple wires were used to monitor the temperature distribution in the slab. Each set of thermocouples consists of 6 gauges which were fixed on a wooden rod in equidistance. One set of thermocouples was installed at the slab corner at the side which would be loaded by the HVS wheel. One set of thermocouples was installed at the slab center. The other set of thermocouple was installed in a concrete block (1 ft × 1ft × 9 in.) which would be placed under the shade of the HVS. The thermocouple readings will be taken at every 10 min. intervals.

Temperature differentials between the top and bottom of the slab were computed and plotted against time for Slabs 1C, 1G, 2C, 2E and 2G in Figures 33, 34, 35, 36 and 37, respectively. It can be seen that the temperature differentials fluctuated between positive values in the daytime to negative values at night. For Slabs 1C and 1G, the maximum positive temperature differential was around +15° F while the maximum negative temperature differential was around –10° F. For Slab 2C, the maximum positive temperature differential was around +22° F while the maximum negative temperature differential was around –16° F. For Slab 2E, the maximum positive temperature differential was around +17.5° F while the maximum negative temperature differential was around –11° F. For Slab 2G, the temperature data collection was suspended several times due to lightening strikes on the thermocouple data acquisition system. Thus, Figure 37 shows only the available temperature differential data.

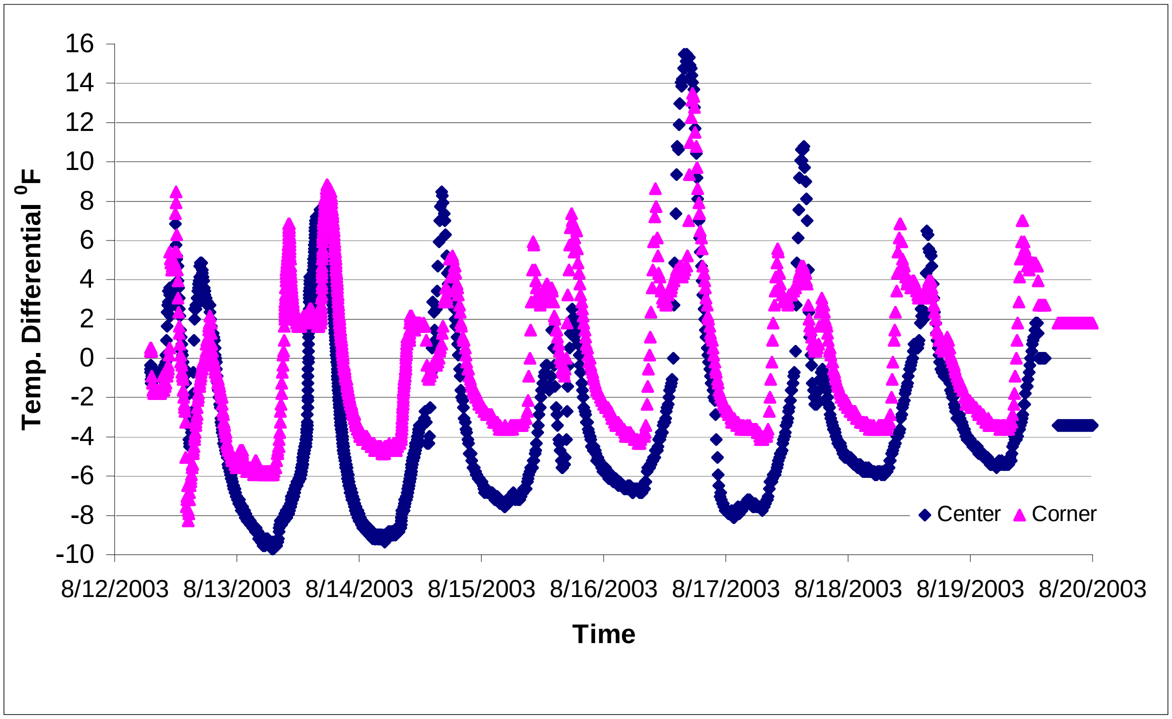

Figure 33. Temperature differentials at Slab 1C

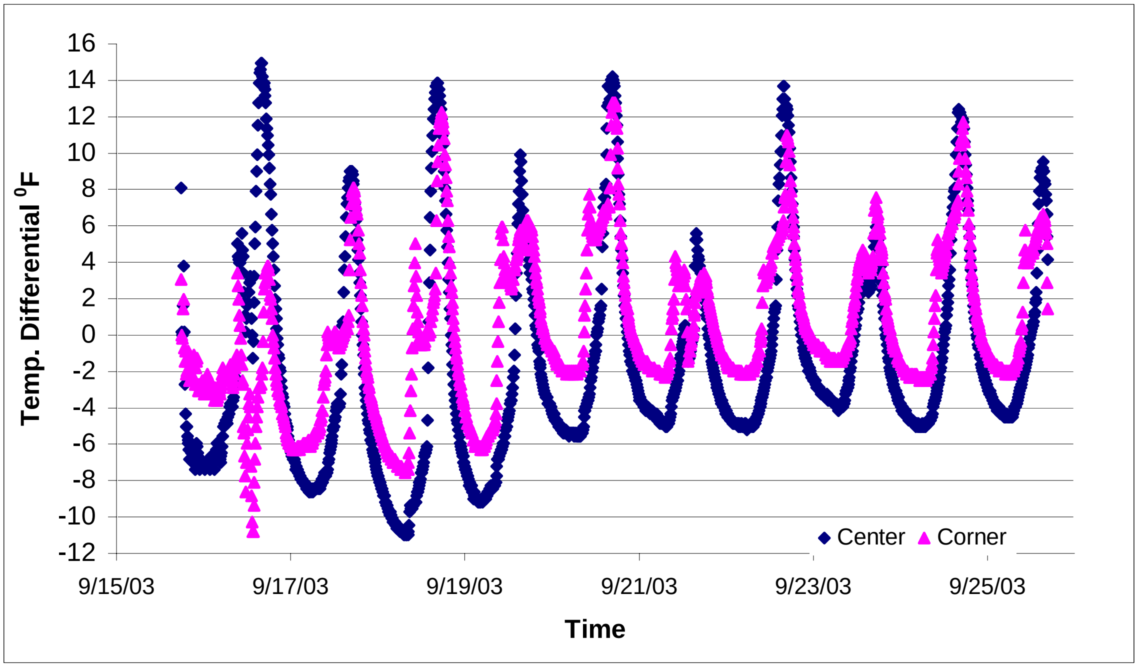

Figure 34. Temperature differentials at Slab 1G

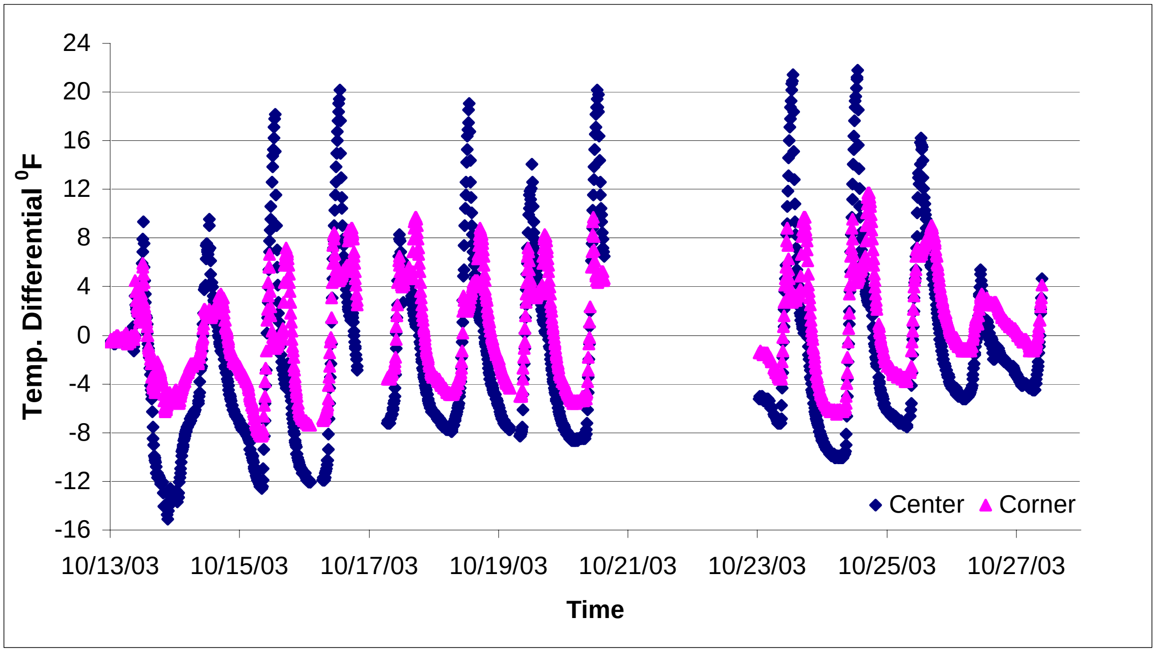

Figure 35. Temperature differentials at Slab 2C

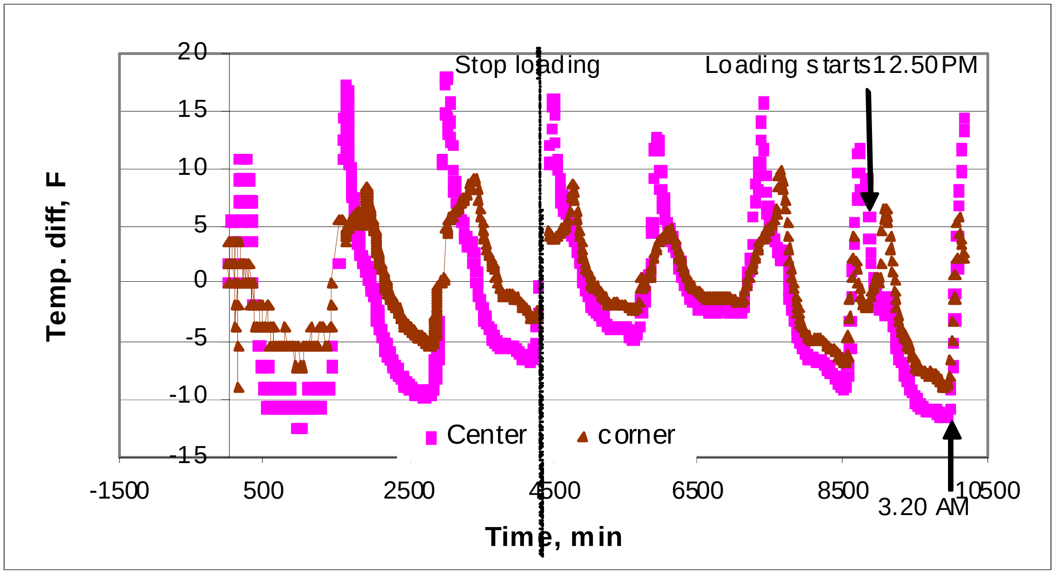

Figure 36. Temperature differentials at Slab 2E

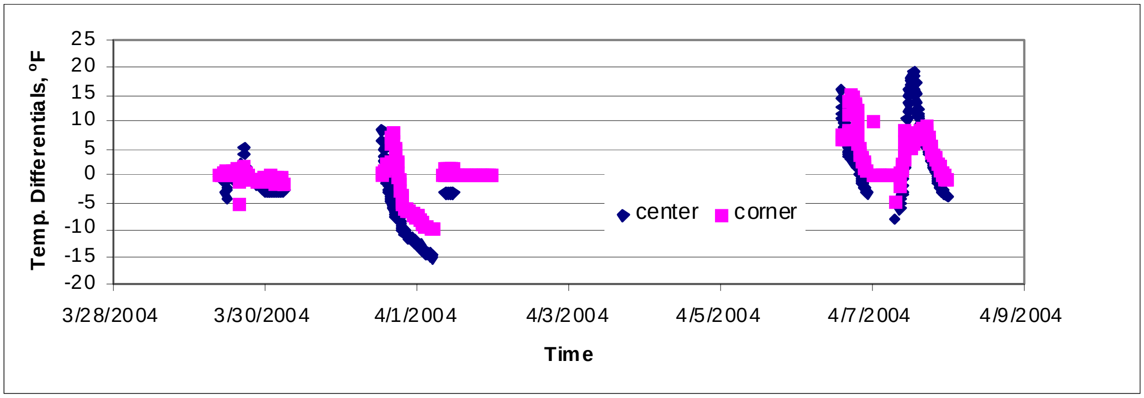

Figure 37. Temperature differentials at Slab 2G

5.3 Impact Echo Test

The impact echo test was used to detect cracks and flaws in concrete. Impact echo test is a non-destructive test on concrete and masonry structures that is based on the use of stress waves (P waves, R waves and S waves) that propagate through concrete and masonry and are reflected by internal flaws and external surfaces. An impact echo instrument consists of two transducers, a mechanical impactor, a data acquisition system and a computer. A small steel ball is used to make a mechanical impact against a concrete and masonry surface and that impact generates low frequency stress waves that propagate into the structure. The reflected stress waves from flows and external surfaces can be detected by the transducers.

P-wave (surface wave) velocity is measured by using two transducers as shown in Figure 38. These two transducers are rigidly clamped in a spacer bar that holds them at a fixed distance, L (typically 300 mm), apart from one another. The impactor is applied at about 150 mm from one of the transducers. This arrangement of transducers and impactor can separate the P wave from the R and S waves. The objective is to measure the precise arrival times of the P wave fronts at the two transducers. If these times are t_1 and t_2, then the wave speed is given by

$$V_s = \frac{L}{t_2 - t_1}$$

P-wave speed in a homogeneous, semi-infinite, elastic solid is a function of Young's modulus of elasticity, the mass density, and Poisson's ratio of the material.

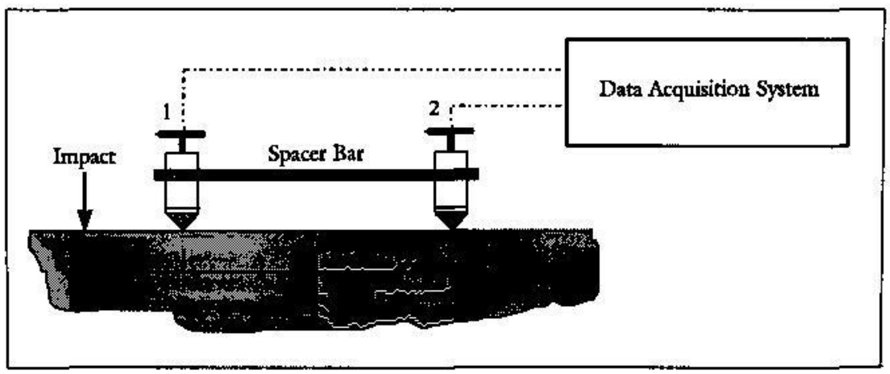

Figure 38. Schematic representation of test set-up for wave speed measurement

The impact echo test and the determination of the P-wave speed were done according to ASTM C 1383 standard test method. An example of the P waves recorded from an impact echo test for P-wave speed measurement is shown in Figure 39.

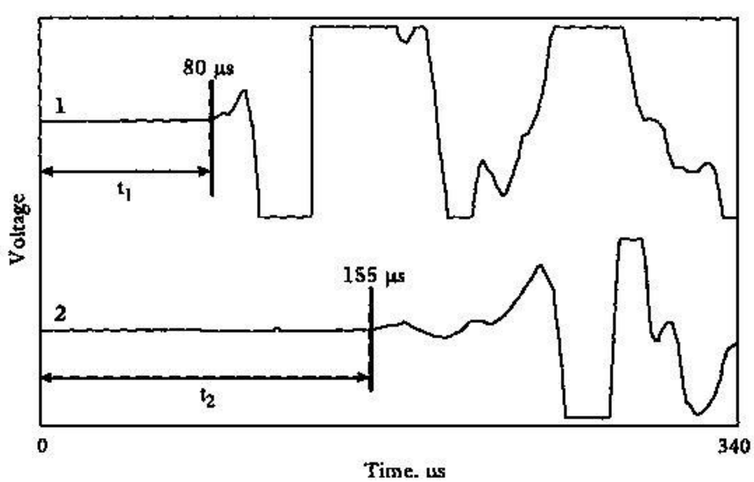

Figure 39. Waveforms from impact echo test for P-wave speed measurement

The corner and the middle edge of the slab were chosen for the impact echo P-wave speed measurement. The results of stress analyses indicated that these were two areas of highest stresses when the test slab was loaded by the HVS wheel, and thus were possible locations for crack development. P-wave speeds at the marked locations were measured at regular time intervals to detect the possible development of cracks. Initiation of cracks tends to reduce of the apparent elastic modulus of the material, and subsequently will reduce the wave speed through the material. Steel template as shown in Figure 40 was made to conveniently mark the hammer (impact) and transducer (receiver) locations on the concrete slab. The locations of the impact and receiver on the test slab for the impact echo test for P-wave speed measurement are shown in Figure 41.

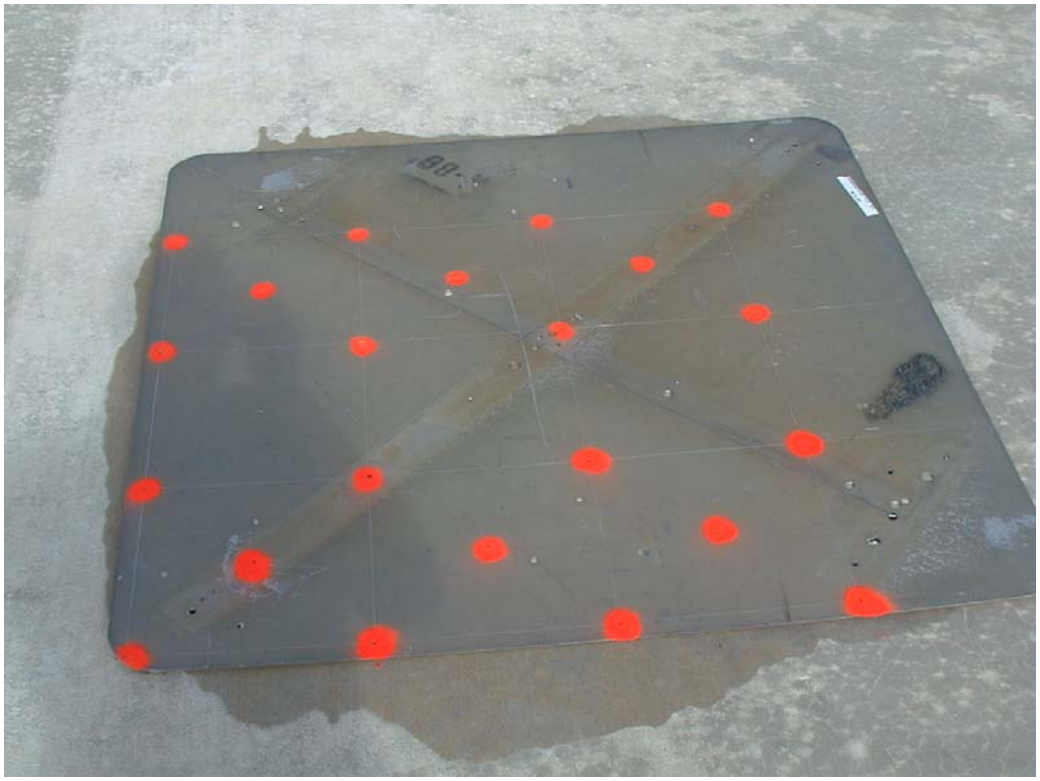

Figure 40. Steel template for marking impact and receiver locations

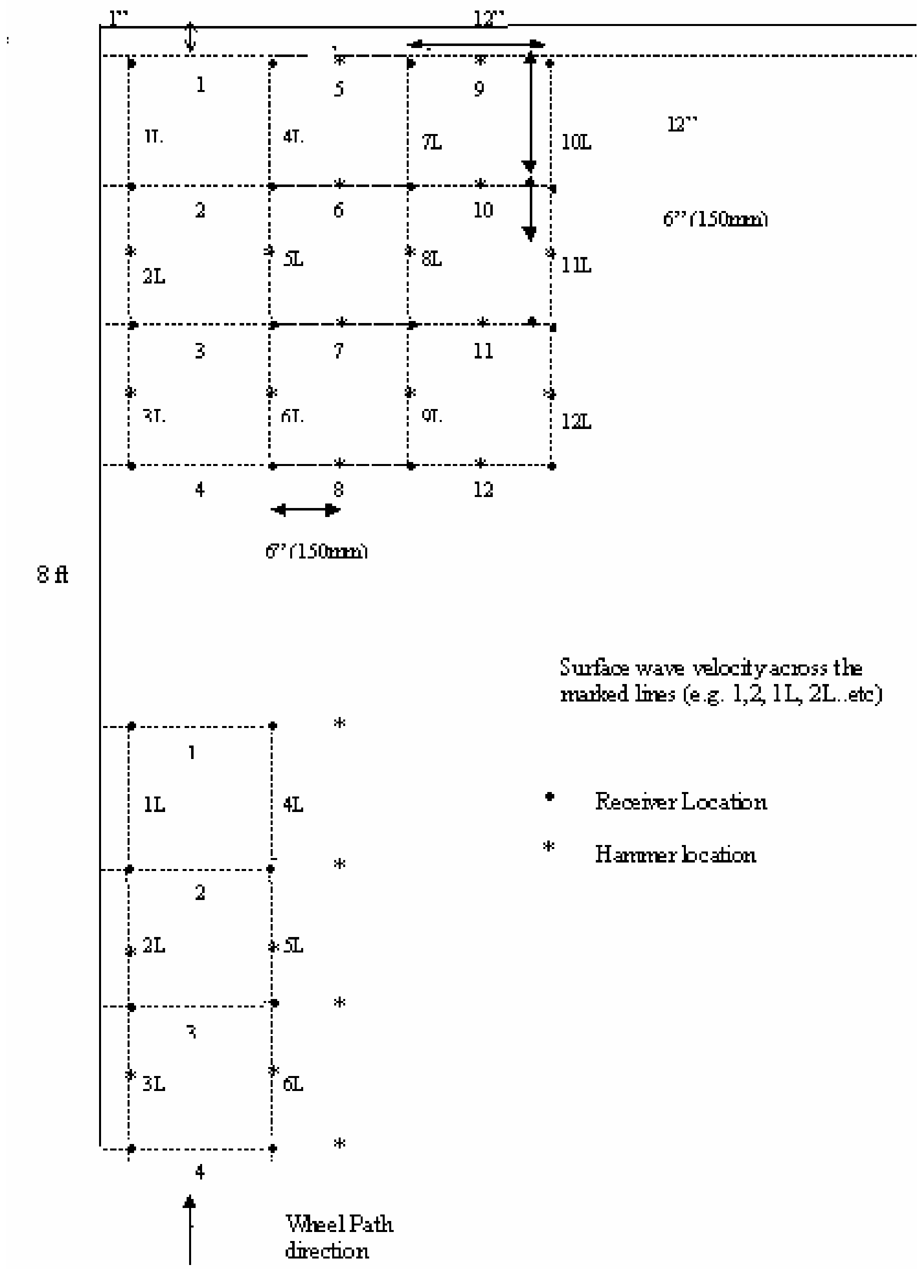

Figure 41. Receiver and impact locations on test slab for impact echo test

Impact echo tests for P-wave speed measurement were run on Test Slabs 1C and 1G successfully. However, due to problems encountered with the data acquisition system of the impact echo equipment during the later part of this study, this test was not used for the rest of the test slabs.

5.4 FWD Test

FWD tests were conducted on the test pavement sections to determine the modulus of subgrade reaction, edge coefficient and join coefficient, which are needed in the modeling of the concrete slab in the FEACONS program. FWD tests were run at midday between 12 PM and 3.00PM and at early morning between 6AM and 8.00AM. At mid day, the temperature differential tends to be positive and slab tends to curl down at the edges and joints. This is the best time to run the FWD test for evaluation of joints and edges because the slab is more likely to be at full contact with the subgrade at the edges and joints. At midnight to early morning, the temperature differential tends to be negative and the slab tends to curl down at the center of the slab. This is an ideal time to run the FWD test at the center of the slab for evaluation of the condition of the concrete slab and the subgrade. Two FWD tests were run at early morning by placing the FWD load at the slab center on Slabs 1G and 2C. Three different FWD loads (around 5000, 9000 and 12000 lbs) were applied at each loading position. Each test was duplicated during the same time interval. The test results and the configuration of geophones and the load on the slab for Slabs 1G and 2C are shown in Table A-1 and Table A-2, respectively in Appendix A. FWD tests were run at midday to estimate the joint and edges stiffness by placing the load at the slab joint (IG and 1F), slab free edge (1G) and confined edge (1E and 2E). The test results and the configuration of geophones and the load on the slab for joint, corner and free edge are shown in Tables A-3, A-4 and A-5, respectively. Each test was duplicated during the same time interval and tested for three load cases.

CHAPTER 6
OBSERVED PERFORMANCE OF THE TEST SLABS

6.1 Crack Initiation and Propagation

6.1.1 Cracks on Slab 1C

Shrinkage cracks were observed at a few places on the finished surface of Slab 1C within a few hours after the placement of the concrete. Figure 42 shows the shrinkage cracks induced on the slab. The first load related crack was detected on the 15th day of loading, which was one day after the load had been increased to 18 kips. The first detected crack was a corner crack, which occurred on the wheel path at the north end of the slab. Figure 43 shows a picture of this corner crack. This corner crack extended from the joint at 25 inches from the edge to the edge at 35 inches from the joint. HVS loading was continued for another day, at which point another corner crack, which extended from the joint at 47 inches from the edge, was observed. Figure 44 shows a picture of the cracked Slab 1C at the end of HVS testing. Figure 45 shows the initial and final crack map for Slab 1C.

Figure 42. Shrinkage cracks on Test Slab 1C

Figure 43. Corner crack on Slab 1C

Figure 44. Cracked Slab 1C at the end of HVS testing

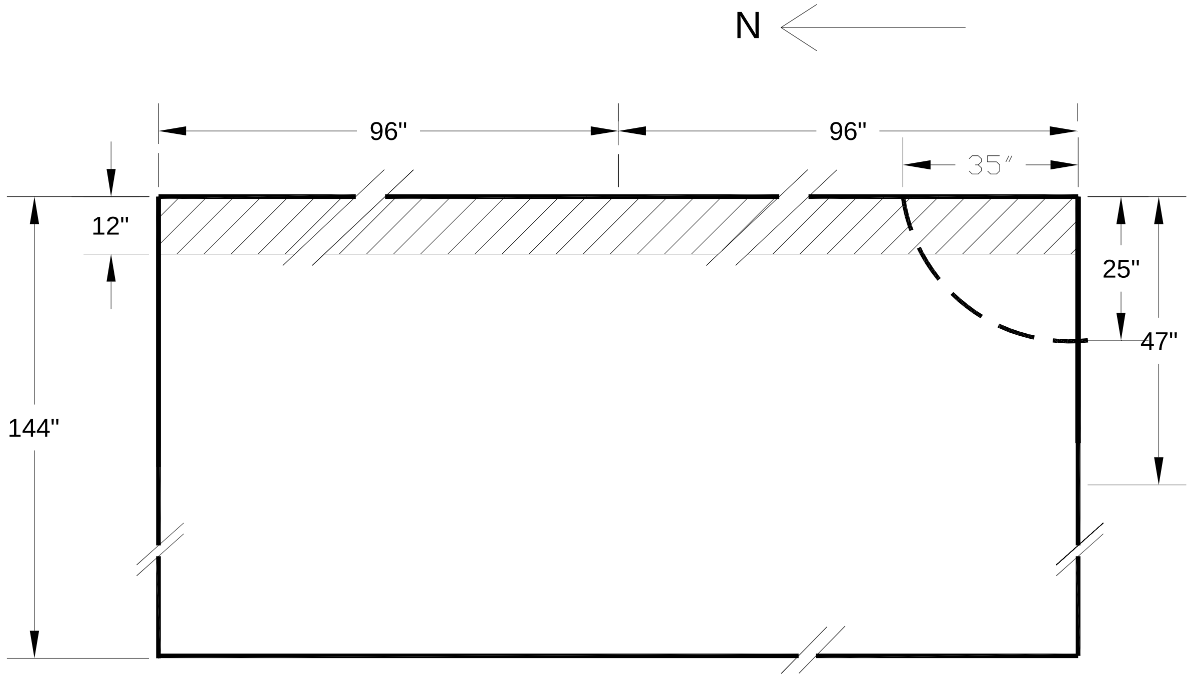

(a) Initial crack on Slab 1C

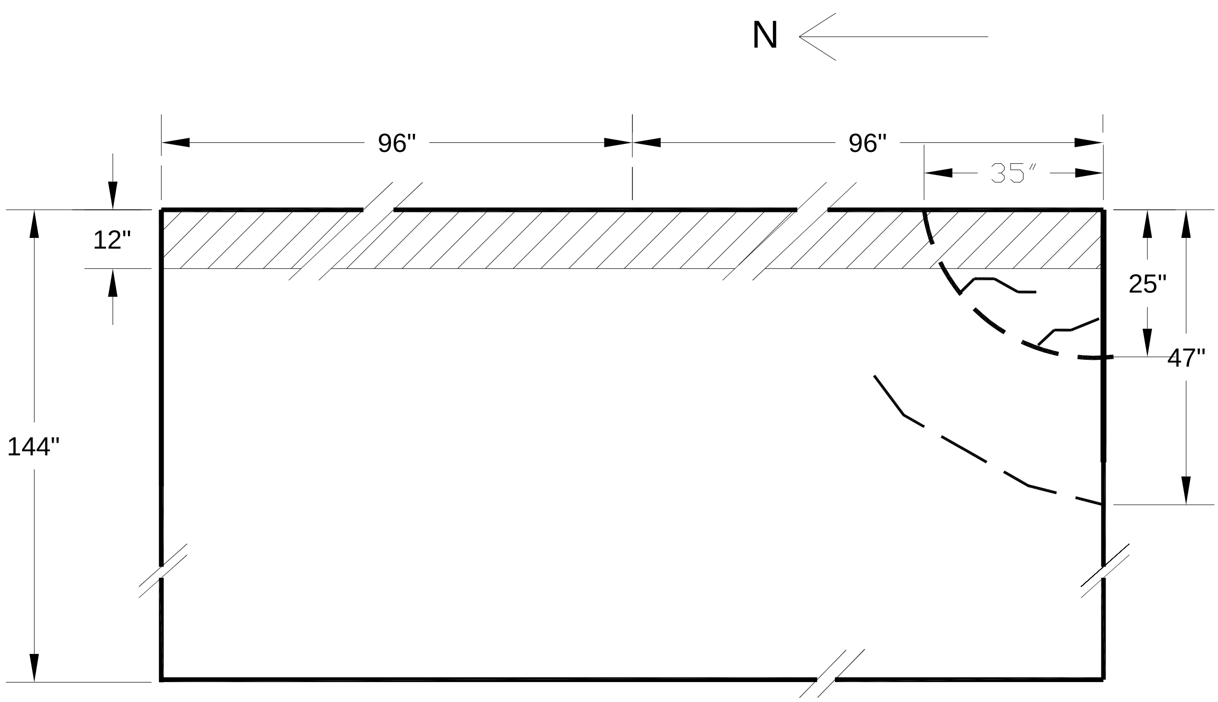

(b) Final cracks on Slab 1C

Figure 45. Crack map of Slab 1C

6.1.2 Cracks on Slab 1G

For Slab 1G, cracking was detected after 11 days of HVS loading and 2 days after the HVS load was raised to 15 kips, with a total of 107,152 load repetitions at 12 kips and 20,464 load repetitions at 15 kips. At the southern end of the slab, there was a corner crack, which extended from the joint at 30 inches from the edge to the edge at 33 inches from the joint. This crack happened to run over the location of strain gauge no. 3. Figure 46 shows a picture of this corner crack. There was also a similar crack on the northern end of the slab, which extended from the edge at 34 inches from the joint. However, this crack did not propagate all the way to the joint. In addition to the corner cracks, there were two transverse cracks at the mid-edge of the slab (89 and 100 inches from the southern joint of the slab). Figure 47 shows the transverse cracks at the mid-edge of the slab. These cracks propagated towards the center of the slab with additional HVS loading. Figure 48 shows the propagation of the mid-edge cracks with additional

Figure 46. Corner crack at the southern end of Slab 1G

Figure 47. Transverse cracks at the mid-edge of Slab 1G

Figure 48. Crack propagation at the mid-edge of Slab 1G with additional loading

loading. The portions of the cracks that are marked as 1, 2 and 3, as shown in the picture, indicate the amount of crack propagation on the 1st, 2nd and 3rd day after crack initiation. Figure 49 shows the initial and final crack map of Slab 1G.

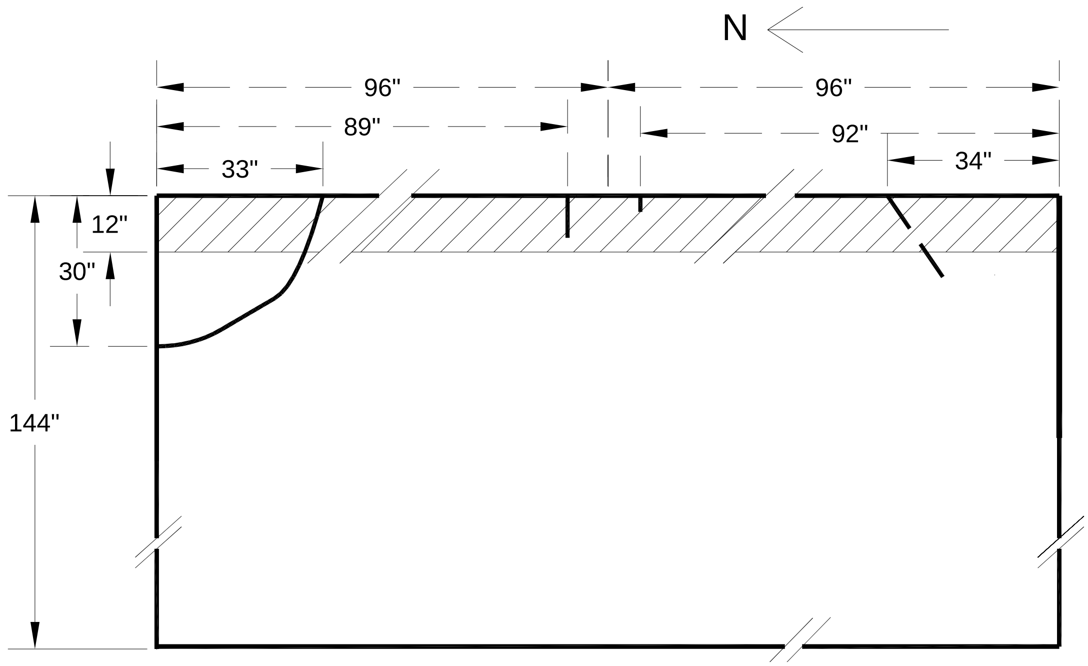

(a) Initial cracks on Slab 1G

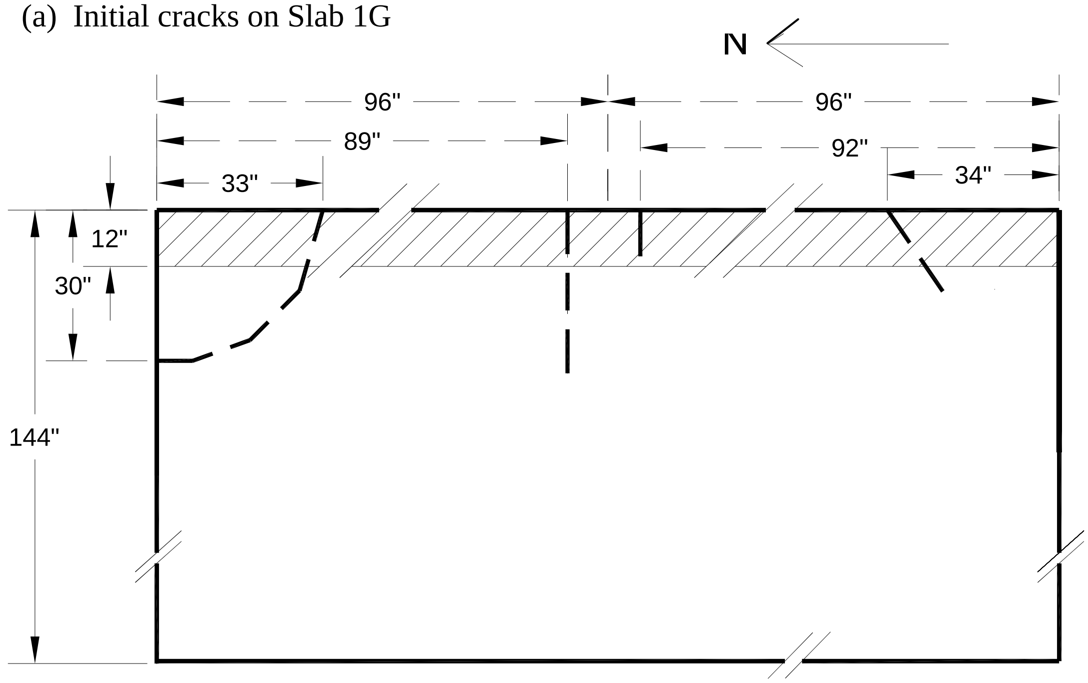

(b) Final cracks on Slab 1G

Figure 49. Crack map of Slab 1G

6.1.3 Cracks on Slab 2C

For Slab 2C, cracks were first detected after 3 days of HVS loading, with a total of 33,176 load repetitions at 12 kips. There were two transverse cracks at about 1 foot off from the center of the slab on the wheel path. Figure 50 shows a picture of these two transverse cracks. Additional hairline cracks were detected after 7 days of loading, with a total of 82,243 load repetitions at 12 kips. Figure 51 shows a picture of the cracks on Slab 1C after 7 days of HVS loading. Figure 52 shows the initial and final crack map of Slab 2C.

Figure 50. Transverse cracks at mid-edge of Slab 2C

Figure 51. Cracks on Slab 2C at the end of HVS testing

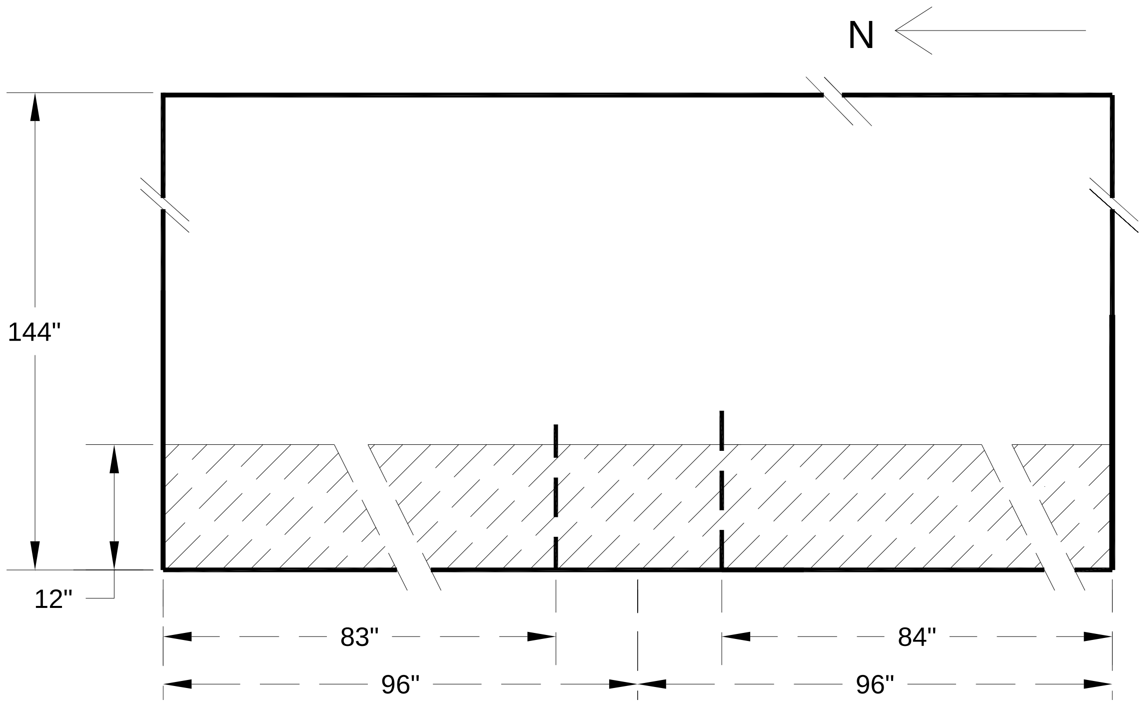

(a) Initial cracks on Slab 2C

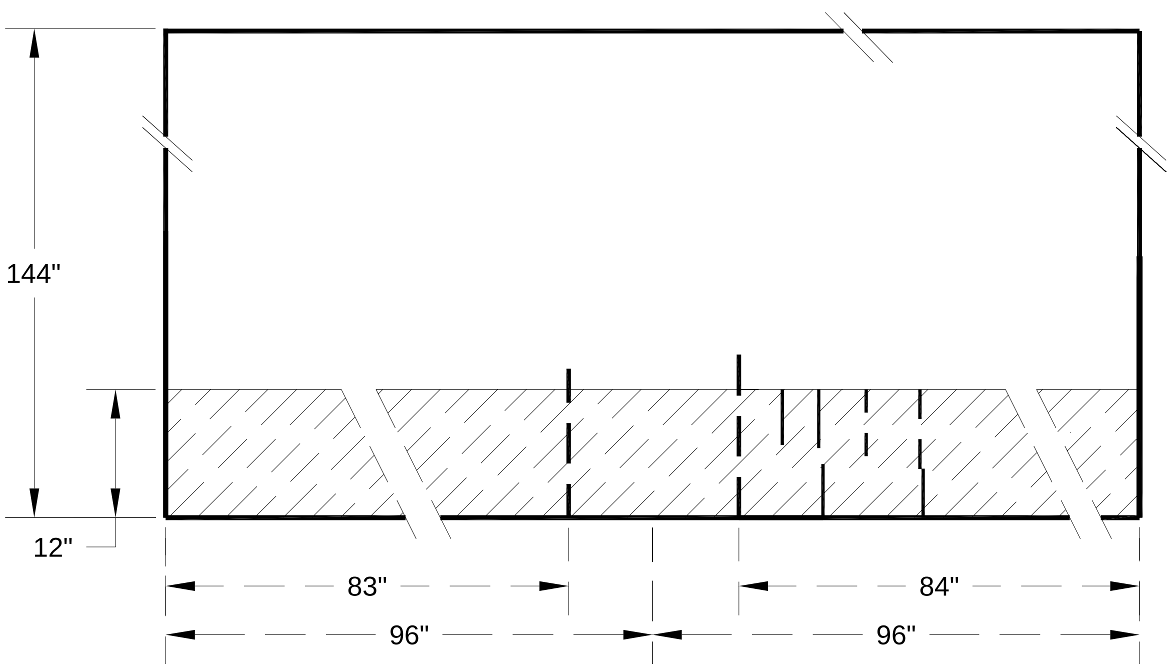

(b) Final cracks on Slab 2C

Figure 52. Crack map of Slab 2C

6.1.4 Cracks on Slab 2E

For Slab 2E, cracks were first detected at the 7th day after the start of HVS loading, with a total of 40,809 load repetitions at 12 kips. The HVS loading was halted for 3 days due to a mechanical problem with the HVS after 3 days of loading. A transverse crack was first detected one day after HVS loading at 12 kips was resumed (or at the 7th day of test). This crack extended from the loading edge to the opposing edge at the middle of the slab. Figure 53 shows the transverse crack that developed on Slab 2E. Figure 54 shows the crack map of Slab 2E.

Figure 53. Transverse crack on Slab 2E at the middle of the slab

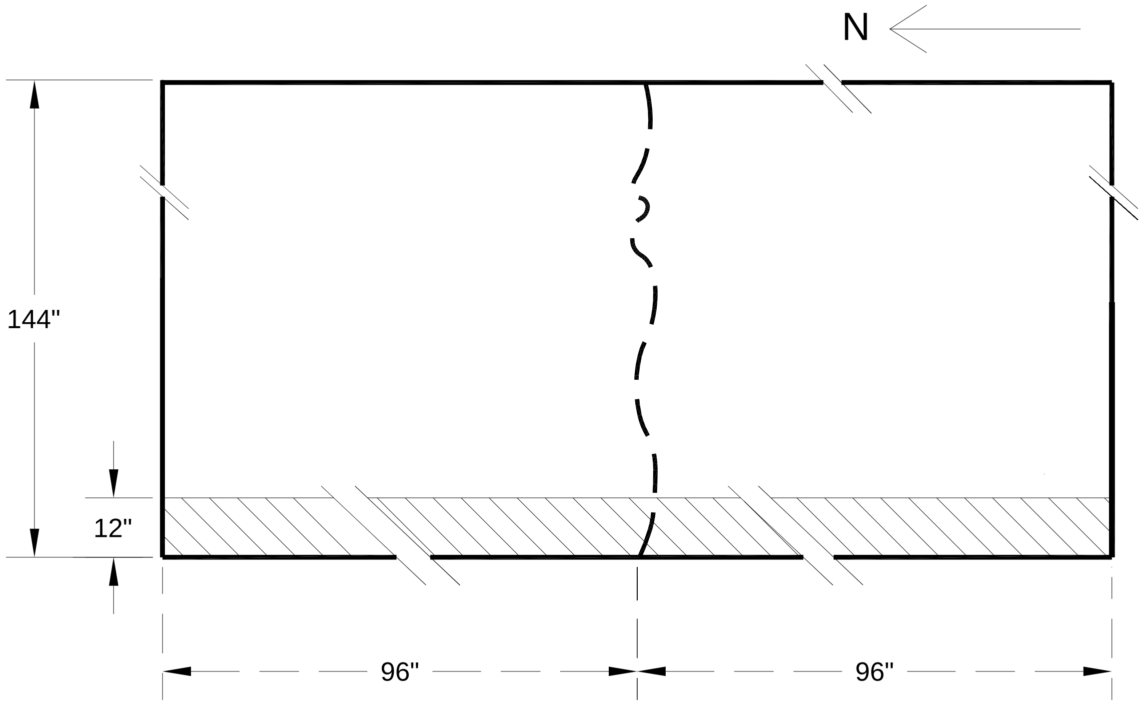

Figure 54. Cracks on Slab 2E

6.1.5 Cracks on Slab 2G

For Slab 2G, the first crack was detected at the 6th day of loading with 50,933 passes of HVS wheel load at 12 kips. Two transverse cracks were noted to start from the edge. One transverse crack started at 9 inches south of the mid-point, while the other started at 36 inches north of the mid-point. Figure 55 shows a picture of the transverse cracks that developed on Slab 2G. Figure 56 shows the initial and final crack map of Slab 2G.

Figure 55. Transverse cracks on Slab 2G at the middle of the slab

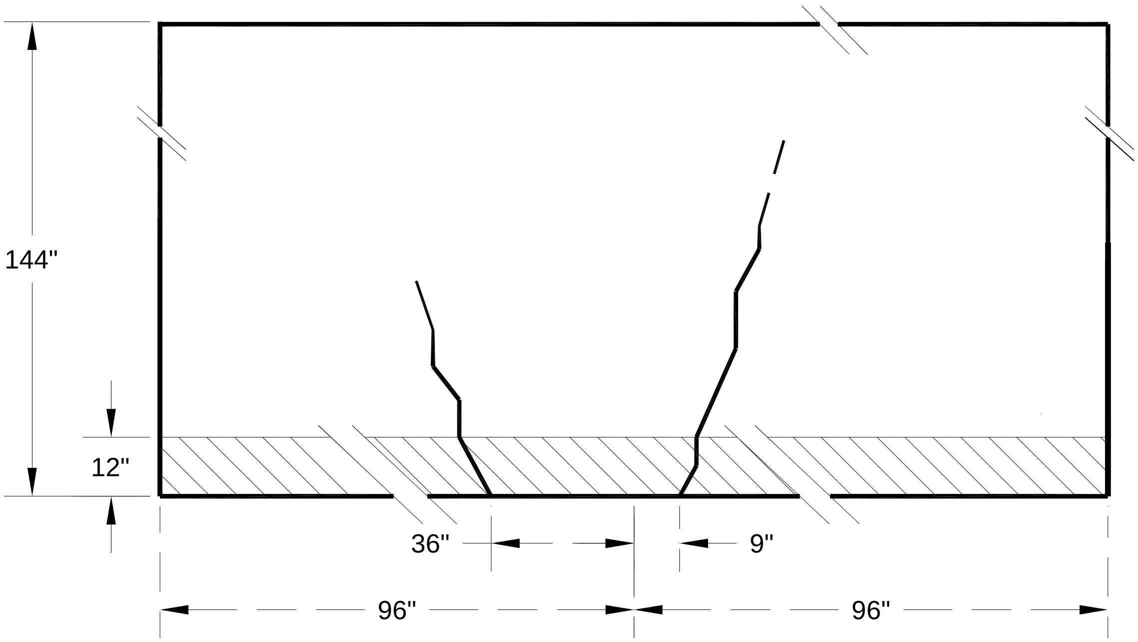

(a) Initial cracks on Slab 2G

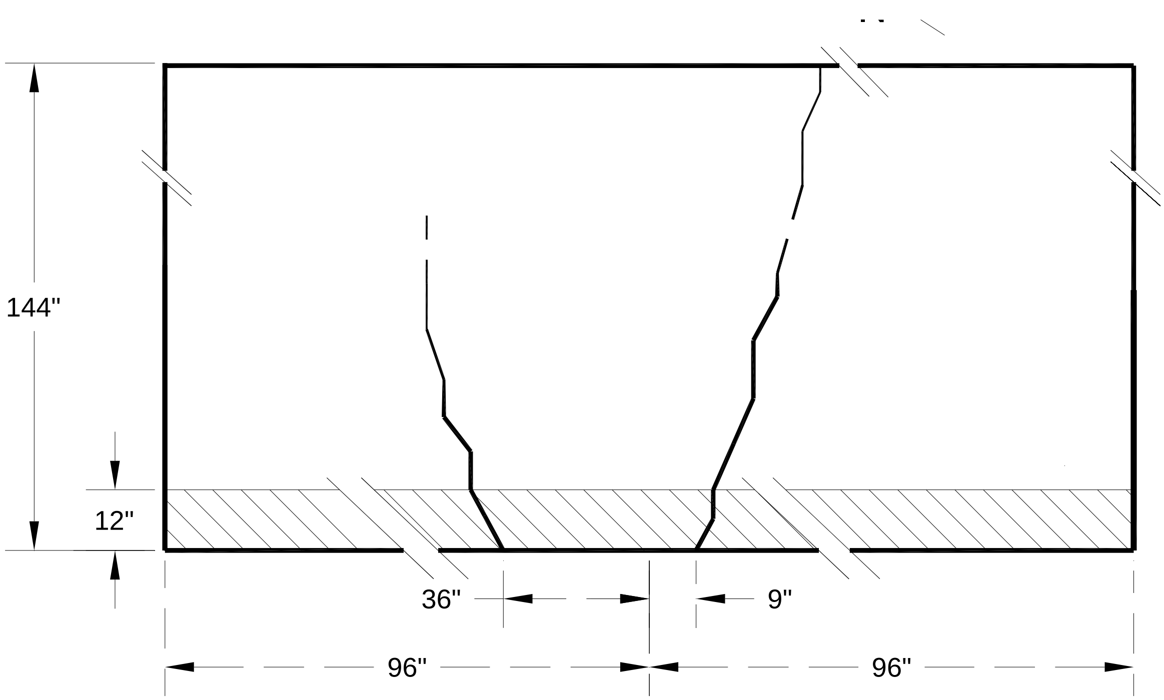

(b) Final cracks on Slab 2G

Figure 56. Crack map of Slab 2G

CHAPTER 7
ANALYSIS OF DATA

7.1 Estimation of Model Parameters

As presented in Chapter 3, the FEACONS program was used to perform stress analyses to determine the optimum locations for strain gauges. In those previous analyses, some assumed values for the various pavement parameters were used with the purpose of determining the locations of maximum stresses rather than determining the magnitudes of the maximum stresses accurately. However, in analyzing the performance of the test slabs under the HVS loading, the temperature-load induced stresses on the test slabs needed to be determined accurately. This necessitated the accurate estimation of the various pavement parameters needed by the FEACONS program to perform the stress analyses effectively. The modulus of subgrade reaction of the test slab was estimated by back-calculation of the FWD deflection basins using the FEACONS program. The deflection basins caused FWD loads applied at the slab center was used in this case. The effect of joint and edge stiffness was assumed to be negligible for the deflection at the slab center. Loading area of the FWD is circular with a 12-inch diameter. A twelve-inch by twelve-inch square loading area was used in the finite element mesh to model the loading plate. The other pavement parameters used in the FEACONS analyses were as follows:

(1) Concrete thickness – 9 inches
(2) Concrete modulus of elasticity – 4000 ksi
(3) Poisson’s ratio – 0.2
(4) Slab sizes – 12 ft × 16 ft
(5) Applied load –12 kips
(6) No temperature effect.

The computed and measured deflections at the locations of the geophones for Slab 1G are shown in Figure 57. The measured deflections in the X direction were noted to be different from those in the Y direction. The differences in deflections in the two directions may be due to cracks on the slab. The computed deflection basin was obtained by using a modulus of subgrade reaction of 0.9 kci. The computed deflection for Slab 2C is shown in the Figure 58. For Slab 2C, the modulus of subgrade reaction was estimated to be 1.1 kci. The lower modulus of subgrade reaction for the Slab 1G could be due to deterioration of the asphalt layer prior to the placement of the concrete slab at Slab 1G. FDOT personal had noticed the deterioration of the asphalt layer at Slab 1G and had used a cold asphalt patch to repair the damaged area before placement of the replacement concrete slab.

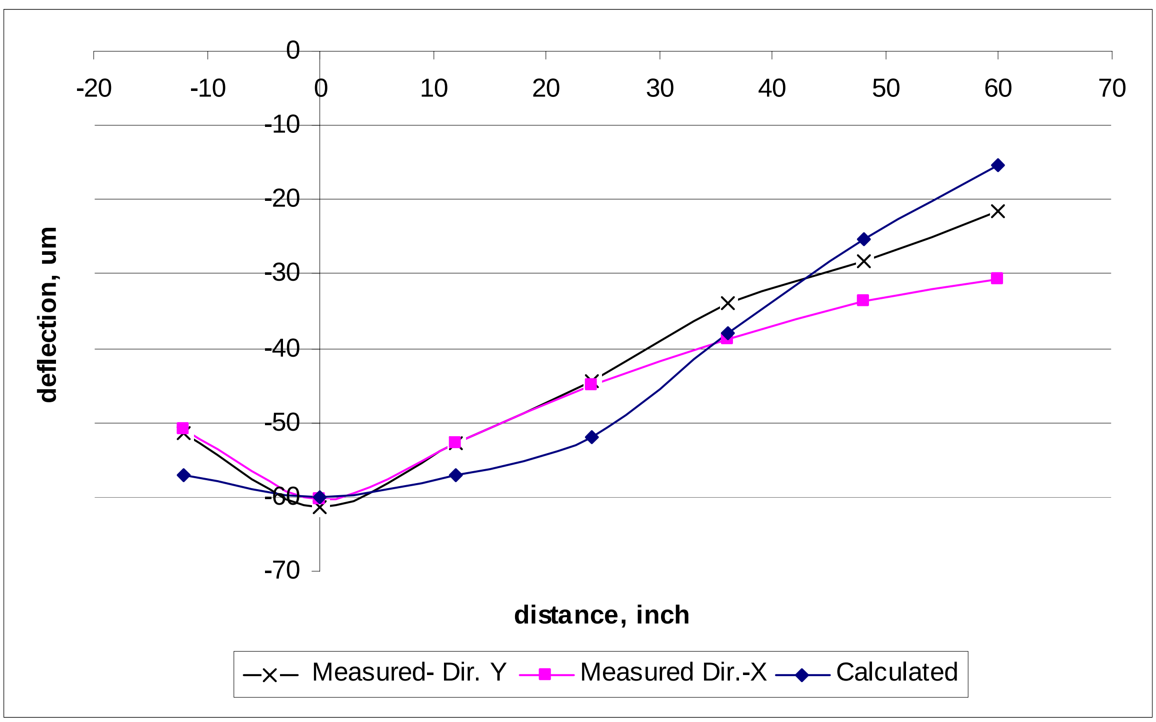

Figure 57. Measured and computed deflection basins caused by a 9-kip FWD load at slab center for Slab 1G

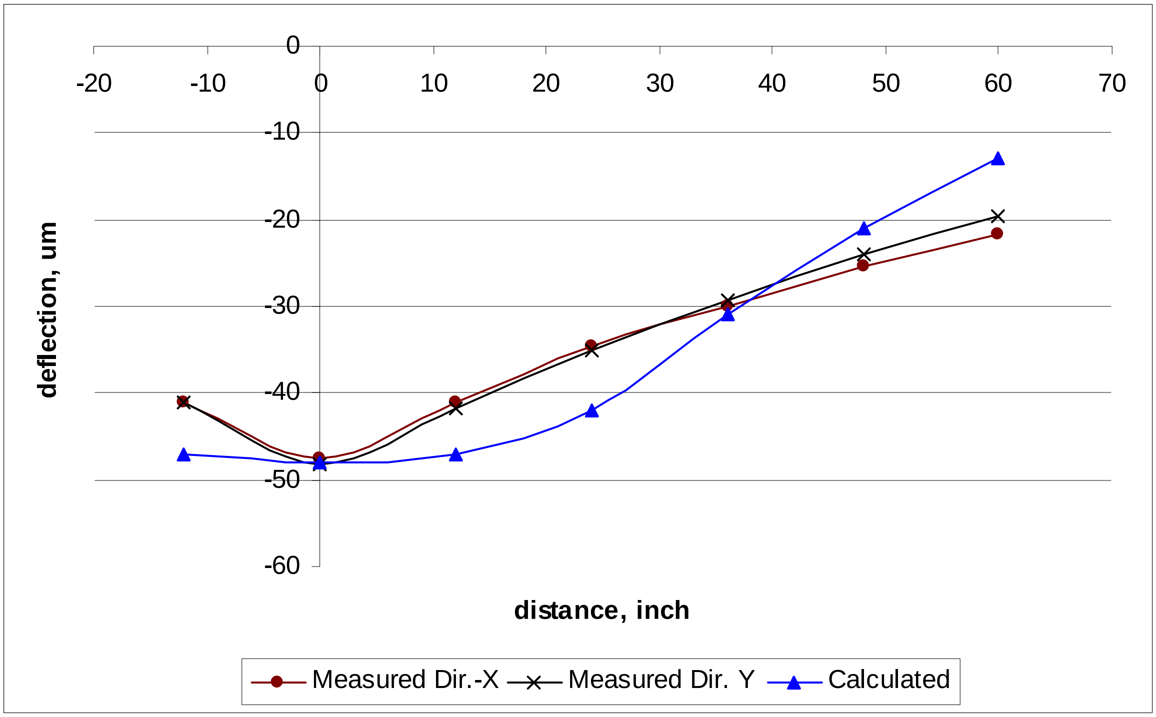

Figure 58. Measured and computed deflection basins caused by a 9-kip FWD load at slab center for Slab 2C

Results of FWD tests at the slab joint were used to estimate the joint coefficients. The estimated modulus of subgrade reaction and the values of the other known pavement parameters were used in the FEACONS program to compute the analytical deflections. The computed and measured defections at the slab joint for Slab 1G are shown in Figure 59. The linear and torsional coefficients of the joint were 200 ksi and 600 K-in/in. These coefficients gave a fairly good match between the computed and the measured deflection at the joint.

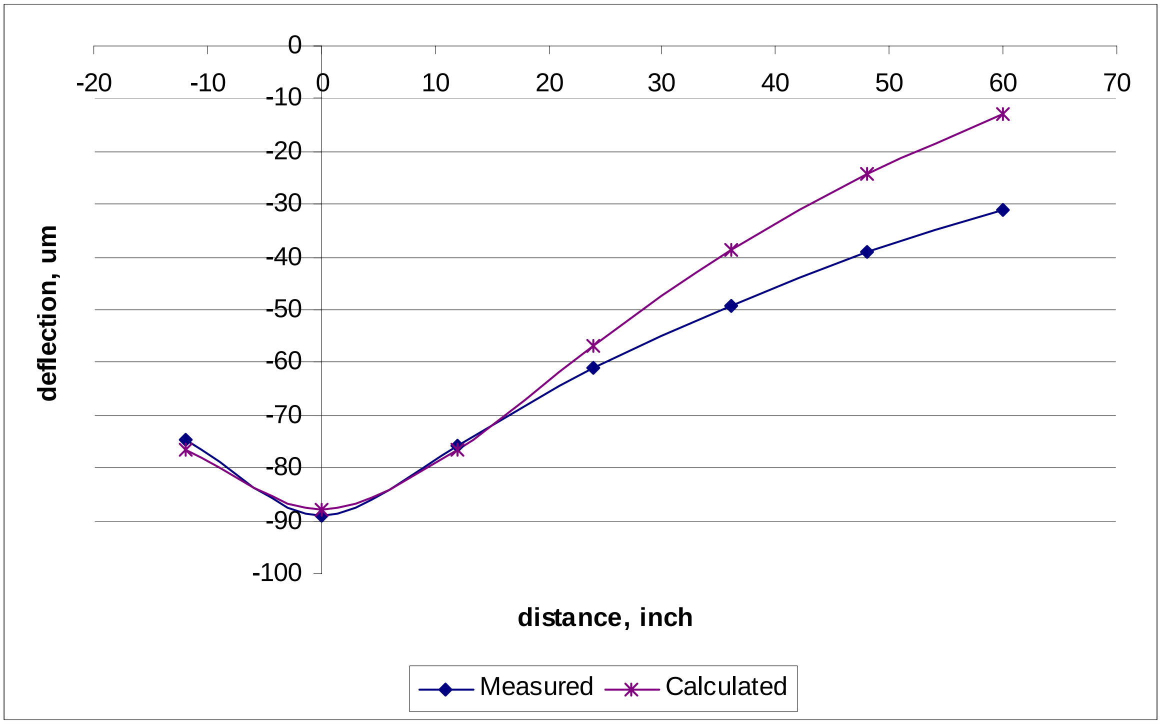

Figure 59. Measured and computed deflection basin caused by a 9-kip FWD load at slab joint for Slab 1G

Results of FWD tests at the free edge of the test slab were used to estimate the edge coefficients. The estimated subgrade modulus and the other known pavement parameters were used in the FEACONS program to calculate the deflections caused by a 9-kip FWD load at the slab edge. An edge stiffness of 10 ksi gave a fairly good match between the computed and measured deflection at the free edge. Figure 60 shows the computed and measured deflections for the free edge of Slab 1G. Similarly, the edge coefficient for a confined edge was estimated by using the results of FWD tests run at a confined edge. The edge coefficient for a confined edge was determined to be 23 ksi.

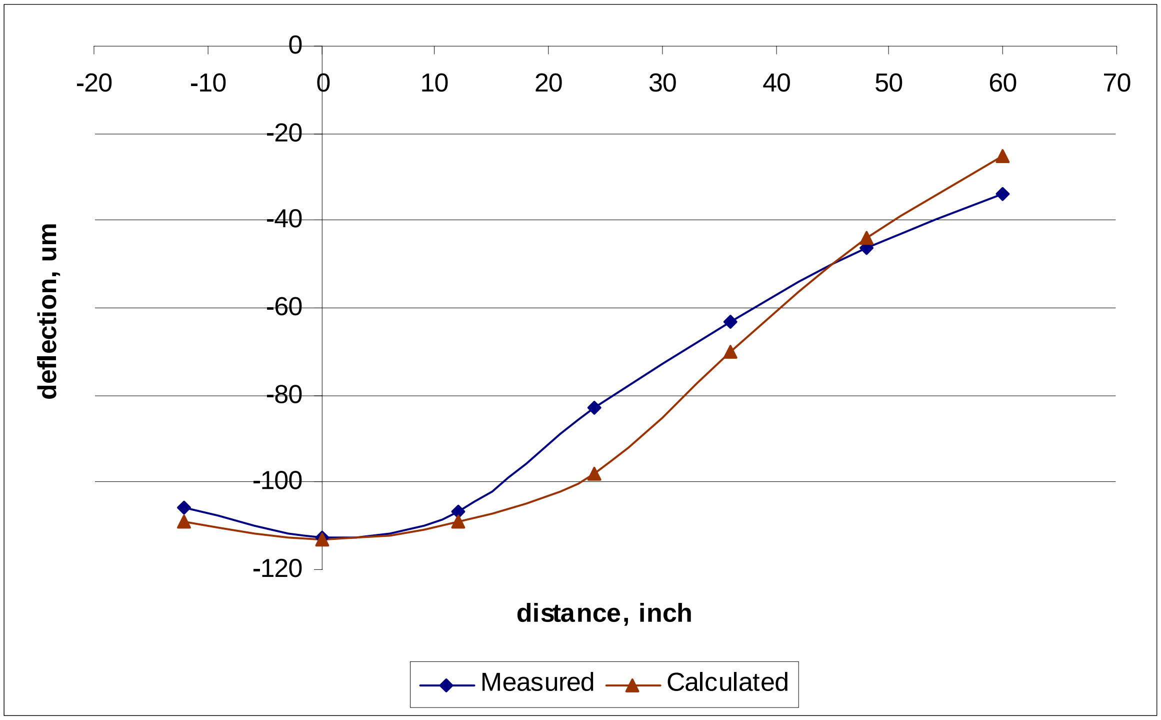

Figure 60. Measured and computed deflection basins caused by a 9-kip FWD load at a free edge for Slab 1G

7.2 Analysis of Dynamic Strain Data

Dynamic strains in the test slabs caused by the moving HVS wheel load were collected at 7 strain gauge locations. Two of the gauges were placed in the transverse direction (YY) while the other 5 gauges were installed in the longitudinal direction (XX), as described in Section 3.2. The main purposes for the measurement of these dynamic strains were (1) to detect crack development in the slab, (2) to verify the stresses and strains as computed by the FEACONS computer program, and (3) to evaluate the stress distribution in the concrete slab caused by moving wheel loads.

7.2.1 Analysis of Measured Dynamic Strains for Detection of Cracks

The changes in the measured dynamic strains could be used to detect the development of cracks and the locations of the cracks. Figure 61 shows the plots of dynamic strains as measured by gauge 3 as a HVS wheel passed over it, before and after a crack developed on Slab 2C. From the plots for Day 2 and Day 3, when the crack had not yet developed, it can be seen that the measured strains started to increase gradually after the load passed over the slab joint (at around the time of 18.7 seconds on the plot) and approached the location of the gauge. The measured strain peaked when the load was directly over the gauge (at around the time of 20.3 seconds on the plot). After the load passed over the gauge, the strain would quickly reversed from positive to negative as can be seen from the plots.

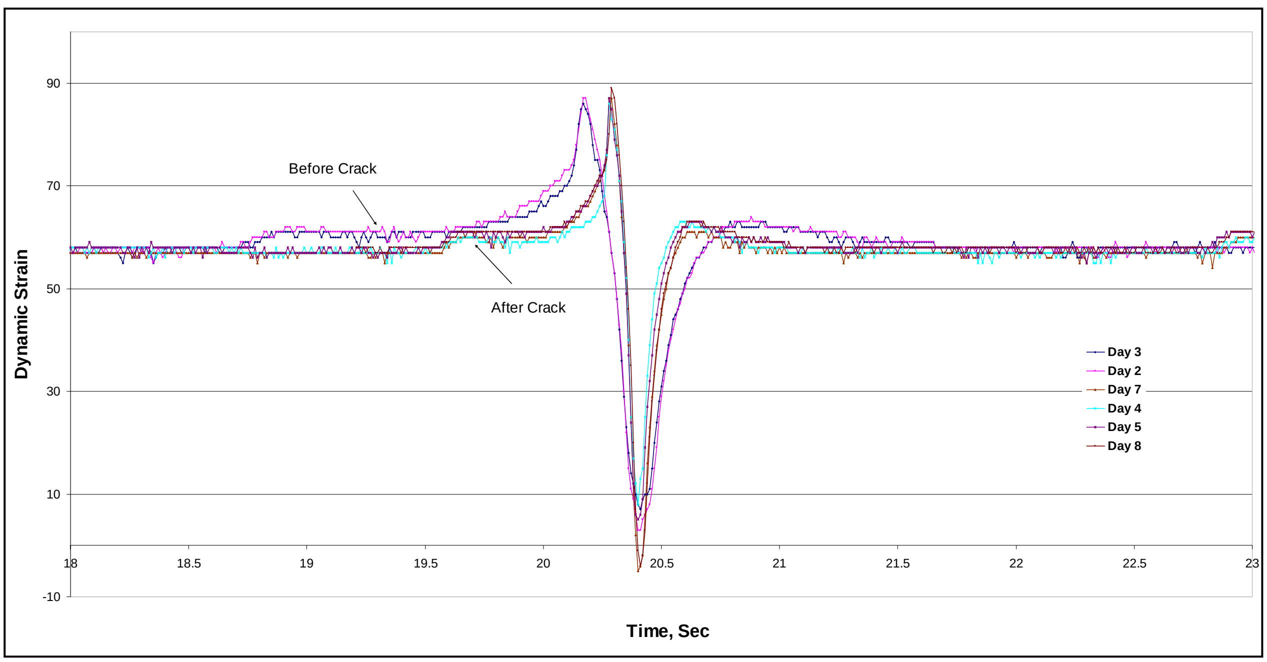

Figure 61. Measured dynamic strains from gauge 3 on Slab 2C

A change in the plots of dynamic strains can be observed after Day 3, when a crack was observed. From the plots for Days 4, 5, 7 and 8, it can be seen that the dynamic strain did not start to increase until the load passed over the crack (at around the time of 19.6 seconds). It can also be seen that, due to the formation of the crack, the magnitudes of the maximum positive and negative strains are noticeably higher than those before the crack.

For Slab 2E, cracks were first detected one day after HVS loading at 12 kips was resumed (or at the 7^{th} day of test). Figure 62 shows the plots of measured dynamic strains from gauge 4, as a HVS wheel passed over it, before and after crack initiation. A plot of the maximum measured compressive strain from gauge 4 versus time is shown in Figure 63. It can be seen from Figure 63 that the magnitude of the measured compressive strain drastically increased after testing was resumed on the 7^{th} day, indicating the initiation of crack on the 7^{th} day, though the crack was observed on the 8^{th} day.

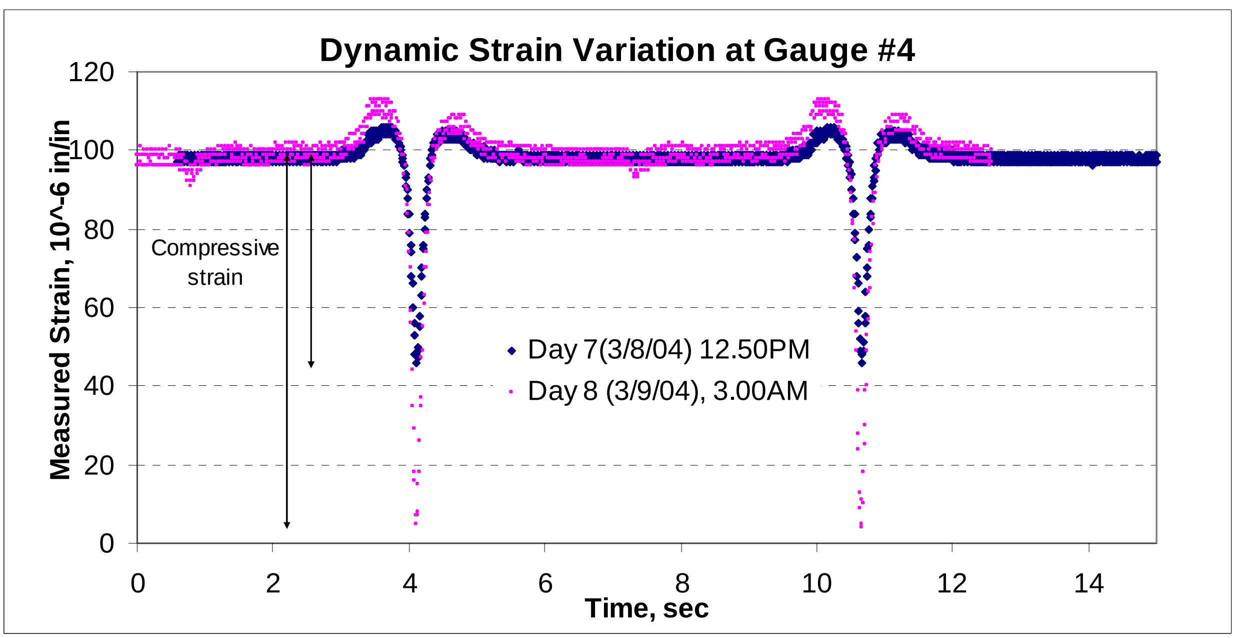

Figure 62. Measured dynamic strains from gauge 4 on Slab 2E

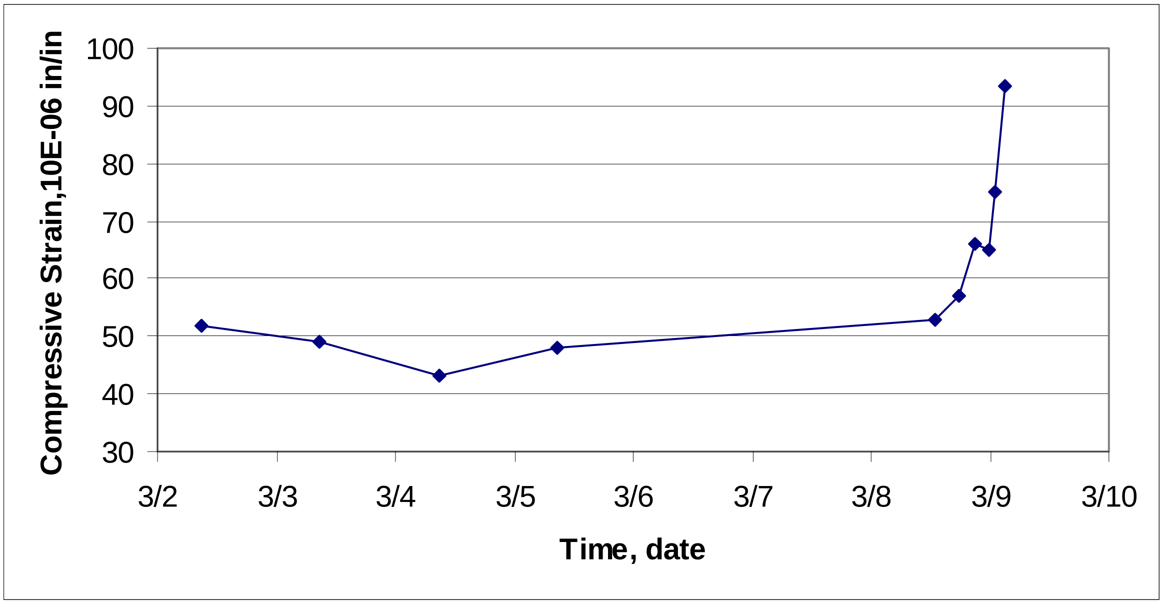

Figure 63. Maximum measured compressive strain from gauge 4 on Slab 2E

7.2.2 Comparison of Measured Strains with Computed Strains

The FEACONS program was used to compute the strains in the concrete caused by the HVS wheel load. The pavement parameters as needed by the FEACONS model were determined as described in Section 7.1. The stress at each gauge location was computed using the FEACONS model for the case of a static load at several specified locations on the wheel path. These static load locations were converted to a time scale that indicates the time the HVS test wheel passed over these locations. The computed stresses were used to calculate the strains using the elastic modulus and Poisson's ratio of the concrete. Figures 64 through 69 show the comparison of theoretical strains using the FEACONS model and the measured dynamic strains at gauge locations 1, 2, 4, 5, 6and 7 on Slab 1C. Gauge number 3 had picked up lot of noise, and thus the comparison between theoretical and measured is not presented for this gauge.

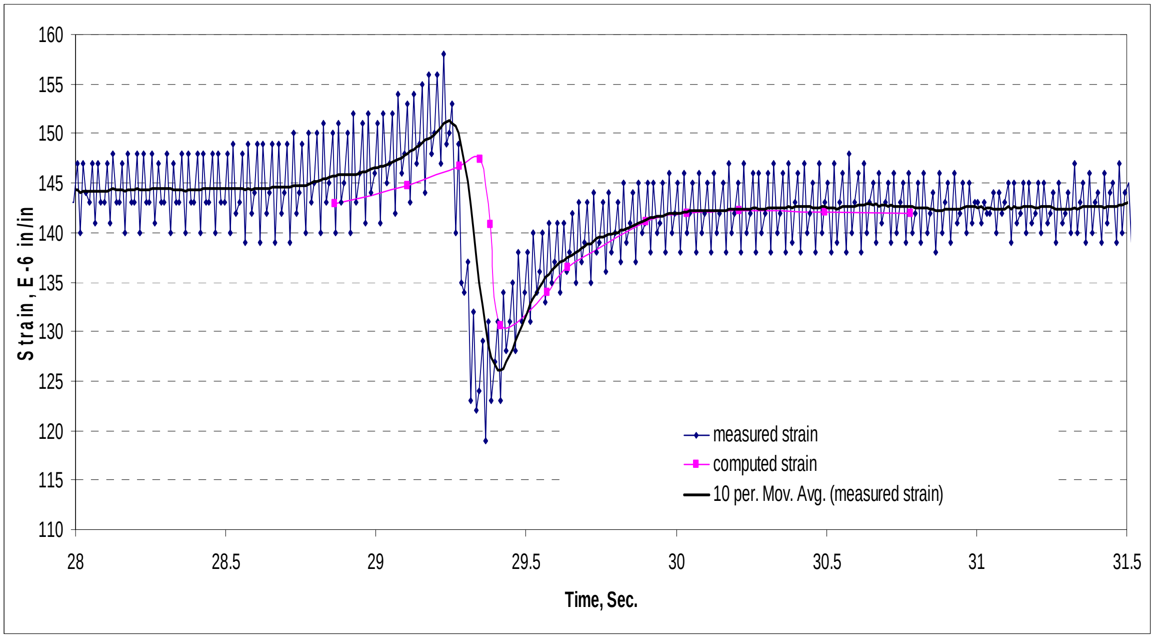

Figure 64. Measured and computed strains for gauge 1 on Slab 1C

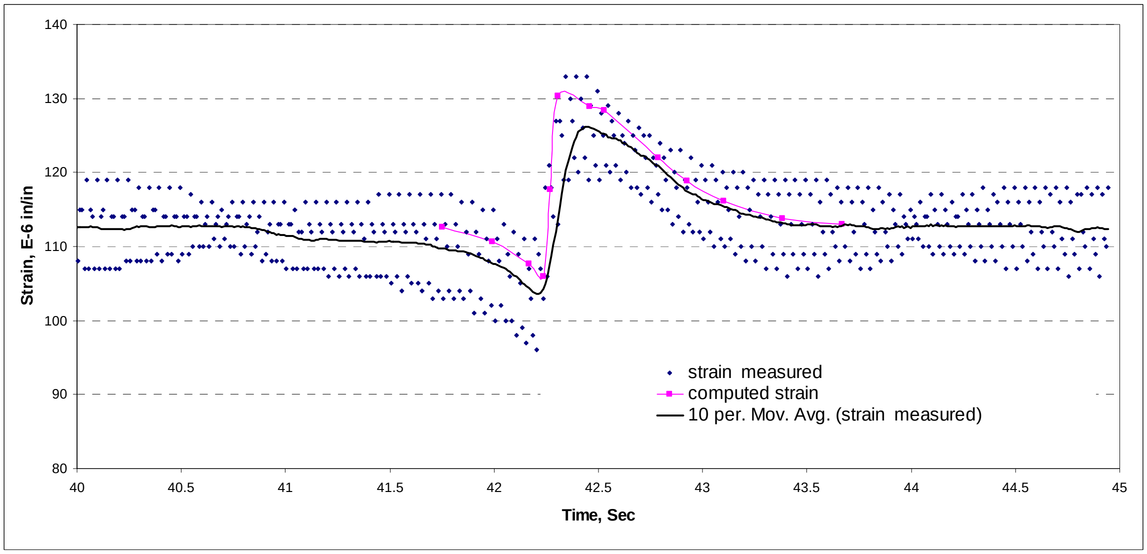

Figure 65. Measured and computed strains for gauge 2 on Slab 1C

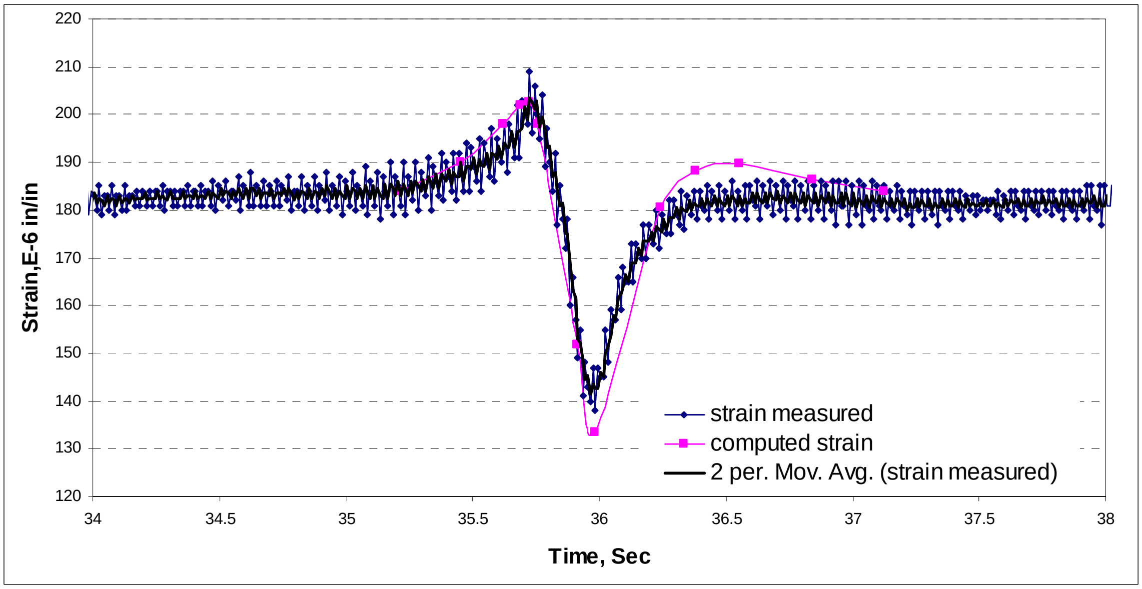

Figure 66. Measured and computed strains for gauge 4 on Slab 1C

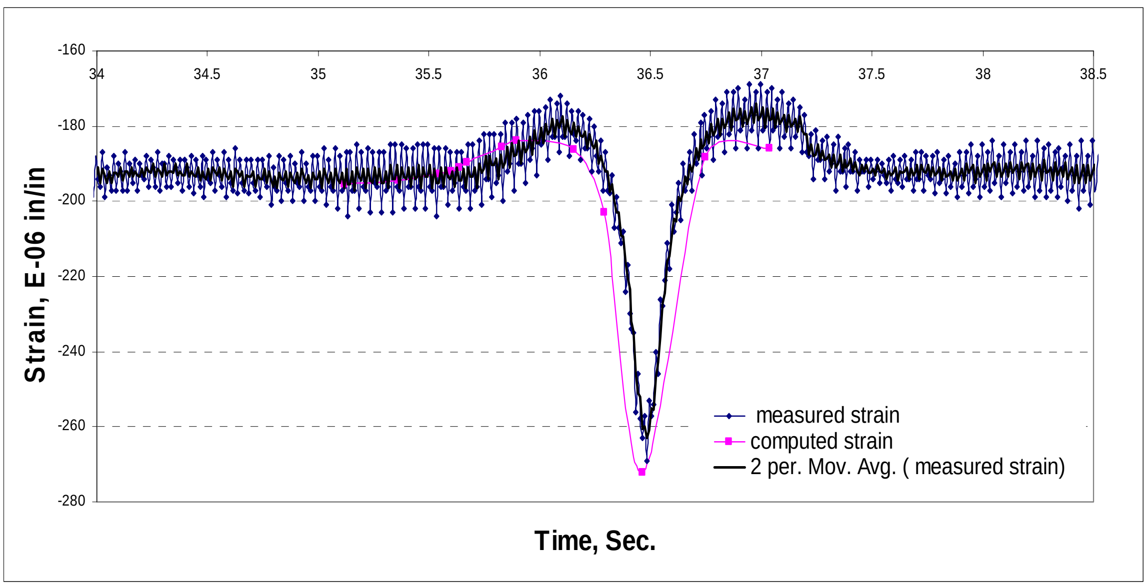

Figure 67. Measured and computed strains for gauge 5 on Slab 1C

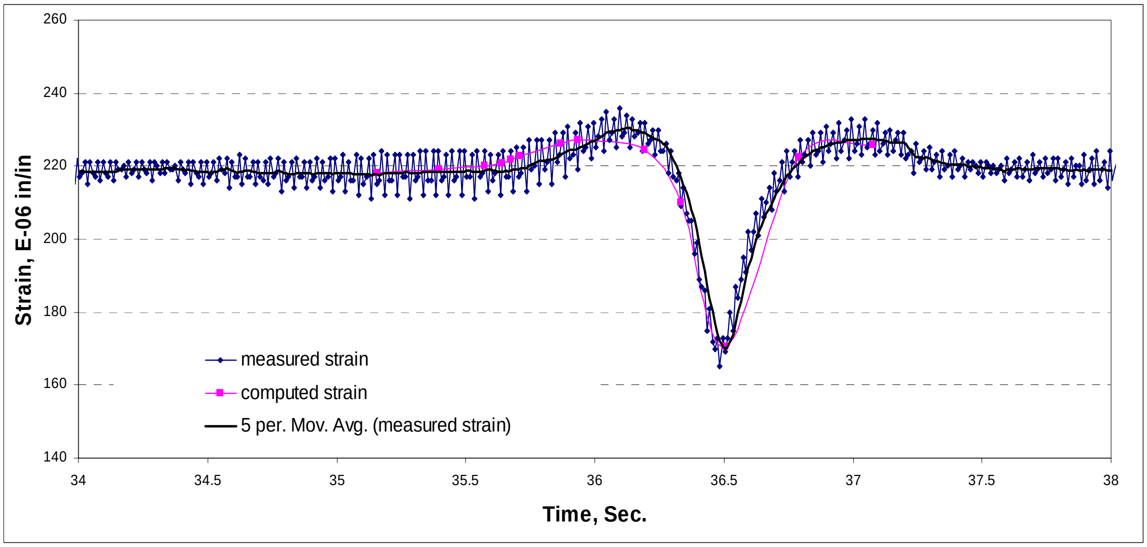

Figure 68. Measured and computed strains for gauge 6 on Slab 1C

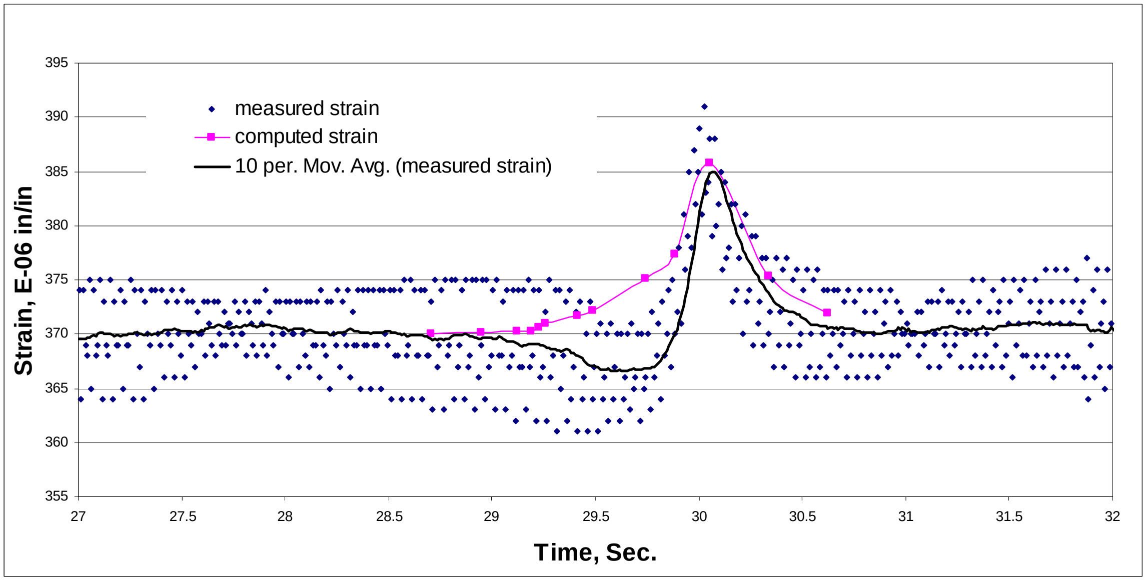

Figure 69. Measured and computed strains for gauge 7 on Slab 1C

It can be seen from these figures that the computed strains are generally fairly close to the measured values. The closeness of the analytical strains to the measured strains indicates that the FEACONS program can model the response of the concrete slab fairly well and can be used to analyze the behavior of the slab under other critical load and thermal conditions.

7.3 Analysis of Static Strain Data

The FEACONS program models the wheel loads as static loads no matter whether the loads are moving or stationary. Questions arise as to whether it is valid to model a moving load as a static load as done in the FEACONS program, and the possible difference between the stresses caused by a static load and those caused by a moving load of the same magnitude. This question was investigated by comparing the measured strains from the installed strain gauges when a test slab was loaded by a moving HVS wheel load, with those when the slab was loaded by a static wheel load of the same magnitude. However, the attempt to apply a static wheel load of a fixed and specified magnitude ran into some technical challenges. In the initial attempt, the HVS wheel was placed on the specified location and the load was gradually increased to the specified magnitude. When the load was noted to have reached the specified magnitude, the load was then released immediately. The reason that the static load had to be applied in this manner was due to the fact that it required some time before a static HVS load could be stabilized to a specified level. Figure 70 shows the responses of gauges 1 and 2 when a static wheel load was placed at the slab corner of Slab 1G and gradually increased to an intended magnitude of 12-kip, and then released immediately. As can be observed from Figure 70, the measured strains increased as the applied load was increased. As the load was released when it reached the intended magnitude, the measured strains were observed to drop suddenly. There were two main concerns with this method of loading. First, there was not a time during the test when the applied load was truly static. Second, it cannot be ascertained that the exact intended load magnitude was reached when the load was released. Due to these concerns, a second method for applying the static load was used.

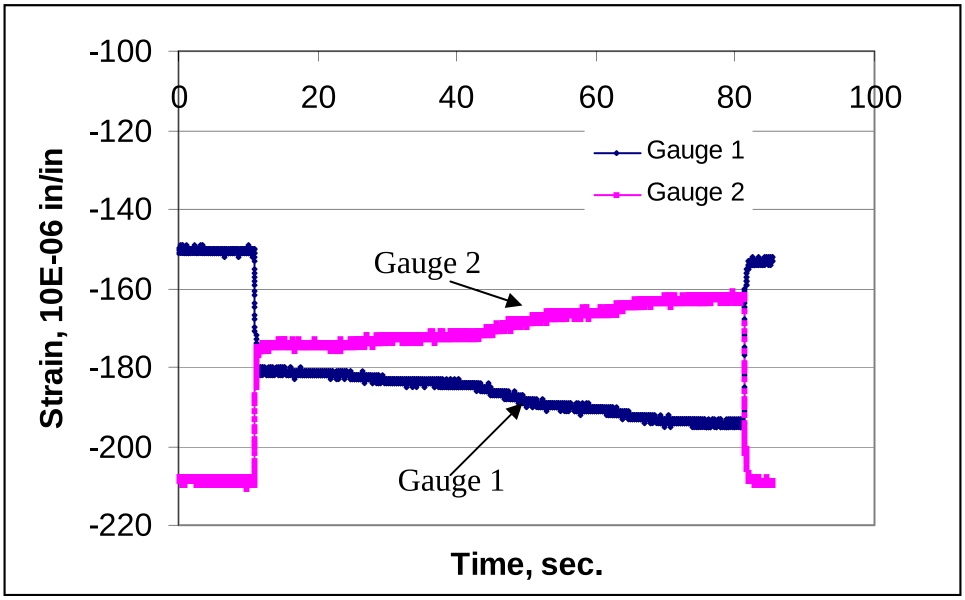

Figure 70. Measured strains at Slab 1G in the first method of applying a static load

In the second method for applying a static load, the HVS wheel was first placed at a location away from the intended load location. The wheel load was increased until it reached and stabilized at the intended load level. The HVS wheel was then moved slowing to the intended test location, and kept at the intended load location for about 10 seconds. Figure 71 shows the plot of measured strains versus time from gauges 1 and 2 for a static load applied at the corner of Slab 2G on the 3rd day of loading. It shows that the strain during the static loading period remained fairly constant except for some noises picked up by the data acquisition system. It can also be seen that the static loading did not cause any residual strains in the concrete. After the wheel load was moved away from the load location, the measured strains from gauges 1 and 2 can be seen to return to their original values before loading.

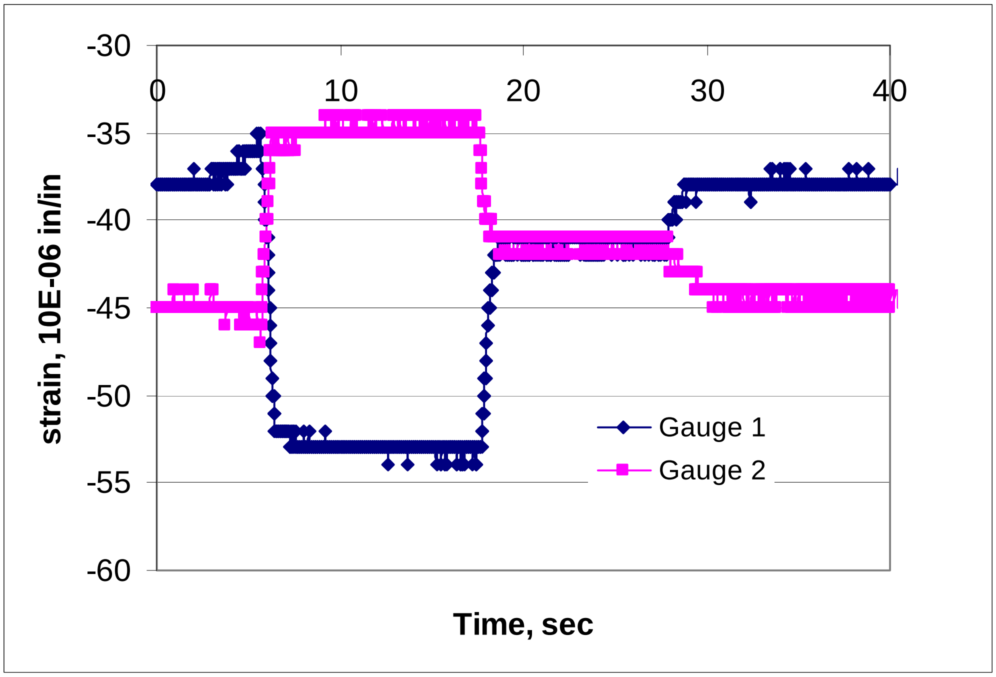

Figure 71. Measured strains at Slab 2G in the second method of applying a static load

The measured strains due to static loads were compared with those due to moving loads of the same magnitude. Figure 72 shows the comparison of the maximum measured strains from gauges 1 and 4 on Slab 2G caused by a 12-kip static load with the maximum measured strains due to a moving load of the same magnitude. It can be seen that the difference between the measured static and dynamic strains is small and fluctuates between positive and negative values. This means that there is no significant difference between the pavement response from a static load and that from a moving load of this speed. Thus, it is proper to model a moving load of this speed as a static load, as done in the FEACONS analysis.

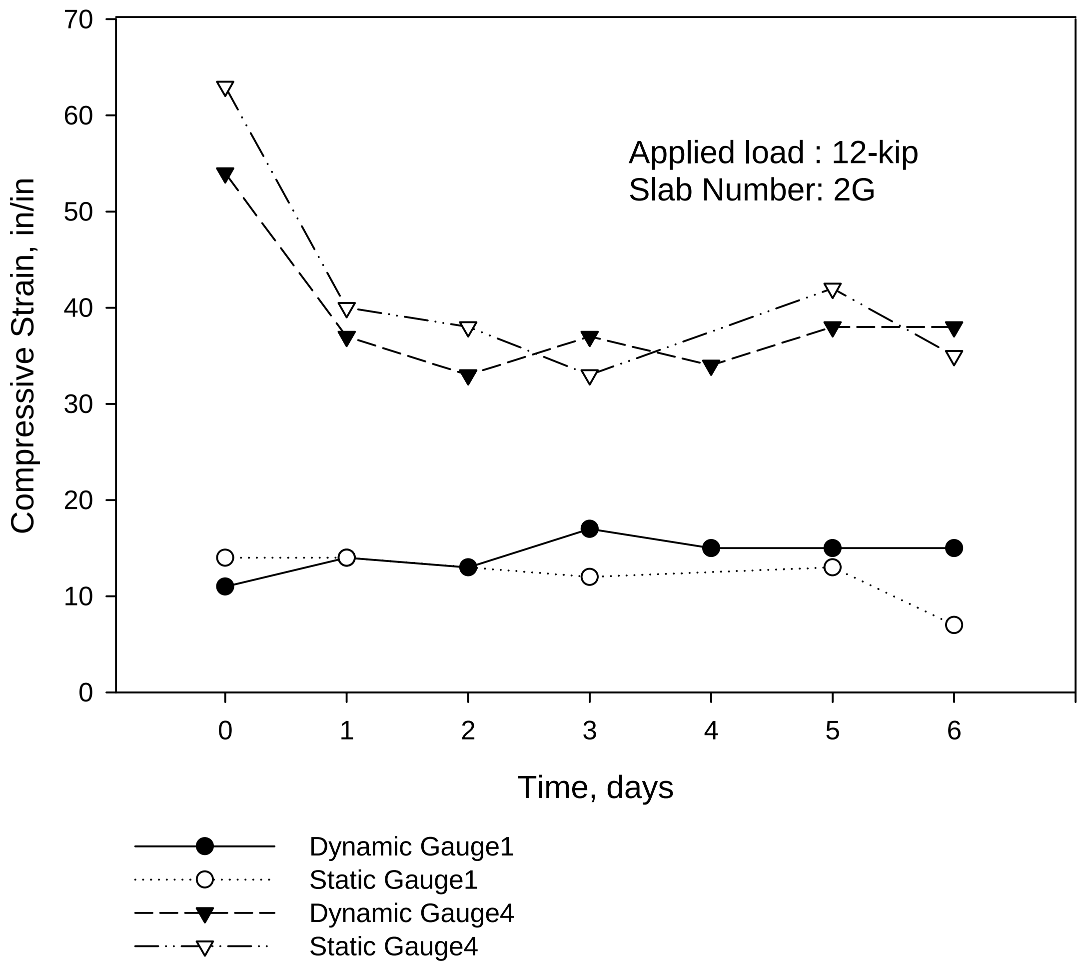

Figure 72. Comparison of maximum measured dynamic and static strains

7.4 Impact Echo Test Results

The impact echo test was used to measure the P-wave speed along the grid lines marked on the corner and the mid-edge of the test slab. These impact echo tests were performed during the times when the HVS was stopped for maintenance. The grid lines used on Slab 1G are shown on Figure 73. On the same figure is also shown the location of the corner crack which appeared later on that slab. The plots of measured P-wave speed along lines 3, 4, 8,10,15,16 at the corner of the Slab 1G are shown in Figures 74 through 79, respectively. The plots show generally an increase in P-wave speed with

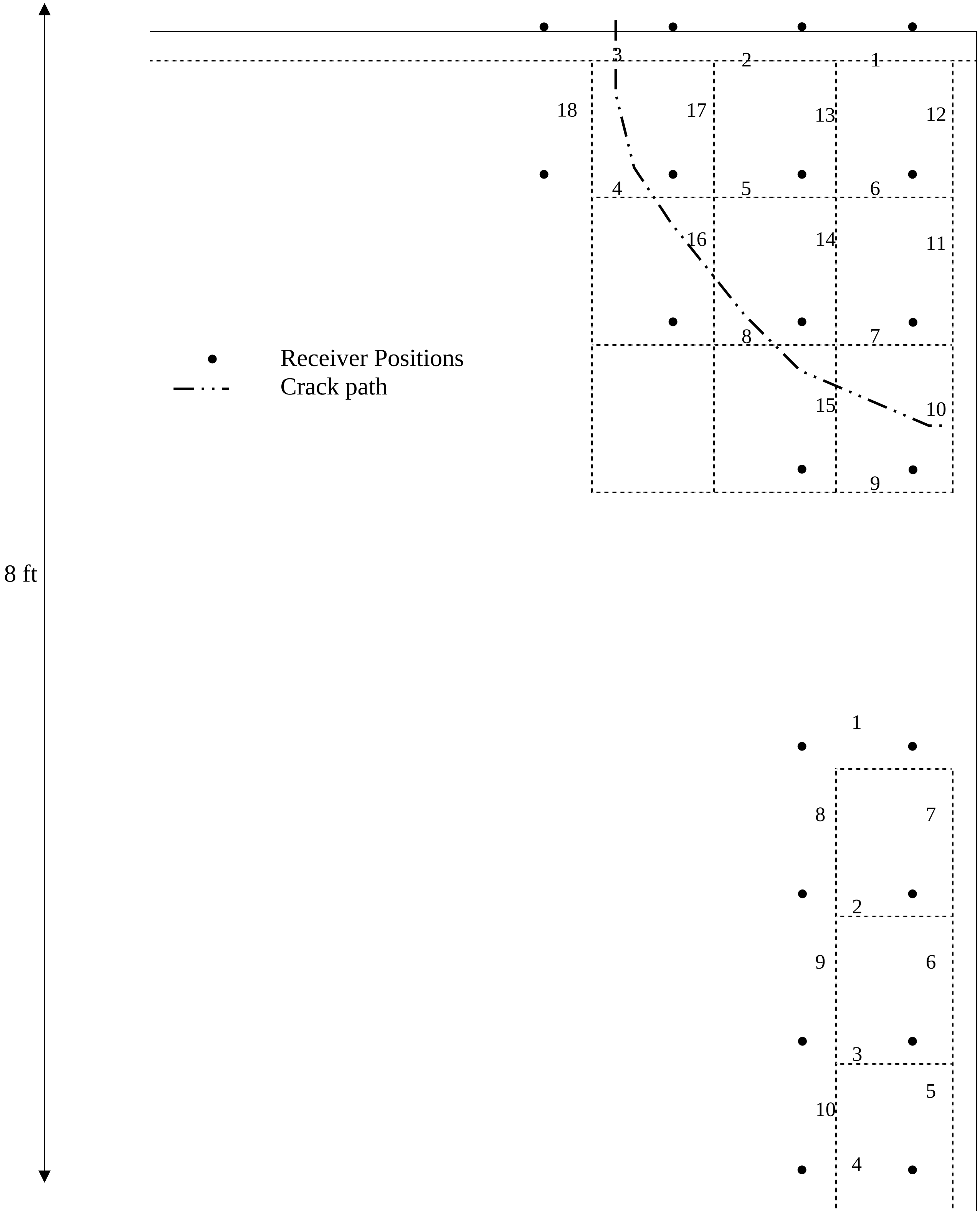

Figure 73. Grid lines for impact echo test and location of corner crack on Slab 1G

time as the concrete gained strength and its elastic modulus increased. However, after the corner crack was formed across the grid lines on 9/27/03, the P-wave speed can be seen to decrease drastically.

Impact echo test data collected at the mid edge and the northbound corner of Slab 1C did not show any reduction of the P-wave speed since the cracks did not developed in the middle or northbound corner of the slab.

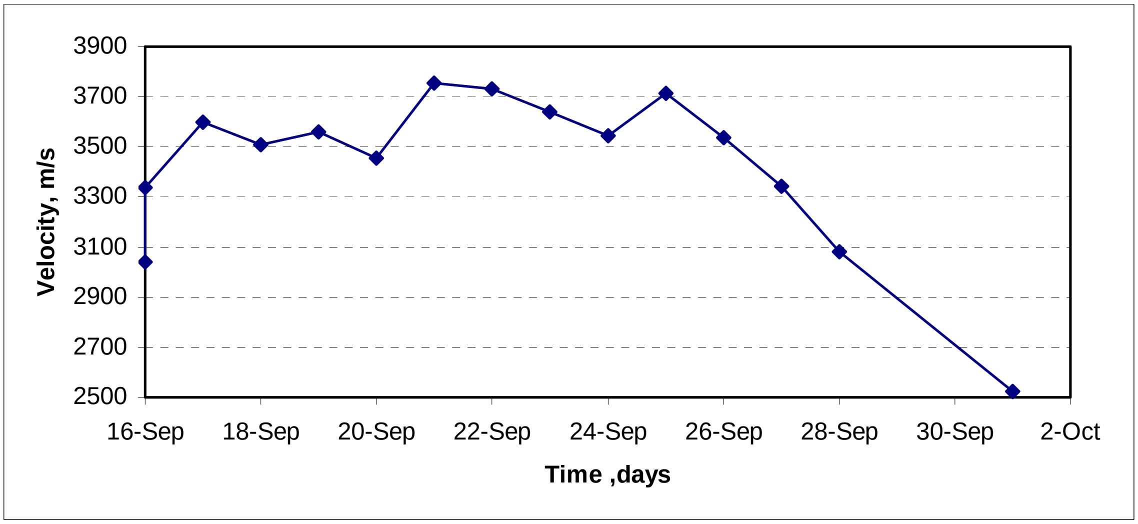

Figure 74. Measured P-wave speed along line 3 at corner of Slab 1G

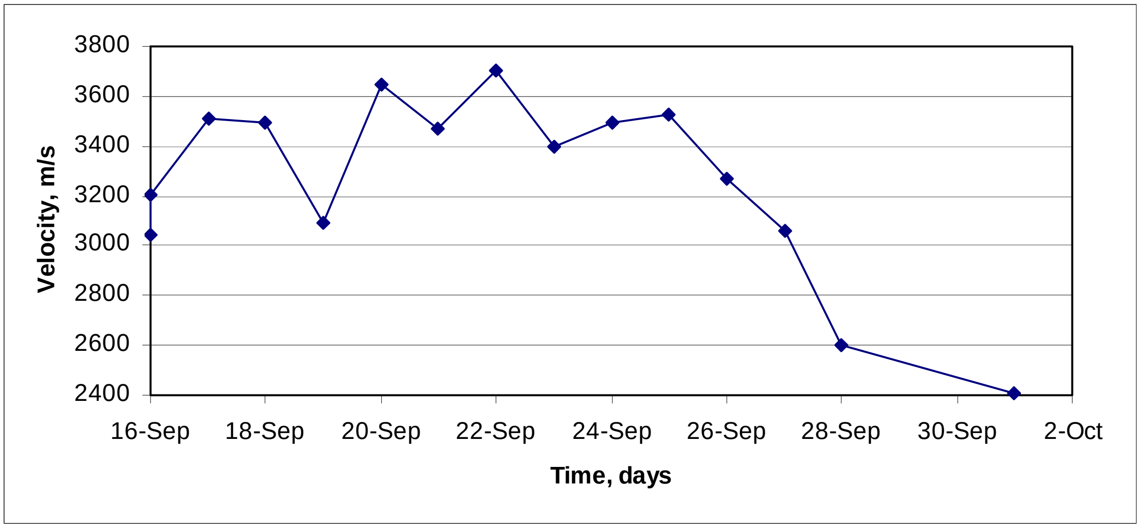

Figure 75. Measured P-wave speed along line 4 at corner of Slab 1G

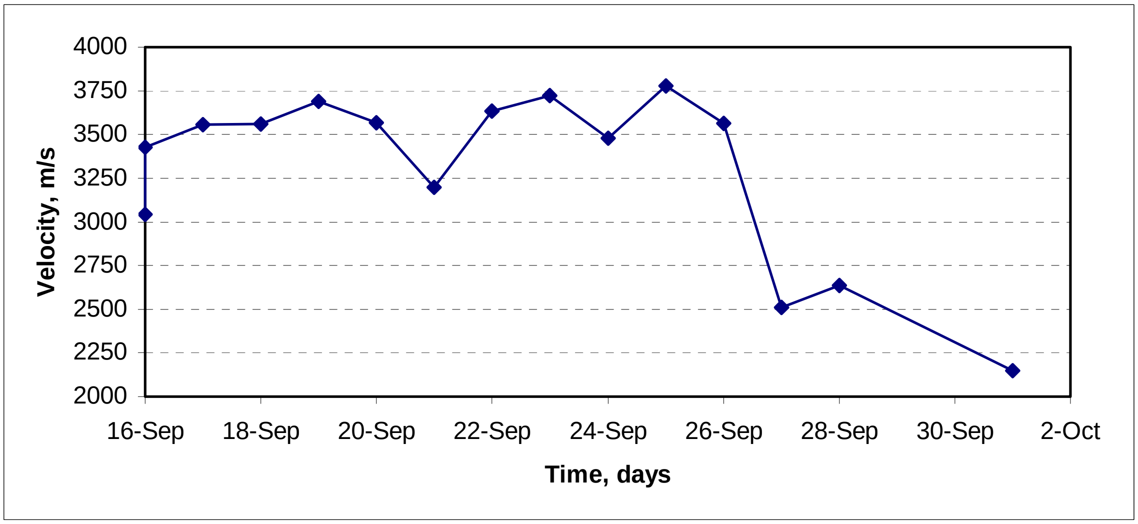

Figure 76. Measured P-wave speed along line 8 at corner of Slab 1G

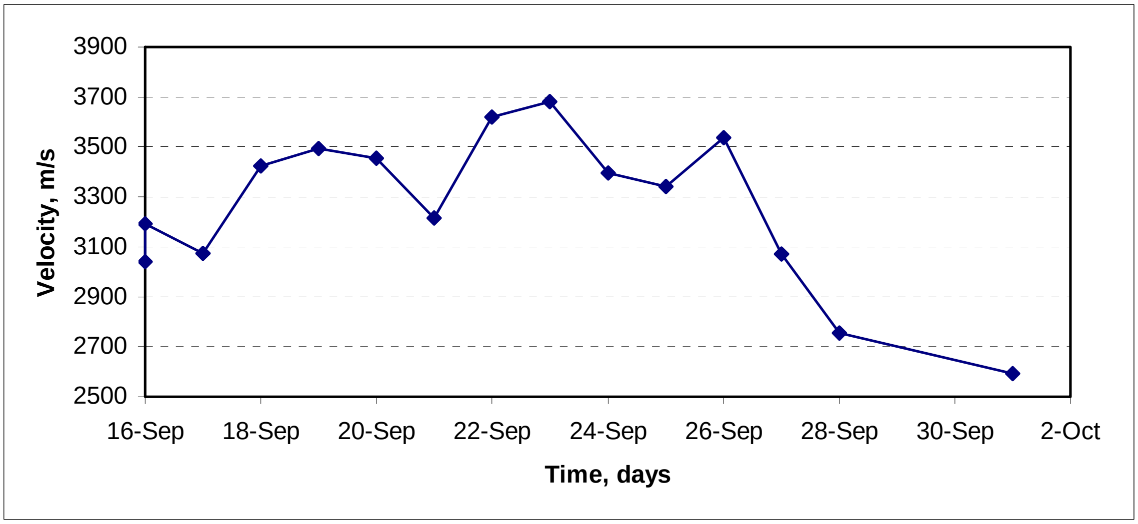

Figure 77. Measured P-wave speed along line 10 at corner of Slab 1G

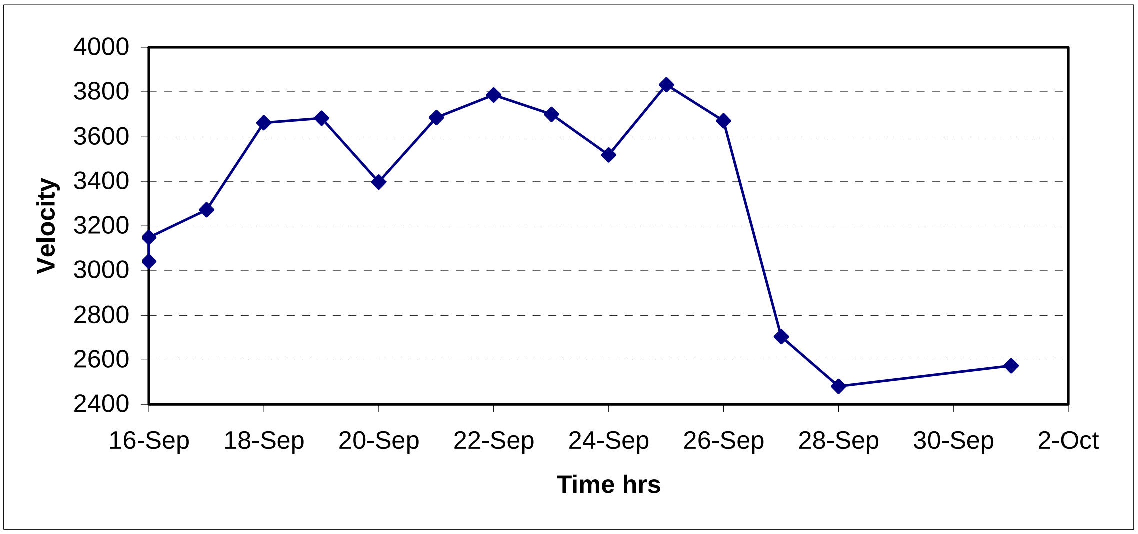

Figure 78. Measured P-wave speed along line 15 at corner of Slab 1G

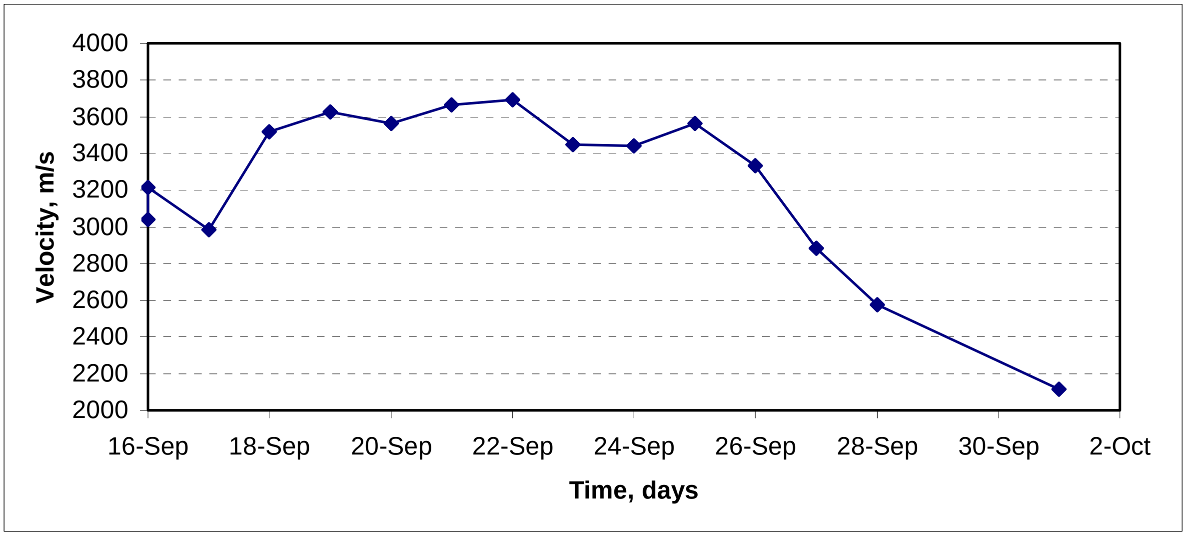

Figure 79. Measured P-wave speed along line 16 at corner of Slab 1G

7.5 Analysis of Performance of Concrete Mixes

7.5.1 Computation of Stresses in the Test Slabs

The FEACONS program was used to calculate the maximum stresses in each test slab due to the HVS loads at various times. The applicable pavement parameters (i.e., effective modulus of subgrade reaction, joint stiffnesses and edge stiffness), concrete elastic modulus, HVS load, and the temperature differential in the concrete slab for each particular condition were used in each analysis. The coefficient of thermal expansion of the concrete was assumed to be $4.5 \times 10^{-6}/\ °F$.

The concrete elastic modulus is an important material property that affects the stress/strain behavior of the concrete slab, and is a needed input to the FEACONS model. The elastic moduli of the concrete at the various ages were obtained from the results of elastic modulus tests, and are shown in Table 5 in Chapter 4. When an elastic modulus from direct measurement was not available, it was first estimated from the compressive strengths of the concrete at the corresponding age by the following equation:

$$E = 33\ w^{1.5} \times f_c^{0.5} \qquad \text{(Eq. 1)}$$

where E = elastic modulus, in psi

w = unit weight, in pci

f_c = compressive strength , in psi

The computed elastic modulus (E) from the above equation was then adjusted by multiplying by the ratio of the measured and the computed elastic modulus values as computed from the available data.

In order to evaluate the likelihood for the concrete to crack at the various times and conditions, the maximum computed tensile stresses were divided by the flexural strength of the concrete at the corresponding age to obtain the stress-strength ratio. The flexural strengths of the concrete at the various ages were obtained from the results of flexural strength tests as shown in Table 5. When the flexural strength from direct measurement was not available, it was first estimated from the compressive strength of the concrete at the corresponding age by the following equation:

$$R = 7.5 \times f_c^{0.5} \qquad \text{(Eq. 2)}$$

where R = flexural strength, in psi

f_c = compressive strength , in psi

The computed flexural strength (R) from the above equation is then adjusted by multiplying by the ratio of measured flexural strength to computed flexural strength as computed from the available data.

The ratios between the computed stress and the flexural strength were computed at curing times of 4, 6, and 8 hours and 1, 3, 7, 9, and 28 days, at which the samples were tested for their compressive strength, elastic modulus and flexural strength in the laboratory. The computation of stress to strength ratios for Slabs 1C, 1G, 2C, 2E and 2G are shown in Tables 11 through 15, respectively. Figure 80 shows the plots of stress to strength ratio versus the number of 12-kip HVS wheel load passes for these five test slabs.

Table 11. Computation of Stress to Strength Ratios for Test Slab 1C (Mix 1)

Time (hrs)	Temperature Differential (° F)	Accumulated HVS Passes	Applied Load (kips)	Compressive Strength (psi)	Elastic Modulus (ksi)	Computed Stress (psi)	Flexural Strength (psi)		Computed Stress / Strength
							Computed	Measured or Adjusted	
4	3.2	0	12	980	1711	227.0	235	258	0.88
6	4.9	0	12	1700	2254	253.0	309	340	0.74
8	1.8	0	12	2260	2599	246.0	357	392	0.63
24	7.4	5311	12	4750	3767	321.0	517	569	0.56
72	7.0	29090	12	5280	3972	324.0	545	599	0.54
168	6.5	74680	12	5960	4220	326.0	579	637	0.51
216	6.5	86001	12	6026	4243	327.0	582	640	0.51
216	6.5	86001	15	6026	4243	390.0	582	640	0.61
312	*6.5	145000	15	6158	4290	391.0	589	647	0.60
312	*6.5	145000	18	6158	4290	455.0	589	647	0.70
360	*6.5	156300	18	6224	4313	457.0	592	651	0.70
672				6653	4459		612	673	

* data is not available. Assumed the temperature differential of the last day of data collection

Table 12. Computation of Stress to Strength Ratios for Test Slab 1G (Mix 2)

Time (hrs)	Temperature Differential (° F)	Accumulated HVS Passes	Applied Load (kips)	Compressive Strength (psi)	Elastic Modulus (ksi)	Computed Stress (psi)	Flexural Strength (psi)		Computed Stress / Strength
							Computed	Measured or Adjusted	
4	– 6.1	0	12	710	1267	206	200	220	0.94
6	6.3	0	12	1100	1577	257	249	274	0.94
8	7.7	1015	12	1520	1854	275	292	322	0.85
24	14.9	9134	12	3340	2749	362	433	477	0.76
72	13.9	44987	12	4803	3300	381	520	572	0.67
168	13.7	95187	12	5540	3540	396	558	614	0.64
216	12.4	115996	12	5633	3579	385	563	619	0.62
216	12.4	115996	15	5633	3579	453	563	619	0.73 (15 kips)
264	9.5	139128	15	5727	3618	428	568	624	0.69 (15 kips)
672				6520	3950		606	666	

Table 13. Computation of Stress to Strength Ratios for Test Slab 2C (Mix 3)

Time (hrs)	Temperature Differential (° F)	Accumulated HVS Passes	Applied Load (kips)	Compressive Strength (psi)	Elastic Modulus (ksi)	Computed Stress (psi)	Flexural Strength (psi)		Computed Stress / Strength
							Computed	Measured or Adjusted	
4	1.4	0	12	480	1030	217	164	164	1.32
6	– 3.4	0	12	860	1388	216	220	220	0.98
8	– 7.2	990	12	1170	1627	208	257	257	0.81
24	9.5	8914	12	2770	2629	319	395	434	0.73
72	20.2	33176	12	3883	3223	435	467	514	0.85
168	20.2	82243	12	5020	3826	472	531	585	0.81
672				6510	4366		605	666	

Table 14. Computation of Stress to Strength Ratios for Test Slab 2E (Mix 4)

Time (hrs)	Temperature Differential (° F)	Accumulated HVS Passes	Applied Load (kips)	Compressive Strength (psi)	Elastic Modulus (ksi)	Computed Stress (psi)	Flexural Strength (psi)		Computed Stress / Strength
							Computed	Measured or Adjusted	
4	– 1.8	0	12	630	1221	221	188	188	1.18
6	0	0	12	1250	1730	234	265	260	0.90
8	0	1000	12	1560	1920	243	296	296	0.82
24	17.2	7695	12	3440	2620	372	440	525	0.71
72	15	30780	12	4340	2920	372	494	595	0.63
168	5	40809	12	4980	3230	299	529	650	0.46
192									
192									

Table 15. Computation of Stress to Strength Ratios for Test Slab 2G (Mix 5)

Time (hrs)	Temperature Differential (° F)	Accumulated HVS Passes	Applied Load (kips)	Compressive Strength (psi)	Elastic Modulus (ksi)	Computed Stress (psi)	Flexural Strength (psi)		Computed Stress / Strength
							Computed	Measured or Adjusted	
4	3.2	0	12	670	1174	228	194	186	1.22
6	4.9	0	12	1210	1569	252	261	250	1.01
8	1.8	1000	12	1830	1775	248	321	308	0.81
24	7.4	7000	12	3850	2514	301	465	530	0.57
72	7.0	20000	12	4650	2789	309	511	563	0.55
168	6.5	70000	12	5530	2953	311	558	600	0.52

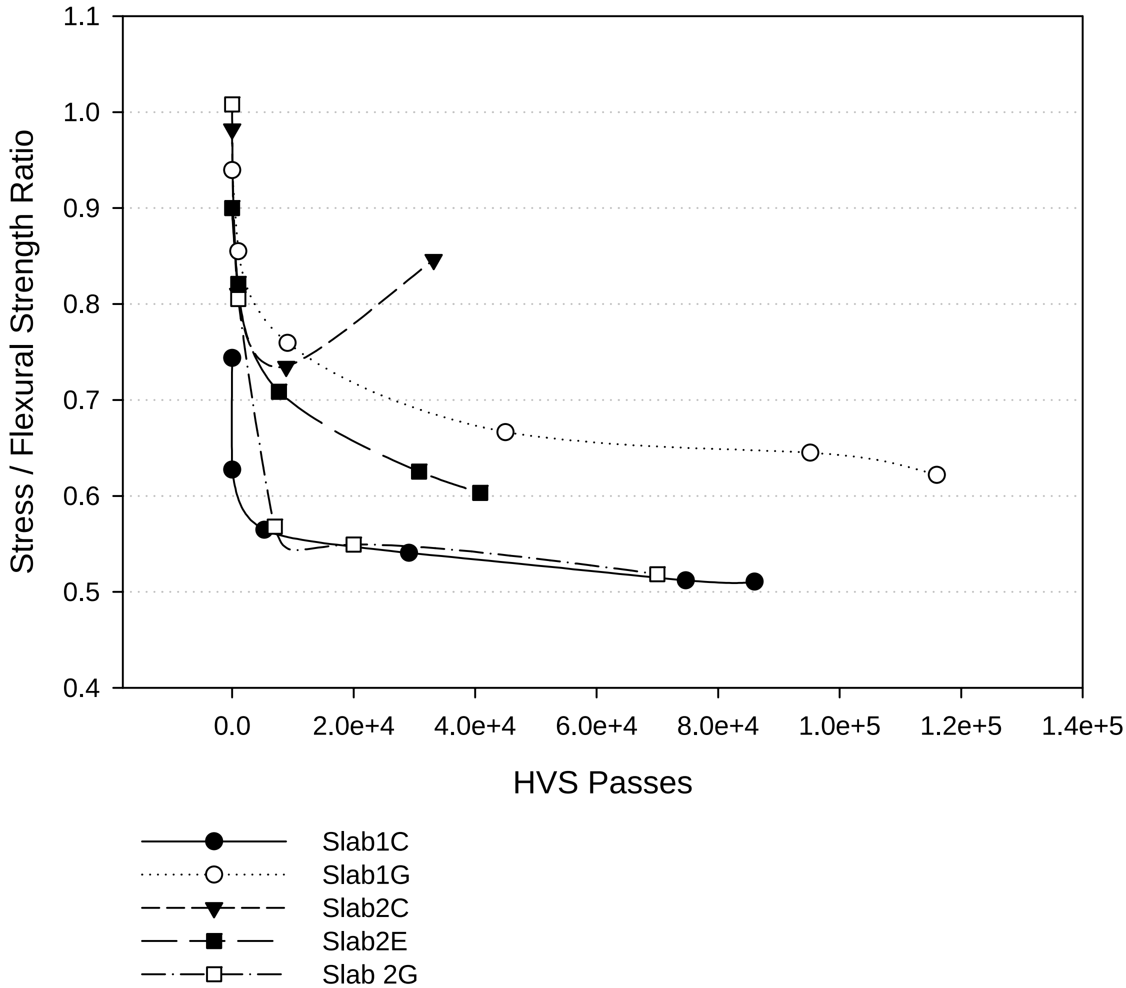

Figure 80. Stress/ flexural strength ratio versus HVS passes

7.5.2 Relating Stress/Strength Ratio to Observed Performance

The computed stress/strength ratios for the mixes as shown in Figure 80 can be used to explain the observed performance of the different test slabs. Slab 1C and Slab 2G used the same mix design (with a cement content of 850 lbs/yd^3) and had similar strength and stress/strength ratio at later ages. However, the mix used in Slab 2G had a much lower early strength and a much higher stress/strength ratio at early age. The computed stress/strength ratio for Slab 2G at early age (6 hours) was higher than 1.0. This explains why Slab 2G failed prematurely, while Slab 1C performed well.

Slabs 1G, 2C and 2E show the same trend in stress/strength ratio at early age of the concrete. Slab 1G performed well, and can be explained by its computed stress/strength ratio less than 1 throughout. However, cracks developed on Slab 2C on the 3rd day of loading due to a high temperature gradient (+20° F) present in the concrete slab, which induced higher stresses in the slab. This can be seen from the sharp increase in the stress/strength ratio for Slab 2C on the third day.

The crack that developed in Slab 2E was postulated to be caused by the locking up of the dowel bars at the joint. It was noted that the crack on Slab 2E was different from the cracks on the other slabs. While the cracks on other slabs propagated gradually from the loading edge to the joints or the opposite edge, the crack that developed on Slab 2E was a single transverse crack that cut across the entire slab and occurred in a short time. That crack occurred right after the HVS loading was resumed after three days of shutdown due to a mechanical problem. From the appearance of the deep transverse crack across the middle of the slab, it was postulated that the crack might be caused by the high stresses from the locking up of the dowel bars at both joints. When the slab tried to contract at night but could not due to the locked dowel bars at the joint, the tensile stresses would be induced, which could crack the slab across the center.

7.5.3 Required Concrete Properties for Performance

The results from this experimental study show that loading a concrete slab at the early age when the induced stress may be higher than the strength of the concrete will adversely affect the performance of the slab. What should the required properties of the concrete for slab replacement be? Basically, the concrete used should be such that the anticipated maximum tensile stresses should be less than the flexural strength of the concrete at the time when the slab is open to traffic.

Using the pavement conditions of the test slabs in this study (9-inch slab on a strong foundation) and an applied wheel load of 12 kips, the stress/strength ratios of concrete of different compressive strengths are computed for different temperature differentials in the slab. In doing these computations, the elastic modulus of the concrete was assumed to be related to the compressive strength by Equation 1, and the flexural strength was related to the compressive strength by Equation 2, as presented earlier. The coefficient of thermal expansion of concrete was assumed to be 4.5×10^{-6}/ °F. Figure 81 shows the plot of the computed stress/strength ratio as a function of compressive strength by using the assumed relationships as given by Equations 1 and 2, for a 9-inch concrete slab with similar foundation as that of the test slab and subjected to a 12-kip wheel load.

It is to be noted that if the relationships among the compressive strength, elastic modulus and flexural strength are different, the plot of computed stress/strength ratio versus compressive strength would be different. Using the limited data from this study, the relationship between compressive strength and the elastic modulus was developed, and plotted in Figure 82. The relationship between the flexural strength and the compressive strength was also developed and plotted in Figure 83.

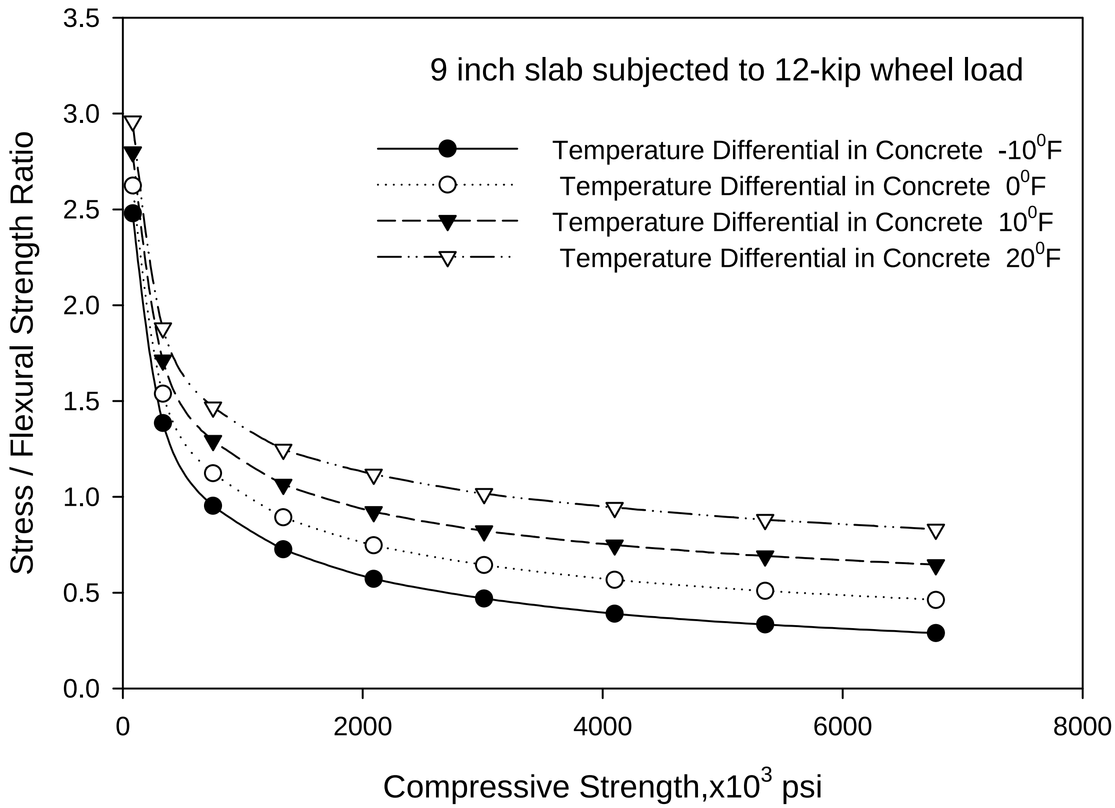

Figure 81. Computed stress/strength ratio versus compressive strength of concrete using ACI equations for relating f_c, E and flexural strength

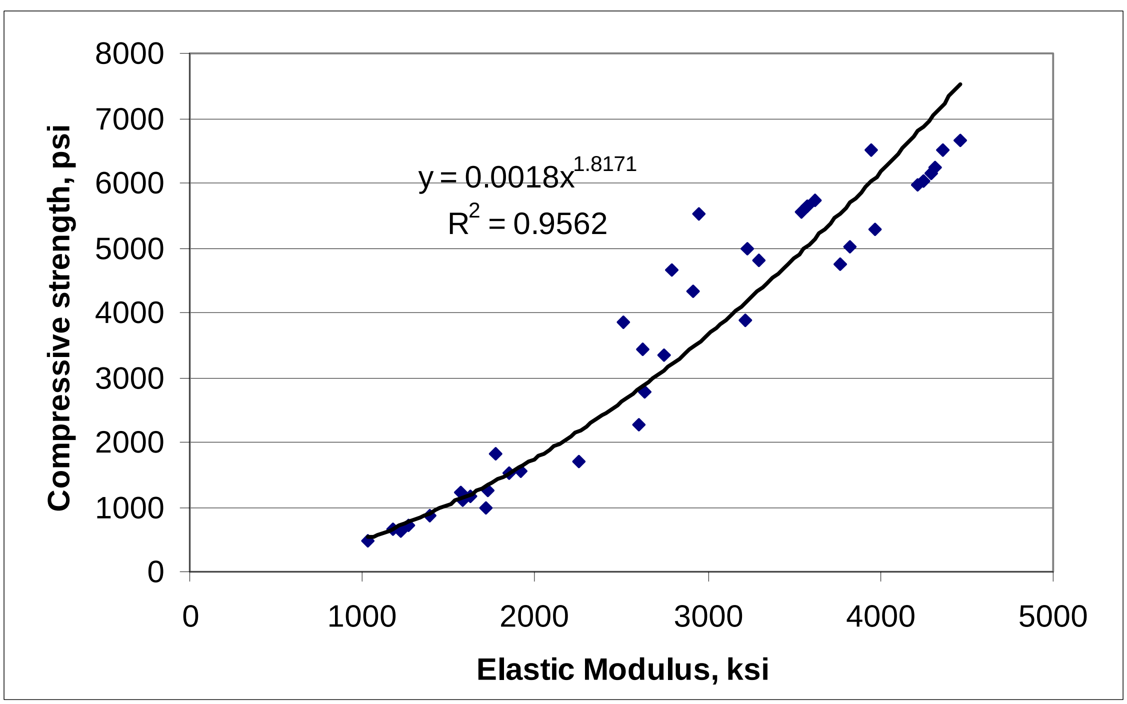

Figure 82. Relationship between compressive strength and elastic modulus

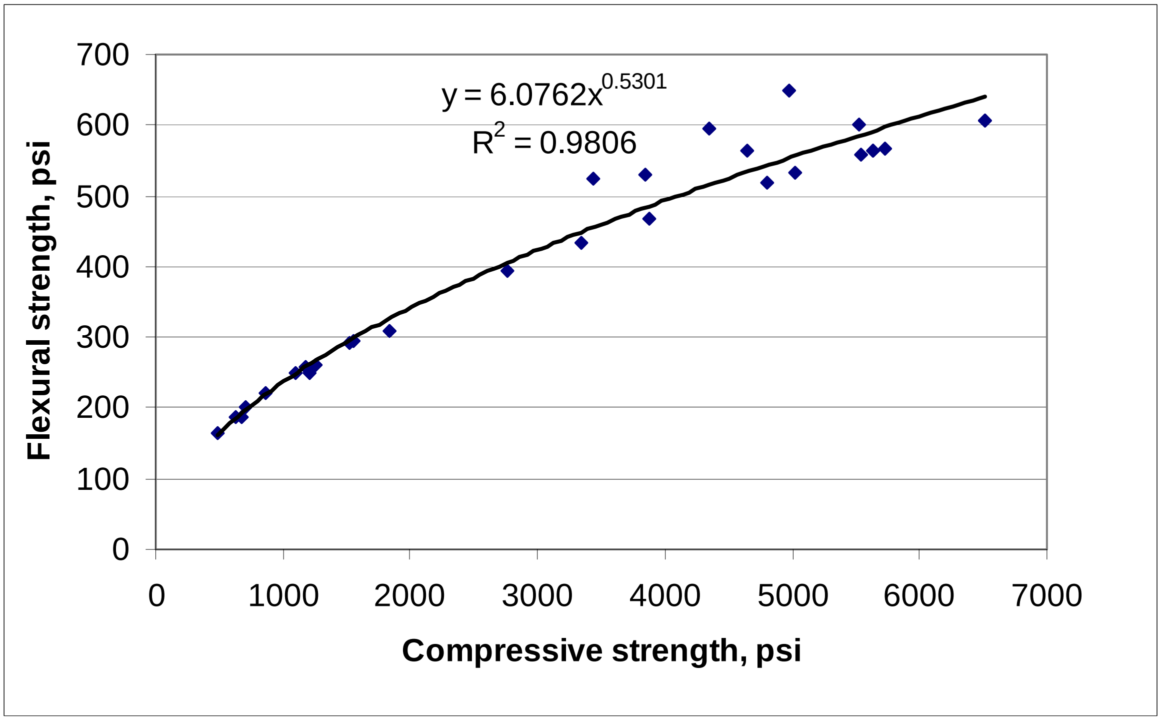

Figure 83. Relationship between flexural strength and compressive strength

The following regression equations were developed from the available data:

$$f_c = 0.0018\ E^{1.8171} \quad R^2 = 0.9562 \qquad \text{(Eq. 3)}$$

$$R = 6.0672\ f_c^{0.5301} \quad R^2 = 0.9806 \qquad \text{(Eq. 4)}$$

Figure 84 shows the plot of computed stress/strength ratio versus compressive strength by using Equations 3 and 4 for relating compressive strength to elastic modulus and flexural strength.

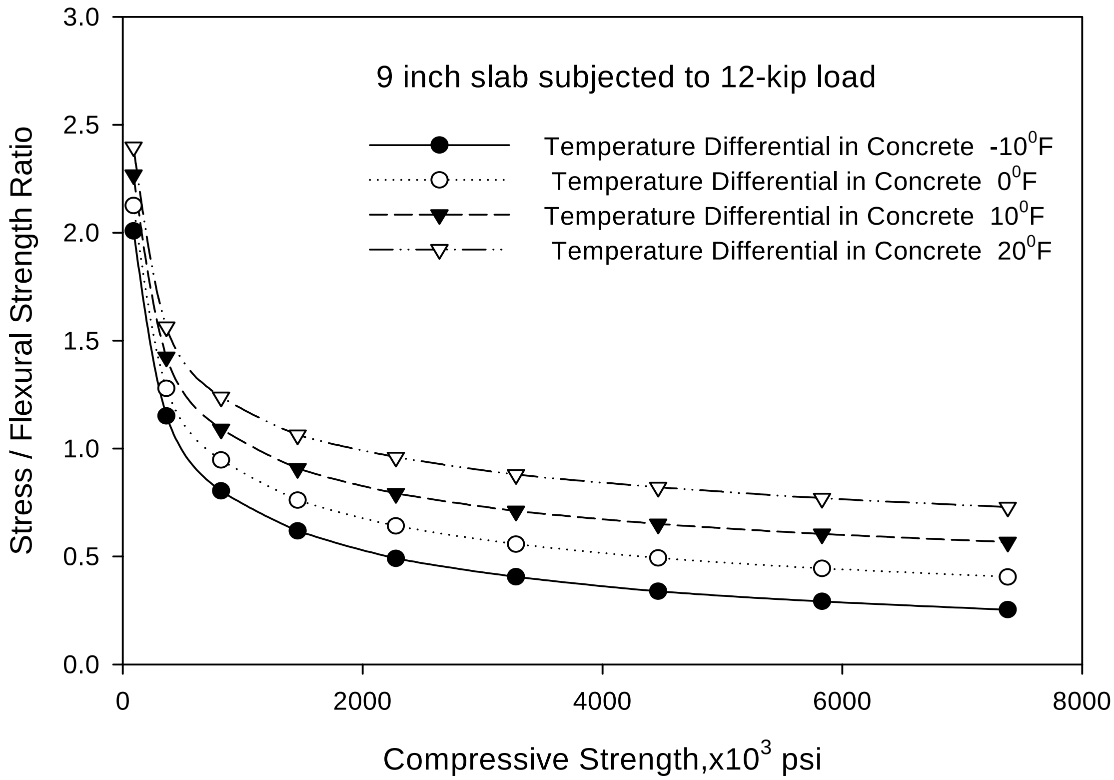

Figure 84. Computed stress/strength ratio as a function of compressive strength using the developed relationship between f_c, E and flexural strength

CHAPTER 8
CONCLUSIONS AND RECOMMENDATIONS

8.1 Summary of Findings

Five 9-inch thick concrete replacement slabs were constructed and tested by a Heavy Vehicle Simulator (HVS), which applied a 12-kip super single wheel load in a uni-directional mode along the edge of the slab beginning at 6 hours after the placement of concrete. Two of the test slabs (1C and 2G) used a concrete with a cement content of 850 lbs per cubic yard of concrete, while the other three test slabs (1G, 2C and 2E) used a concrete with a cement content of 725 lbs per cubic yard of concrete. The results of the experiments indicated that Slabs 1C and 1G performed well, while Slabs 2C, 2E and 2G cracked prematurely under the 12-kip wheel loads.

The FEACONS (Finite Element Analysis of CONcrete Slabs) computer program was used to model the response of the test slabs and to compute the stresses in the concrete slabs due to the applied loads and the temperature differentials in the concrete slabs. The good performance of Slabs 1C and 1G, which had different cement contents and different strengths from one another, was attributed to the fact that the temperature-load induced stresses were much lower than the flexural strengths of the concretes. The premature cracking of Slabs 2C and 2G, which also had different cement contents and different strengths from one another, was attributed to the fact that the temperature-load induced stresses exceeded the estimated flexural strength of the concrete during the early age of the concretes.

The premature cracking of Slab 2E could not be explained by the computed temperature-load induced stresses. From the appearance of the deep transverse crack across the middle of the slab, it was postulated that the cracking might be caused by the locking-up of the dowel bars at both joints.

Impact echo tests were used successfully in this study to detect cracks in a concrete slab. This was manifested by a sudden drop in the apparent measured speed of P waves across the location of cracks. Cracks in the concrete slab were also successfully detected from observed changes in the measured strains from strain gages that had been installed in the concrete.

The predicted strains in the concrete slab as calculated by the FEACONS program matched fairly well with the measured strains from the installed strain gages. The measured maximum strains caused by a moving HVS wheel load were found to match fairly well with the measured maximum strains caused by a static wheel load of the same magnitude. This indicates that it is proper to model a moving load of this type by a static load as used in the FEACONS program.

Plots of stress to flexural strength ratio versus compressive strength of concrete were developed for a typical 9-inch concrete replacement slab subjected to a 12-kip wheel load and different temperature differentials in the concrete slab. When the ACI equations were used to relate the compressive strength to elastic modulus and flexural strength of concrete (as presented in Figure 81), a compressive strength of 1600 psi or above at the time of the loading of the concrete slab, with a temperature differential of 10° F, would be required to ensure that the induced stress would not exceed the flexural strength (or the stress to strength ratio of less than 1). When the relationships between the compressive strength, elastic modulus and flexural strength as developed from the limited test data from this study were used (as shown in Figure 84), a compressive strength of 1100 psi or above at the time of the loading of the concrete slab, with a temperature differential of 10° F, would be required to ensure that the stress to strength ratio would be less than 1.

8.2 Conclusions

The results from this study show that the performance of a concrete replacement slab depends not just on the cement content of the concrete mix, as two concrete slabs with the same concrete mix design can have drastically different performance. The performance of a concrete replacement slab will depend on whether or not the concrete will have sufficient strength to resist the anticipated temperature-load induced stresses in the concrete slab. The strength development of a concrete depends not only on the mix design but also the condition under which the concrete is cured. The anticipated temperature-load induced stresses are a function of the slab thickness, effective modulus of subgrade reaction, modulus of the concrete, coefficient of thermal expansion of the concrete, anticipated loads and anticipated temperature differentials in the concrete slab. The anticipated stress must be lower than the anticipated flexural strength of the concrete at all times to ensure good performance.

Based on the limited test results from this study, it appears that for a 9-inch slab placed on an adequate foundation and a maximum temperature differential of +10° F in the concrete slab, a minimum required compressive strength of 1100 to1600 psi for the concrete at the time of application of traffic loads may be adequate. It may be feasible to lower the minimum required compressive strength of 2200 psi at 6 hours, as specified by the current FDOT specifications, to 1600 psi at 6 hours, subject to further testing and verification.

8.3 Recommendations

Due to the limited scope of this study and the limited amount of testing performed in this study, no recommendation for changes in FDOT specifications for concrete replacement slab should be made at this point. It is recommended that further testing and research in this subject area be conducted, with particular focus on the following areas:

1. The use of maturity meter to accurately determine the strength of the in-place concrete, and to determine the time when the concrete will have sufficient strength to be open to traffic.
2. Determination of the relationships between compressive strength, flexural strength and elastic modulus of typical concretes used in replacement slabs in Florida. Accurate determination of these relationships is needed in order to determine the required strength of the concrete before the pavement slab can be open to traffic.
3. Determination of temperature distributions in typical concrete pavement slabs in Florida. This information is needed in order to accurately determine the maximum temperature-load induced stresses in the concrete slabs. The strength of the concrete needs to be higher than this maximum induced stress to avoid cracking.

APPENDIX A
FWD DATA

Table A-1. FWD Test at Center of Slab 2C

Morning Test - 6AM to 9AM

Center Loading on 2C

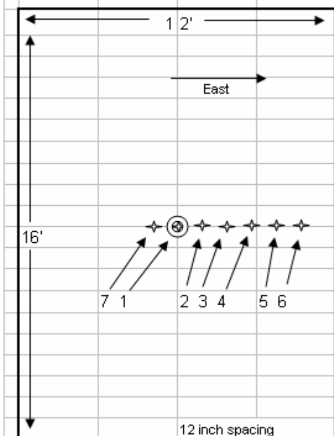

Location: 2C **Geophone:** Date: 11/18/2003

Description: **Slab** **Plate:**

	Load	D1	D2	D3	D4	D5	D6	D7
Test 15	5760	1.17	1	0.83	0.73	0.61	0.51	1.01
Time: 07:18	9045	1.89	1.63	1.37	1.19	1.01	0.86	1.63
	12227	2.7	2.33	1.98	1.7	1.46	1.26	2.33
	Temp	Pav. Sur.	63					
		Air	64					

	Load	D1	D2	D3	D4	D5	D6	D7
Test 16								
Time: 07:26	5732	1.18	1.03	0.87	0.75	0.63	0.54	1.03
	8982	1.88	1.63	1.37	1.18	1	0.85	1.62
	12184	2.69	2.33	1.96	1.7	1.43	1.24	2.31
	Temp	Pav. Sur.	63					
		Air	65					

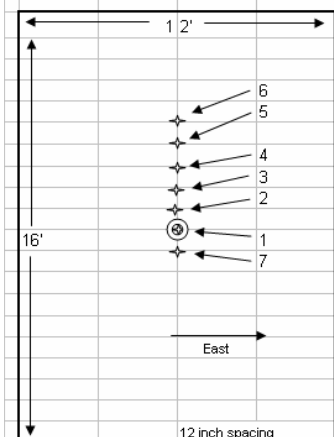

Location: 2C **Geophone:** Date: 11/18/2003

Description: **Slab** **Plate:**

	Load	D1	D2	D3	D4	D5	D6	D7
Test 13	5784	1.15	1	0.88	0.71	0.59	0.48	1.01
Time: 07:11	9041	1.91	1.66	1.39	1.16	0.95	0.78	1.63
	12184	2.72	2.36	2	1.65	1.37	1.12	2.33
	Temp	Pav. Sur.	63					
		Air	65					

	Load	D1	D2	D3	D4	D5	D6	D7
Test 14								
Time: 07:17	5768	1.12	0.96	0.88	0.71	0.53	0.44	0.97
	9077	1.92	1.65	1.38	1.16	0.97	0.8	1.64
	12212	2.7	2.33	1.96	1.65	1.37	1.12	2.32
	Temp	Pav. Sur.	63					
		Air	65					

Note: Load was placed at the center of slabs.

Table A-2. FWD Test at Center of Slab 1G

Morning Test - 6AM to 9AM

Center Loading on 1G

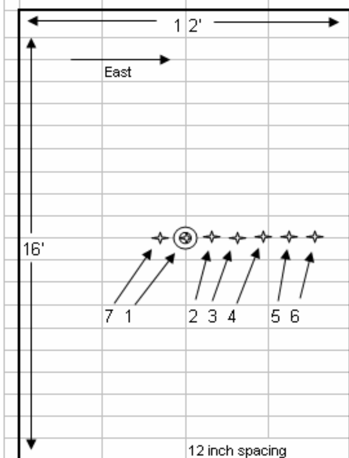

Location: 1G **Geophone:** Date: 11/18/2003

Description: Slab **Plate:**

	Load	D1	D2	D3	D4	D5	D6	D7
Test 10	5510	1.44	1.23	1.04	0.91	0.78	0.7	1.2
Time: 06:58	9030	2.35	2.06	1.75	1.52	1.3	1.17	2.01
	11973	3.39	2.96	2.52	2.19	1.92	1.74	2.87
	Temp	Pav. Sur.	63					
		Air	65					

	Load	D1	D2	D3	D4	D5	D6	D7
Test 11	5450	1.41	1.21	1.02	0.88	0.74	0.65	1.18
Time: 06:59	8978	2.39	2.09	1.78	1.54	1.34	1.22	2.02
	11989	3.38	2.96	2.51	2.19	1.91	1.74	2.85
	Temp	Pav. Sur.	63					
		Air	65					

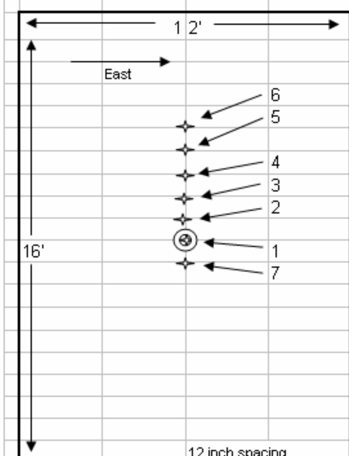

Location: 1G **Geophone:** Date: 11/18/2003

Description: Slab **Plate:**

	Load	D1	D2	D3	D4	D5	D6	D7
Test 9	5550	1.43	1.21	1	0.78	0.62	0.51	1.18
Time: 06:54	9038	2.44	2.09	1.76	1.35	1.12	0.86	2.04
	12025	3.43	2.89	2.4	1.89	1.53	1.2	2.86
	Temp	Pav. Sur.	63					
		Air	65					

	Load	D1	D2	D3	D4	D5	D6	D7
Test 12	5709	1.46	1.23	1	0.78	0.7	0.63	1.22
Time: 07:03	8922	2.39	2.03	1.72	1.35	1.01	0.78	2
	12013	3.38	2.86	2.4	1.88	1.47	1.16	2.82
	Temp	Pav. Sur.	63					
		Air	65					

Note: Load was placed at the center of slabs.

Table A-3. FWD Test at Joint 1G-1F

Midday Test - Noon to 4PM

Joint Loading 1G & 1F

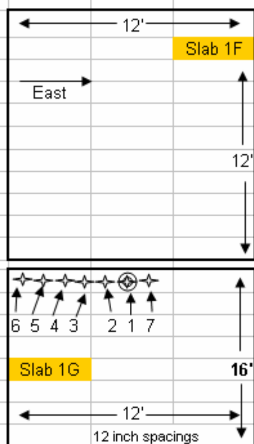

Location: 1G & 1F **Geophone:** **Plate:** Date: 11/18/2003

	Load	D1	D2	D3	D4	D5	D6	D7
Test 35	5923	2.2	1.92	1.54	1.26	0.99	0.8	1.88
Time: 13:51	9085	3.56	3.04	2.45	1.99	1.57	1.26	3
	11989	4.85	4.17	3.38	2.77	2.2	1.78	4.13
	Temp	Pav. Sur.	88					
		Air	86					

	Load	D1	D2	D3	D4	D5	D6	D7
Test 36	5923	2.16	1.89	1.51	1.21	0.96	0.76	1.87
Time: 13:54	8986	3.5	2.97	2.38	1.93	1.52	1.22	2.93
	11961	4.82	4.12	3.34	2.73	2.17	1.75	4.08
	Temp	Pav. Sur.	88					
		Air	85					

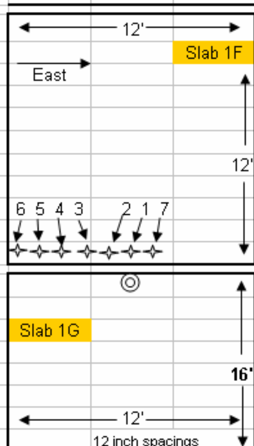

Location: 1G & 1F **Geophone:** **Plate:** Date: 11/18/2003

	Load	D1	D2	D3	D4	D5	D6	D7
Test 37	5871	1.55	1.54	1.38	1.13	0.94	0.76	1.52
Time: 13:58	9030	2.67	2.5	2.23	1.83	1.54	1.24	2.45
	11922	3.58	3.47	3.09	2.53	2.15	1.73	3.44
	Temp	Pav. Sur.	88					
		Air	83					

	Load	D1	D2	D3	D4	D5	D6	D7
Test 38	5923	1.61	1.54	1.37	1.12	0.93	0.74	1.52
Time: 14:00	8970	2.64	2.52	2.25	1.85	1.56	1.26	2.49
	11906	3.6	3.46	3.08	2.53	2.15	1.72	3.43
	Temp	Pav. Sur.	88					
		Air	83					

Note: Load was placed 6 feet from edge.
Dowels are located at joints.
Drawing not to scale.

Table A-4. FWD Test at Free Edge-1G

Edge Loading 1G-Free End

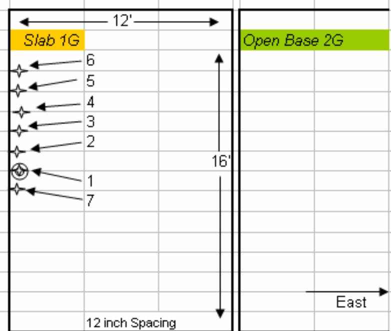

Location: 1G **Geophone:** **Plate:** Date: 11/18/2003

	Load	D1	D2	D3	D4	D5	D6	D7
Test 47	5661	2.75	2.61	2.04	1.56	1.14	0.83	2.59
Time: 14:43	8807	4.5	4.26	3.31	2.53	1.85	1.36	4.22
	11707	6.12	5.76	4.46	3.43	2.52	1.85	5.7
	Temp	Pav. Sur.	81					
		Air	82					

	Load	D1	D2	D3	D4	D5	D6	D7
Test 48	5669	2.77	2.63	2.04	1.55	1.13	0.83	2.63
Time: 14:44	8787	4.46	4.22	3.27	2.49	1.82	1.34	4.19
	11691	6.07	5.73	4.44	3.4	2.5	1.84	5.67
	Temp	Pav. Sur.	81					
		Air	83					

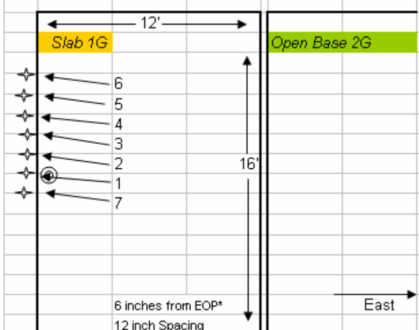

Location: 1G **Geophone:** **Plate:** Date: 11/18/2003

	Load	D1	D2	D3	D4	D5	D6	D7
Test 49	5661	2	1.64	1.52	1.24	0.96	0.76	1.8
Time: 14:45	8811	3.29	2.7	2.5	2.02	1.57	1.23	2.94
	11747	4.48	3.7	3.39	2.77	2.16	1.68	4
	Temp	Pav. Sur.	81					
		Air	82					

	Load	D1	D2	D3	D4	D5	D6	D7
Test 50	5621	1.96	1.63	1.52	1.24	0.98	0.77	1.81
Time: 14:46	8791	3.26	2.67	2.48	2	1.57	1.24	2.95
	11707	4.43	3.67	3.37	2.74	2.15	1.68	4.01
	Temp	Pav. Sur.	81					
		Air	83					

Note: Load was placed at the center of Slab on the edge.
No cracks were found along slab.
EOP - edge of pavement
Dowels are located at joints.
Drawing not to scale.

Table A-5. FWD Test at a Confined Edge

Midday Test - Noon to 4PM

Edge Loading 1E-**Adjacent Slab** 2E

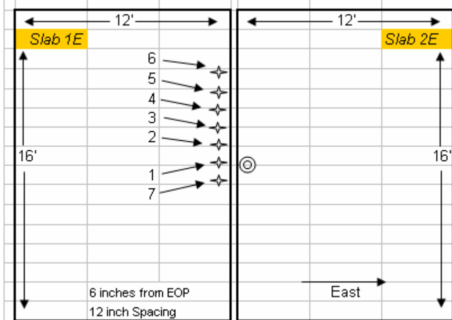

Location: 1E & 2E **Geophone:** **Plate:** Date: 11/18/2003

	Load	D1	D2	D3	D4	D5	D6	D7
Test 23	5720	1.4	1.31	1.11	0.93	0.75	0.62	1.33
Time: 13:06	8898	2.3	2.15	1.84	1.52	1.24	1.02	2.17
	11830	3.15	2.94	2.52	2.08	1.7	1.39	2.97
	Temp	Pav. Sur.	79					
		Air	82					

	Load	D1	D2	D3	D4	D5	D6	D7
Test 24	5645	1.37	1.29	1.11	0.93	0.74	0.6	1.31
Time: 13:21	8902	2.28	2.14	1.82	1.53	1.23	1.01	2.16
	11806	3.14	2.95	2.54	2.11	1.7	1.39	2.96
	Temp	Pav. Sur.	79					
		Air	81					

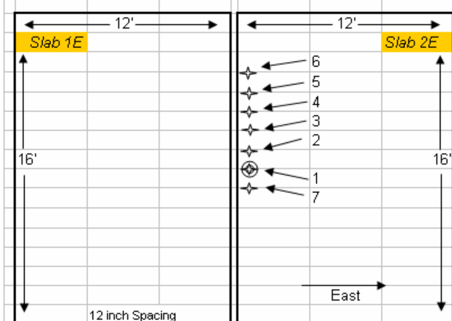

Location: 1E & 2E **Geophone:** **Plate:** Date: 11/18/2003

	Load	D1	D2	D3	D4	D5	D6	D7
Test 21	5474	1.87	1.53	1.24	0.98	0.75	0.61	1.57
Time: 13:03	8851	2.96	2.57	2.09	1.64	1.26	1.01	2.61
	11787	4.35	3.55	2.89	2.27	1.77	1.41	3.62
	Temp	Pav. Sur.	80					
		Air	82					

	Load	D1	D2	D3	D4	D5	D6	D7
Test 22	5661	1.91	1.5	1.19	0.94	0.72	0.57	1.54
Time: 13:04	8863	3.04	2.55	2.04	1.62	1.27	0.99	2.61
	11854	4.18	3.5	2.85	2.25	1.76	1.39	3.57
	Temp	Pav. Sur.	80					
		Air	81					

Note: Load was placed at the center of Slab on the edge.

Dowels are located at joints.

Drawing not to scale.